Crustal growth during island arc accretion and transcurrent deformation, Natal Metamorphic Province, South Africa: new isotopic constraints

Christopher J Spencer[1,2*], Robert J Thomas[3], Nick M W Roberts[2], Peter A Cawood[1], Ian Millar[2], Simon Tapster[2]

[1]Department of Earth and Environmental Sciences, University of St Andrews, St Andrews, KY16 9AL, UK

[2]NERC Isotope Geosciences Facilities, British Geological Survey, Keyworth, Nottingham, NG12 5GG, UK

[3] Council for Geoscience, P.O. Box 572, Bellville, 7535, South Africa

*Corresponding author; current address: Department of Applied Geology, Curtin University, Perth WA 6845, Australia; cspencer@curtin.edu.au

Keywords: Natal orogeny; accretion; oblique collision, crustal growth; zircon U-Pb-Hf

Abstract

The Natal Metamorphic Province consists of, from north to south, the Tugela, Mzumbe, and Margate terranes. These were accreted to the southeastern margin of the Kaapvaal Craton in the late Mesoproterozoic, and followed by intrusion of a large suite of A-type granitoid bodies. New U-Pb data from zircon, titanite, and monazite further constrains the temporal framework of these geological events.

The Tugela and Mzumbe terranes record protracted magmatism in an island arc complex from ~1200 Ma to 1160 Ma, followed by the accretion of these terranes onto the southern margin of the Kaapvaal Craton at ~1150 Ma. Arc magmatism in the Margate Terrane

continued until ~1120 Ma and was followed by extension and bimodal volcanism immediately prior to accretion to the Kaapvaal/Mzumbe continental margin at ~1090 Ma. This accretion was accompanied by high-pressure and high-temperature metamorphism, juxtaposition of the Mzumbe and Margate terranes along the Melville Thrust, and the formation of a number of syntectonic intrusive units derived from melting of the pre-existing arc crust. After accretion, extensional collapse is evidenced by the intrusion of mafic/ultramafic and alkaline intermediate magmatic suites at ~1085 Ma, resulting from mafic underplating and/or lower crustal delamination. Nd and Hf isotopic data imply the magmatic rocks of the Natal Metamorphic Province were derived from relatively juvenile continental crust, initially generated by island arc magmatism and subsequently reworked during the accretion event(s). The combined Kaapvaal-NMP region (the southern margin of the enlarged Kalahari Craton) then experienced extensive sinistral transcurrent deformation centered along a series of discrete steep shear zones that are found from the Kaapvaal cratonic margin to the southernmost portion of the Natal Metamorphic Province. This deformation is accompanied by low-pressure, (ultra)high-temperature metamorphism, isobaric cooling, and intrusion of the voluminous A-type Oribi Gorge Suite porphyritic granites and charnockites throughout the Mzumbe and Margate Terranes.

1. Introduction

The Mesoproterozoic Natal Metamorphic Province (NMP) is comprised of ~1.3 to 1.0 Ga lithotectonic terranes which were accreted onto the SE margin of the Archaean Kaapvaal Craton (Figs. 1 and 2). From south to north these terranes are the Margate, Mzumbe, and Tugela terranes (Thomas, 1989a). The NMP, along with a similar age metamorphic

47 province in the Northern Cape of South Africa and southern Namibia, form part of the
48 Namaqua-Natal belt that is thought to be associated with arc accretion and escape
49 tectonics whereby late sinistral shearing in Natal is mirrored by conjugate dextral shears
50 in Namaqualand (Jacobs et al., 1993) that formed immediately prior to the assembly of
51 the Rodinia supercontinent. The timing of intrusion, deformation and metamorphism, and
52 the geochemical/isotopic composition of the rocks within the NMP, has been the focus
53 of many studies (see references and data compilations within Eglington, 2006 and
54 McCourt et al., 2006). This study adds to the growing body of geochronological and
55 isotopic data of the NMP, places further constraints on its orogenic evolution, and will
56 address several outstanding questions concerning the temporal framework of the Natal
57 Orogeny. Most of the previous studies have been conducted piecemeal over the last 25
58 years, and employed a variety of geochronological techniques by various laboratories.
59 This approach has ensured that there still remain several ambiguities, unresolved
60 questions and untested hypotheses. In order to provide a consistent U-Pb zircon
61 geochronological data framework by laser ablation inductively coupled plasma-mass
62 spectrometry (ICP-MS) and isotope-dilution thermal ionization mass spectrometry (ID-
63 TIMS) techniques, we have re-sampled most of the main intrusive units from the
64 Mzumbe and Margate Terranes and dated some units for the first time. This
65 geochronological framework is augmented by the first whole-rock and zircon Hf isotope
66 data from Natal, coupled with U-Pb zircon, titanite, and monazite age data recording
67 metamorphism and whole-rock Nd isotopes of many of the intrusive units throughout the
68 Mzumbe and Margate terranes. This dataset is used to provide an up-to-date and

69 comprehensive interpretation of the timing and nature of the tectono-magmatic events in
70 the NMP.

71 ## 2. Regional Setting

72 The Tugela Terrane comprises a series of NE directed, flat-lying thrust nappes,
73 predominantly composed of supracrustal sequences; mainly layered amphibolites with
74 subordinate quartzofeldspathic gneisses and ultramafic rocks with some intrusive
75 tonalitic orthogneisses (Matthews, 1972; Thomas et al., 1994, Johnston et al., 2003). The
76 terrane underwent upper-amphibolite to lower-granulite grade metamorphism,
77 overprinted by greenschist facies assemblages (Bisnath et al., 2008). Matthews (1972)
78 interpreted the terrane as an ophiolite complex, which was obducted over the rigid
79 Kaapvaal cratonic margin at about 1135 Ma (Jacobs et al., 1997). The southern margin of
80 the Tugela Terrane is defined by the major sub-vertical Lilani-Matigulu Shear Zone,
81 which coincides with the southernmost geophysical boundary of the Kaapvaal Craton (de
82 Beer and Meyer, 1984; Barkhiuzen and Matthews, 1990; Jacobs and Thomas 1994; de
83 Wit and Tinker, 2004). South of the Lilani-Matigulu Shear Zone, the Mzumbe and
84 Margate terranes are composed of arc-related, felsic to mafic metavolcanic and
85 metasedimentary gneisses, the oldest of which (Quha gneiss) have been dated at ca. 1235
86 Ma (Thomas et al., 1999). The supracrustal gneisses were intruded at about ~1200 Ma by
87 juvenile calc-alkaline I-type granitoids (e.g. the Mzumbe gneiss), likely in an island arc
88 setting (Thomas and Eglington, 1990). The Mzumbe and Margate Terranes are separated
89 by the Melville Thrust, a ~1 km wide, southerly dipping zone of high-strain (Thomas,
90 1989a). Apart from differing rock assemblages, the most apparent difference between the
91 terranes is the metamorphic grade; the Margate Terrane displays (ultra)high-temperature

92 granulite-facies metamorphism, whereas the Mzumbe Terrane is dominated by
93 amphibolite-facies rocks (Thomas, 1989a; Thomas et al., 1992; Jacobs and Thomas,
94 1994). The three Natal terranes accreted northwards during the first phase of the Natal
95 Orogeny during a tectonic phase generally termed D_1 (e.g. Jacobs and Thomas, 1994;
96 Jacobs et al., 1997). The Mzumbe and Margate Terranes are intruded by several suites of
97 granitic and subordinate mafic rocks. The most voluminous of these are the large
98 metaluminous, A-type granite/charnockite plutons known as the Oribi Gorge Suite
99 (Thomas, 1988, 1991b), which intrudes both the Mzumbe and Margate terranes after they
100 were juxtaposed. These are interpreted to have been derived from the partial melting of
101 lower crustal rocks (Thomas, 1988). The plutons exhibit ductile deformation especially
102 near their contacts with the supracrustal gneisses, and were emplaced during a major
103 phase of sinistral ductile transcurrent shearing, generally termed D_2 (Jacobs et al., 1993;
104 Fig 12; Jacobs and Thomas, 1994). Published U-Pb zircon determinations point to a
105 protracted timescale for this tectono-magmatic event between ~1080 and 1030 Ma (see
106 review in Eglington et al., 2003). Following transcurrent deformation, the latest stage of
107 magmatism in the Natal Province is represented by a restricted number of undeformed
108 granitic dykes in the Margate Terrane (Mbizana Microgranite) dated at 1026 ± 3 Ma
109 (Thomas et al., 1993b). In the sections that follow, we provide a new set of isotopic data
110 that cover a large portion of the Mzumbe and Margate Terrane, with which many of the
111 models discussed are tested and modified.

112 ## 3. Unit description, Petrography, and Zircon textures

113 Sample lithologies and mineral assemblages are listed in Table 1.

114 ### 3.1. Mzumbe Granitoid Suite

115 The Mzumbe Granitoid Suite forms the oldest pre-tectonic granitoid in the Mzumbe
116 Terrane (Thomas, 1989a). It intrudes the supracrustal rocks of the Mapumulo Group. The
117 age of the Mzumbe Granitoid Suite has been previously constrained by an 8-point Rb-Sr
118 isochron age of 1212 ± 56 Ma and a TIMS U-Pb multigrain zircon age of 1207 +10/-11
119 Ma (Thomas and Eglington, 1990). This suite comprises a complex series of sheet-like
120 granitoid bodies ranging from quartz diorite to leucogranodiorite which Thomas (1989b)
121 interpreted as a comagmatic series of primitive, low-K, calc-alkaline granitoids formed
122 from the partial melting of a descending slab of oceanic lithosphere adjacent to the
123 Kaapvaal continental margin during the earliest phase of convergence in the NMP.
124 A sample of gneissic quartz-diorite from the Mzumbe Suite (CS13-16) was collected
125 along the Fafa River near Ifafa. The sample is composed of quartz, plagioclase,
126 poikiloblastic hornblende and altered biotite. Thomas (1989) reported colorless
127 clinopyroxene replacing hornblende in some samples, which he interpreted as having
128 formed during prograde metamorphism. CL imaging of zircons in sample CS13-16
129 demonstrates oscillatory zonation, distinct core and rim growth phases and apatite and
130 opaque mineral inclusions (Fig. 3).

131 3.2. Sezela Syenite Suite

132 This suite is composed of alkaline intrusive syenitic rocks which were sampled at the
133 type localities in the Sezela pluton documented by Evans et al. (1991). The pluton
134 comprises an inner relatively mafic grey quartz-monzonite and an outer envelope of pink
135 quartz-monzonite and fluorite-bearing quartz-syenite (Thomas, 1988). The outer pink
136 syenite displays a weak foliation with progressively decreasing amounts of strain in the
137 interior of the pluton (Evans et al., 1987). The pink syenite sample exhibits patchy

perthite mantling plagioclase, quartz, and biotite (see also Evans et al., 1991). Plagioclase is variably altered to sericite and biotite is found in greenish clots, altered to chlorite. The grey quartz monzonite sample exhibits perthitic feldspar, plagioclase, with altered biotite and hornblende. CL images of zircons in the two Sezela Suite samples (pink syenite: CS13-12, grey quartz monzonite: CS12-13) show a range of morphologies and textures. The majority of the zircons are complexly zoned and variably metamict (Fig. 3). Many zircons display distinct core and rim zircon growth phases. The Sezela Syenite Suite was originally defined as one of the youngest intrusive suites in the Mzumbe Terrane. It intrudes the supracrustal rocks of the Mapumulo Group, Humberdale Granite, and Equeefa Amphibolite Suite. Eglington and Kerr (1989) report a 9-point Rb-Sr whole-rock isochron age of 951 ± 16 Ma, which was interpreted as an intrusive age. This age and the presence of minimal deformation fabrics led this suite to be classified late to post-tectonic (Evans et al., 1991), but data from this study discussed below calls this interpretation into question.

3.3. Leisure Bay Formation

The Leisure Bay Formation is part of the Mzimkulu Group, forming the oldest rocks of the Margate Terrane. The formation comprises a sequence of inter-layered pelite, psammite, and calcic granulite-facies migmatitic gneisses with chemical compositions akin to average shales, greywackes, and calcarenites respectively (Mendonidis, 1989). Three generations of folds with their associated axial planar foliations have been recognized (Grantham et al., 1991). The Leisure Bay Formation underwent (ultra)high-temperature, low-pressure (900-1100 ºC, ~5-7 kbar) granulite-facies metamorphism and biotite/hornblende dehydration melting to produce garnet+orthopyroxene leucosomes and

garnet+cordierite restites (Mendonidis and Grantham, 2003). Mendonidis and Grantham (2003) interpreted inclusions of hercynite in cordierite and garnet+quartz symplectites after orthopyroxene+plagioclase, as indicating isobaric cooling after the peak metamorphism. A sample of the Leisure Bay Formation (CS13-20) was collected from the type section as described by Grantham et al. (1991). CL imaging of zircons from this sample reveal oscillatory zonation, distinct core and rim growth phases, and minor opaque mineral inclusions. The zircons are subrounded, and in some cases the zoning is truncated by abraded edges (Fig. 3); this is consistent with the metasedimentary interpretation of Mendonidis, (1989).

3.4. Margate Granite Suite

The most widespread and diverse intrusive unit in the Margate Terrane, covering about ~200 km^2, is known as the Margate Granite Suite (Thomas et al., 1991). It is made up of three variably foliated lithotypes: garnet-biotite augen gneiss, charnockite and more than one generation of leucogranite (± garnet). The intrusions range in form from thin boudinaged veins up to large sheet-like plutons (Thomas et al., 1991). Initially this suite was classified as being made up of peraluminous S-type granites, interpreted as syn-collisional melts generated during the accretion of the Margate Terrane (M_2; Thomas et al., 1991). Recently however, Voordouw and Rajesh (2012) reinvestigated the geochemistry of the rocks and found that ~75% of the Margate Suite granites are magnesian, calc-alkalic, and peraluminous, while the remaining 25% are ferroan, calc-alkalic, and metaluminous to peraluminous. They interpreted the suite to represent a large granitic batholith and the Margate Terrane as a continental magmatic arc. The polyphase Margate Suite is poorly dated, and the timing of intrusion has been constrained by a

zircon SHRIMP U-Pb age of 1057 ± 27 Ma on one of the minor later phases of intrusion (Mendonidis and Armstrong, 2009). Two Rb-Sr whole-rock isochrons of 1011 ± 14 Ma (Nicholson's Point pluton; Eglington et al., 1986) and 1055 ± 60 Ma (Belmont pluton Thomas et al., 1990) have also been reported. The complexity of the Margate Suite is examined by Mendonidis et al. (this issue) who report U-Pb SHRIMP zircon dates from several phases of the suite, which reveal four distinct zircon-forming events: an earliest phase of magmatism (1169 ± 14 Ma), similar to that reported for the Sikombe Granite (Thomas et al., 2003), three intrusive pulses of garnetiferous leucogranite (1135 ± 8, 1088 ± 9, and 1043 ± 4 Ma), and a phase of charnockitisation synchronous with the intrusion, and within the thermal aureole of the Oribi Gorge Granitoid suite (1037 ± 13 Ma). Two samples of the Margate Granite Suite were also taken as part of this study from the type locality (CS13-26) and from Nicholson's Point (CS13-21). They are composed of medium- to fine-grained garnet-bearing leucogranite with myrmekitic orthoclase and albite-rimmed plagioclase. Biotite is mostly chloritised, often associated with garnet, and is likely secondary. CL imaging of zircons in the samples show a low CL response and oscillatory zonation (Fig. 3).

3.5. Glenmore Granite

The Glenmore Granite is an irregular shaped body with an outcrop extent of ~28 km^2 that has been interpreted as a sheet, folded along east-west axes (Talbot and Grantham, 1987). The granite is strongly foliated, peraluminous, with biotite, garnet and occasional rapakivi feldspar textures (Grantham, 1983; Mendonidis, 1989; Mendonidis et al., 1991). It intrudes the Leisure Bay Formation to the south and Margate Granite Suite to the north, with contacts generally concordant to the regional foliation. The granite locally contains

enclaves of Margate Granite, some phases of which, at least, must be older (Thomas, 1988). The Glenmore Granite has given a SHRIMP U-Pb zircon age of 1091 ± 9 Ma (Mendonidis et al., 2002). A sample of the granite was collected from the type locality described by Mendonidis et al. (1991). Poikilitic orthoclase is the dominant feldspar with inclusions of quartz and plagioclase, with abundant myrmekite. Grantham (1983) also reported biotite-quartz symplectites, typically in contact with garnet. CL images of zircons in the granite (sample CS13-22) show oscillatory zonation, distinct core and rim growth phases with minor opaque mineral inclusions (Fig. 3).

3.6. Turtle Bay Suite

The Turtle Bay Suite comprises a bimodal association of two-pyroxene mafic granulites and felsic charnockites (orthopyroxene-bearing granites), spatially associated with the Melville Shear Zone, which constitutes the boundary between the Mzumbe and Margate terranes (Thomas et al., 1992). The two units are interlayered and are likely sheet intrusions. Strong compositional banding is observed in the mafic granulites comprising hydrous (hornblende and biotite-bearing) and anhydrous (pyroxene-rich) layers. The felsic charnockites contains large orthopyroxene poikiloblasts (< 10 mm) with biotite myrmekite. These rocks structurally overlie the Margate Granite Suite along the eastern coastal type section and are intruded by the Mvenyane pluton of the Oribi Gorge Suite in the western section (Thomas, 1988). Previous work has interpreted the two distinct rock types in this suite to genetically unrelated sources (Thomas, 1991d). These are represented by an earlier mafic plagioclase-rich cumulate and a later partial melt of this cumulate leading to highly fractionated pyroxene-bearing granites. A sample of both mafic granulite and felsic charnockite were collected from the coastal type section

described by Thomas (1991d). CL images of zircons in the mafic granulite (CS13-28) reveal very complicated internal structures and show them to be metamict. Zircons from the felsic charnockite (CS13-29) have a low CL response and are metamict with oscillatory zonation (Fig. 3).

3.7. Oribi Granitoid Suite

The Oribi Granitoid Suite comprises ten plutons of very coarse-grained, megacrystic, and locally rapakivi granite/charnockite plutons, which intrude the supracrustal rocks and older granitoids of the Mzumbe and Margate terranes (Fig. 2). Some of the plutons are biotite/hornblende granite-dominated, with very little to no orthopyroxene (Mvenyane) whereas other are nearly exclusively charnockitic (Port Edward, KwaLembe) (Thomas, 1988; Grantham et al., 2012). The plutons are predominately elliptical in map view and become progressively more elongate parallel to the regional foliation towards the northern part of the Mzumbe terrane (Thomas, 1988). Strong regional fabrics are seen along the plutonic margins forming distinct augen gneiss textures. In most plutons, strain partitioning during the D_2 deformation has left the plutonic core devoid of deformation, whereas the Glendale and Umgeni plutons exhibit discrete ductile shear zones that cut through the plutonic core (Fig. 2; Thomas, 1989a; Thomas et al., 1991). Samples were collected from two plutons in the Mzumbe Terrane (Mvoti and KwaLembe) and two plutons in the Margate Terrane (Port Edward and Oribi Gorge).

3.7.1. Mvoti pluton

The Mvoti pluton occurs as an elongate granitoid/charnockite body (~240 km^2), and intrudes the Mapumulo Group and often hosts enclaves of the host rock (Thomas, 1992). The plutonic margins are generally sharp and occasionally mylonitic (Kerr and Finlay,

1981). Plagioclase in the Mvoti pluton is often replaced by sericite and antiperthite and biotite is partially chloritised. This pluton is previously undated, but displays the same intrusive relationships as the other units of the Oribi Gorge plutonic suite. A sample of the Mvoti pluton (CS13-4) was collected along the Mvoti River south of the Embezeni village near the inferred margin of the pluton. Cathodoluminescence (CL) imaging shows the zircons in the Mvoti pluton are complexly zoned and often metamict; many have lozenge shaped apatite inclusions (Fig. 3).

3.7.2. KwaLembe pluton

The previously undated KwaLembe pluton is an elliptical granitoid/charnockite (~420 km^2), which intrudes the undated Mkomazi granitic gneiss on its southern margin and is covered by the overlying Paleozoic Natal Group sedimentary rocks to the north (Evans et al., 1991). Contacts with the Mkomazi gneiss are sharp and concordant with the dominant steep foliation, which lies within the major D_2 Amanzimtoti Shear Zone. Plagioclase is the dominant feldspar with minor myrmekite when in contact with quartz. Secondary biotite is partially chloritised. A sample of the KwaLembe pluton was collected south of the Songeni village along the Mkomazi River. CL images of zircons in the KwaLembe pluton (sample CS13-10) exhibit complex zoning and intense metamictisation (Fig. 3).

3.7.3. Port Edward pluton

The Port Edward pluton is an irregularly shaped enderbite body (> 300 km^2) that intrudes the Munster Metabasite and the Margate Granite suites and often displays diffuse contacts (Grantham, 1983) interpreted to be caused by contact metamorphism (Eglington et al., 1986). Andesine and orthoclase are the dominant feldspars, which often have myrmekitic margins. Orthopyroxene is the main mafic mineral with minor amounts of

secondary biotite. Previous studies have dated the Port Edward pluton at 1025 ± 8 Ma (SHRIMP zircon U-Pb) and 987 ± 19 Ma (whole-rock Rb-Sr), which have been interpreted to represent igneous emplacement and cooling respectively (Eglington et al., 2003). A sample of the Port Edward pluton was collected along the coast of the Indian Ocean along the type section described by Thomas (1991c). Zircons in the Port Edward pluton (sample CS13-19) have sector and oscillatory zonation with minor opaque mineral inclusions as revealed by CL imaging (Fig. 3).

3.7.4. Oribi Gorge pluton

The Oribi Gorge pluton is a large elliptical granitoid/charnockite body (~880 km^2) that intrudes the granulite-facies Margate Granite Suite along its southern side. This pluton is predominately orthopyroxene-bearing ± fayalite and garnet and relatively minor volumes of porphyritic hornblende-biotite granite. The multi-facies relationship in the Oribi Gorge is similar to that of the Farsund charnockite of southern Norway, in which this variation is attributed to heterogeneous assimilation of varying lower crustal lithologies (Vander Auwera et al., 2014). Eglington et al. (2003) report a series of complex inheritance, emplacement, and overgrowth SHRIMP zircon U-Pb ages ranging from 1071 ± 12 Ma to 1029 ± 8 Ma. Thomas (1988) and Thomas et al. (1993) report a U-Pb zircon age for the pluton of 1037 ± 14 Ma and Rb-Sr ages of 1003 ± 29 Ma (whole-rock isochron), 924 ± 49 Ma (biotite), and 882 ± 18 Ma (biotite), probably reflecting emplacement and cooling. A sample (CS13-27) was collected from the type locality within the Oribi Gorge Nature Reserve along the Mzimkhulwana River as described by Thomas (1991c). CL images of zircons in the Oribi Gorge pluton (sample CS13-27) show sector and oscillatory zonation with minor opaque mineral inclusions (Fig. 3).

299 4. Methods

300 Full methods are explained in supplementary text 1.

301 4.1. Whole-rock Hf and Nd isotopes

302 Whole-rock Hf isotopes were performed on a Thermo Scientific Neptune+ multi-
303 collector inductively coupled plasma mass spectrometer system at the NERC Isotope
304 Geoscience Laboratories (NIGL). Nd isotopes were collected using a Thermo Scientific
305 Trition thermal ionization mass spectrometer also at NIGL.

306 4.2. Laser ablation U-Pb geochronology and Hf isotopes

307 U-Pb geochronology of zircon, titanite, and monazite were analyzed by single- and multi-
308 collector sector-field inductively coupled plasma mass spectrometry (LA-SC/MC-SF-
309 ICP-MS) coupled to a New Wave Research UP193UC ArF excimer laser ablation system
310 at the NERC Isotope Geosciences Facilities following the methods described in Spencer
311 et al. (2014). Near concordant (>95% concordance) U-Pb zircon ablation sites were then
312 re-analyzed to measure their Lu-Hf isotopic compositions using a Thermo Scientific
313 Neptune Plus MC-ICP-MS with a New Wave Research UP193UC ArF excimer laser
314 ablation system at the NERC Isotope Geosciences Facilities.

315 4.3. CA-ID-TIMS U- Pb geochronology

316 A subset of the most concordant zircons was removed from epoxy mounts for chemical
317 abrasion isotope dilution thermal ionization mass spectrometry (CA-ID-TIMS). Chemical
318 abrasion following Mattinson (2005), ion exchange chemistry and isotopic analysis using
319 a Thermo-Electron Triton were conducted at NIGL. See supplementary materials for
320 complete methodology.

321 5. Results

5.1. U-Pb Geochronology

Results of U-Pb zircon, titanite, and monazite geochronology are presented in figures 4, 5, 6, 7, 8, S1, S2 and supplementary tables S1, S2, S3, and S4. Laser ablation analyses that display lead loss (> 2% discordance) or inheritance are filtered from the weighted average calculation. Weighted averages of $^{207}Pb/^{206}Pb$ or $^{206}Pb/^{238}U$ ages are reported based on the relative magnitude of 2 sigma uncertainties. For the ID-TIMS analyses, crystallization ages are determined using weighted averages of $^{207}Pb/^{206}Pb$ are used given the ~zero age lower intercepts of sample discordias.

5.2. Zircon Hf isotopes

Weighted averages of Hf isotopic analyses of zircon from each of the above samples are displayed in Fig. 10 and supplementary table S4 and have $\varepsilon Hf_{(t)}$ values between 7.4 and 2.9 with the exception of the Mvoti pluton which has an average of -0.8 ± 0.4. Reduced chi-squared tests reveal that Hf analyses for each sample represent single populations (see Wendt and Carl, 1999) and weighted average uncertainties vary between 0.4 and 1.4 epsilon units.

5.3. Whole-rock Nd, and Hf isotopes

Whole-rock isotope data are summarized in Table 3 and Fig. 10. εNd ranges from -0.3 to 5.6, and εHf from -0.2 to 14.7. Sm/Nd ratios range from 0.21-0.10 and Lu/Hf ratios range from 0.057-0.002.

6. Discussion of the new U-Pb zircon ages and isotopic data

In detail, many of the dates determined in this study are in accordance with prior geochronological studies, although several do not agree with previous ages, requiring a

344 re-evaluation of the timing of tectono-magmatic events. In the following section we
345 review each new determination and compare it with previously published data.

346 6.1. Mzumbe Granitoid Suite (Mzumbe Terrane): sample CS13-16

347 The sample of the gneissic quartz diorite of the Mzumbe Granitoid Suite analyzed in this
348 study gave an age of 1175 ± 19 Ma. This is ~30 Ma younger than the previously reported
349 multi-grain TIMS age of 1207 ± 10 Ma (Thomas and Eglington, 1990). Sample CS13-16
350 showed distinct core-rim relationships; however, each of the core/rim analyses yielded
351 the same age within uncertainty. It is possible there is an older population or grains with
352 older cores that were not captured by our analyses in this sample, which might explain
353 why the age presented by Thomas and Eglington (1990) is older than the crystallization
354 age determined in this study. An alternative is simply that the Mzumbe Granitoid Suite
355 has a protracted magmatic history spanning from ~1175 to ~1207 Ma or includes two
356 temporally discrete phases. Certainly, multiple intrusive phases are apparent in most
357 outcrops.

358

359 Whole-rock Nd, and Hf isotope data (Thomas and Eglington, 1990; this study)
360 demonstrate that the Mzumbe Suite incorporated variable, but small, amounts of
361 isotopically enriched material during petrogenesis (Fig. 10). Furthermore, the lack of
362 reworking of significantly older crustal material, that might have been derived from the
363 nearby Kaapvaal Craton for example, suggests the Mzumbe magmatic arc had a
364 subduction polarity dipping away from the craton, as in the model of Jacobs and Thomas
365 (1994). The incorporation of minor amounts of isotopically enriched crust in island arc
366 settings is not unusual (e.g. see the Honshu, Luzon, and Lesser Antilles island arcs), as

367 reviewed by Dhuime et al. (2011). The Hf and Nd isotope data from the younger
368 sequences (with a few exceptions) fall within a narrow field between εHf of ~3-5 and
369 εNd of ~1-3, indicating the reworking of this arc material with minor incorporation of
370 older material.

371 6.2. Sezela Syenite Suite (Mzumbe Terrane): samples CS13-12 and CS13-13

372 The Sezela pluton of the Sezela Syenite Suite, comprises two phases, an outer pink
373 syenite and an inner grey quartz monzonite. Both phases were sampled in this study and
374 gave statistically identical ages of 1081 ± 19 and 1085 ± 18 Ma, respectively. Both dates
375 are considered to represent the age of crystallization/intrusion showing that the phases are
376 coeval. The Sezela Suite has not previously been dated by zircon, except for an
377 unpublished zircon evaporation Pb-Pb age of 1058 ± 6 Ma (B.M. Eglington, pers. comm.,
378 2014). The suite has been defined as post-tectonic intrusive as it does not have clear cross
379 cutting deformation fabrics (Evans et al., 1991). This interpretation was supported by a
380 Rb-Sr whole-rock isochron age of 951 ± 16 Ma, interpreted as an intrusive age by
381 Eglington and Kerr (1989). Our new data shows that this young age and interpretation is
382 no longer tenable. Furthermore, the grey quartz monzonite phase also yielded a titanite
383 upper intercept U-Pb age of 1030 ± 9 Ma, interpreted as dating the metamorphic growth
384 of titanite in the sample as it coincides with the emplacement ages of the Oribi Gorge
385 Suite. This data clearly means a re-evaluation of the tectonic setting of the Sezela Suite is
386 needed.

387 6.3. Leisure Bay Formation (Margate Terrane): sample CS13-20

388 A meta-psammitic sample from the Leisure Bay Formation yielded a $^{207}Pb/^{206}Pb$ laser
389 ablation age of 1047 ± 17 (MSWD = 0.7) from a population of 15 analyses. Despite

390 complex growth zoning revealed by CL imaging, multiple analyses of single grains either
391 yielded overlapping concordant analyses or discordant analyses with intercepts within
392 uncertainty of the weighted average of the sample.
393 Given the metasedimentary nature of this sample, these ages either represent a single
394 detrital population and thus the maximum depositional age, or a granulite-facies
395 metamorphic event based upon the mineral assemblages. Based upon field relations and
396 geochronology of the granites, which intrude the Leisure Bay Formation and overlap in
397 uncertainty (ID-TIMS age of the Port Edward Pluton: 1034.5 ± 0.5 Ma), such a young
398 age cannot represent the maximum depositional age, so the grains are interpreted as being
399 of metamorphic origin. It is curious that no other detrital component is apparent despite
400 zircon zoning. This is possibly due to a complete resetting of the zircon age during
401 granulite-facies metamorphism. Although these zircons do not have depleted Th/U ratios
402 (0.7-4.4) they have very similar textures to those described from other high-temperature
403 granulite terranes that are detrital in nature but completely reset in terms of U-Pb (Lange
404 et al., 2005; Siebel et al., 2012). Further work is needed to more fully assess the
405 distribution of U and Pb in the zircon lattice, as very high temperature systems have been
406 shown to drastically alter their distribution (Kusiak et al., 2013; Valley et al., 2014;
407 Whitehouse et al., 2014).

408 6.4. Turtle Bay Suite (Margate Terrane): CS13-28

409 A mafic granulite sample taken from the mafic phase of the Turtle Bay Suite, interpreted
410 to be of metaigneous origin by Thomas et al. (1992) produced a $^{206}Pb/^{238}U$ age of 1114 ±
411 19 Ma. Selected analyses were between 4 and 7 % discordant. This date is interpreted to
412 represent an estimate of the crystallization age of the metabasic rock. The same sample

413 also yielded a U-Pb monazite age of 1042 ± 7 Ma (weighted average of 17 analyses from
414 5 different grains; MSWD = 1.5), interpreted as dating a metamorphic event. Monazites
415 from mineral separates were unzoned in Th and Y content (Fig. 8).

416 6.5. Glenmore Granite (Margate Terrane): sample CS13-22

417 Magmatic zircons from the Glenmore Granite gave a laser ablation age of 1092 ± 20 Ma
418 and an ID-TIMS age of 1084.5 ± 0.9 Ma (Figs. 5 and 6). This is identical to the SHRIMP
419 U-Pb zircon age of 1091 ± 9 Ma reported in Mendonidis et al. (2002). CL imaging did
420 reveal thin bright rims on the zircons from the Glenmore Granite, although these rims
421 were too thin to analyze (see Fig. 3).

422 6.6. Margate Granite Suite (Margate Terrane): samples CS13-21 and CS13-26)

423 Two intrusions of the Margate Suite from Margate beach (CS13-26) and Nicholson Point
424 (CS13-21) localities gave ages of 1088 ± 20 and 1099 ± 35 Ma, respectively. The
425 Nicholson Point granite also yielded an ID-TIMS age of 1084.4 ± 1.7 Ma (Figs. 5 and 6).
426 These ages, interpreted to represent the time of intrusion and crystallization of the
427 granites, are statistically identical to that of the older garnet leucogranite phase of the
428 Margate suite reported in Mendonidis et al. (2014; this volume). It is also coeval with the
429 Glenmore Granite. For this reason, Mendonidis et al. (2014; this volume) consider the
430 Glenmore Granite to be part of the Margate Suite.

431 6.7. Oribi Gorge Suite (both terranes): samples CS13-4, 10, 19, 27

432 The Oribi Gorge Suite comprises several highly distinctive plutons. The dating of the
433 suite has, however, proved problematical. Four plutons have given simple, consistent
434 dates (see Fig. 2): Mgeni (1030 ± 20 Ma; Eglington et al., 1989), KwaLembe (1030 ± 16

435 Ma; this study), Fafa (1037 ± 10; Eglington et al., 2003) and Port Edward (1025 ± 8 Ma;
436 Eglington et al., 2003; 1039 ± 18 Ma; this study).
437 The dating of the Oribi Gorge pluton itself has been more complex. Thomas (1988)
438 obtained a U-Pb zircon age of 1037 ± 14 Ma, within uncertainty to that we have obtained
439 in this study (1046 ± 19 Ma), and the other four plutons. However, Thomas et al
440 (1993a/b) and Eglington et al., (2003) obtained a range of dates, interpreted as intrusive,
441 from 1082 to 1029 Ma. In these studies the zircons were often complex, core-rim
442 relationships were common and an inherited component of many grains acknowledged.
443 For example, the interpreted magmatic age (ca. 1080 Ma), attributed by Eglington et al.,
444 (2003) to a sample of the pluton from the Bomela locality was taken right at the contact
445 with the Margate Granite. This age likely represents an inherited, Margate Granite, age
446 (Mendonidis et al. 2014; this volume) rather than an emplacement age (Fig. 11).
447 To further assess the temporal constraints of the Oribi Gorge Suite, zircons from the Port
448 Edward and Oribi Gorge plutons were also analyzed using ID-TIMS which yielded
449 weighted average $^{207}Pb/^{206}Pb$ ages of 1034.4 ± 0.6 Ma (Port Edward pluton) and 1049.3 ±
450 0.8 Ma (Oribi Gorge pluton) (Figs. 5, 6, 9).
451 Although the *in situ* data from this study and those preceding it yielded a suite of
452 imprecise data centered around ~1030 Ma with inheritance as old as ~1080 Ma, the ID-
453 TIMS data presented here provides high-precision ages with at least 13.5 Ma separation
454 between the crystallization of the zircons in the Port Edward and Oribi Gorge plutons (the
455 difference between the minimum uncertainty of the Oribi Gorge pluton and maximum
456 uncertainty of the Port Edward pluton). This separation implies the individual Oribi
457 Gorge plutons were emplaced independently.

458 The observed span of ages of the Oribi Gorge Suite (along with the assumption this
459 applies to the other plutons in the suite) has considerable implications for the timing and
460 duration of tectonic events. This suggests that the sinistral transcurrent deformation, with
461 which the suite is intimately associated, continued for at least 13.5 Ma and possibly
462 longer.
463 The new dataset has, however, introduced a new complexity with regard to the age of the
464 Oribi Gorge Suite. One of the northern intrusions, the Mvoti pluton, situated over 100 km
465 north of the KwaLembe intrusion, yielded a $^{207}Pb/^{206}Pb$ age of 1145 ± 18 Ma, some 115
466 Ma older than the southern plutons (Fig. 4). It also exhibits much lower whole rock and
467 zircon εHf and whole rock εNd values. This age and isotopic signature is strikingly
468 similar to the adjacent Mzumbe Terrane basement, and the sample, like the one from the
469 Bomela locality of the Oribi Gorge pluton, was collected from the contact area. It is thus
470 suggested that the Mvoti age in this study represents inheritance and significant
471 assimilation of the adjacent basement rocks and is not an intrusive age.

472 7. Tectonic Model

473 The data presented allow for a reassessment of the tectonic and temporal framework of
474 the NMP, as summarised in Fig. 12.

475 *Arc magmatism: ca. 1250 to 1150 Ma*

476 The earliest event recorded in the Mzumbe and Margate terranes is the formation of the
477 volcanic arc phase of the Quha Formation, dated at 1235 ± 9 Ma (Thomas et al., 1999).
478 The Quha Formation was subsequently intruded by the Mzumbe Granitoid Suite, which
479 is dated at 1207 ± 10 Ma (Thomas and Eglington, 1990) and 1175 ± 19 Ma (this study).

480 This implies either protracted arc magmatism with synchronous volcano-sedimentary
481 deposition, or two discrete pulses of arc magmatism.
482 The Mzumbe Suite is characterized by I-type granitoids interpreted, together with the
483 Quha Formation, to have formed in an essentially juvenile island arc setting above a
484 south-dipping subduction zone (see also Thomas, 1989b; Jacobs and Thomas, 1994). εHf
485 and εNd display varied isotopic compositions all of which are within uncertainty of, and
486 greater than, the chondritic uniform reservoir, implying limited reworking of significantly
487 older crust (Figs. 10, 11).
488 Evidence of an early stage of arc magmatism is also present in the Tugela Terrane, within
489 the northernmost Tugela and Madidima thrust sheets (Arima and Johnson, 2001). The
490 timing of this arc magmatism is imprecisely constrained between ~1200 and ~1150 Ma,
491 within uncertainty of the Mzumbe arc magmatism, although McCourt et al. (2006) posit
492 the Tugela and Mzumbe arc magmatism formed in two separate island arc systems.
493 *Terrane accretion and first regional metamorphism: 1150 to 1100 Ma*
494 The Tugela and Mzumbe terranes were accreted to the Kaapvaal Craton by ~1140 Ma
495 (Fig. 10; Jacobs et al., 1997; McCourt et al., 2006). This is evidenced by the
496 emplacement of the syntectonic granite sheets of the Mzimlilo Suite of the Mzumbe
497 Terrane (1147 ± 17 Ma; Eglington, et al. 2010) and the aplitic dykes cross-cutting the
498 Mkondeni arc rocks (McCourt et al., 2010).
499 During this time, arc magmatism continued until ~1135 Ma (Margate Granite;
500 Mendonidis et al., 2014, this volume) in the outboard Margate Terrane along with the
501 likely equivalent Sikombe Granite (Thomas, 1990; Thomas et al., 2003). The latest stages
502 of Margate arc magmatism was accompanied by the intrusion of the bimodal Turtle Bay

503 Suite comprising two-pyroxene mafic units (now granulites) and felsic pyroxene
504 granitoids. This magmatism is interpreted to represent a phase of extensional activity
505 during the latest stages of arc magmatism (Thomas et al., 1992). The Turtle Bay Suite is
506 spatially closely related with, and deformed by, the Melville thrust, which juxtaposes the
507 granulite-facies rocks of the Margate Terrane northwards over the amphibolite grade
508 rocks of the Mzumbe Terrane (Thomas, 1989; 1991d; Thomas et al., 1992).
509 The accretion of the Margate Terrane with the Mzumbe/Kaapvaal margin is constrained
510 by the emplacement and deformation of several syn-collision intrusions and zircon
511 overgrowths from ~1100 Ma to ~1090 Ma (e.g. Banana Beach Gneiss, Margate Granite,
512 Glenmore Granite; see Fig. 12 caption for references). Each of these syn-collision
513 igneous bodies, along with older, pre-collision intrusions has a strong penetrative ductile
514 fabric (broadly S_1) associated with crustal thickening and regional low-pressure granulite-
515 facies metamorphism in the Margate Terrane (~4 kbar and >850º) (Evans et al., 1987;
516 Mendonidis and Grantham, 2003), and upper amphibolite facies metamorphism in the
517 Mzumbe Terrane.
518 The assigned age (~1090 Ma) of this metamorphism roughly coincides with the intrusion
519 of the syn-tectonic granitoids found throughout the Margate Terrane followed by the
520 extensional collapse and alkaline/mafic magmatism of the Sezela and Equeefa Suites in
521 the Mzumbe Terrane (see Fig. 11 and references therein). It also explains the presence of
522 Margate Suite type garnet leucogranite plutons, such as the Belmont and Stiebel Rocks
523 plutons north of the Mellville Shear Zone, in the southern Mzumbe Terrane. Although
524 undated by U-Pb zircon the Belmont pluton gave a Rb-Sr isochron dates od ca. 1055 Ma

(Thomas et al., 1993), suggesting that it belongs to the latest, post-accretion phase of the Margate Suite, dated at ca. 1040 Ma (Mendonidis et al., 2014; this volume).

Post-accretion extension: ca. 1080 Ma

The cessation of this tectonomagmatic event can be constrained by the ages of the relatively undeformed Equeefa and Sezela suites. The age of the Equeefa Suite was determined by Eglington et al. (2010) at 1083 ± 6 Ma (SHRIMP zircon U-Pb). Our data shows that, for the first time, that the mafic/ultramafic Equeefa and the intermediate alkaline Sezela suites are coeval with both phases of the latter yielding U-Pb zircon ages of 1081 ± 9 and 1085 ± 8 Ma. Consequently, we interpret the Rb-Sr whole-rock isochron date of 951 ± 16 Ma of the Sezela Suite in Eglington and Kerr (1989) to represent a later cooling or alteration event as it is even younger than the U-Pb titanite age of 1030 ± 9 that we have obtained for the quartz monzonite phase.

Since it is now known that the Equeefa and Sezela suite are coeval, their tectonic significance can be better understood. The dated gabbro-norite body of Equeefa Suite probably resulted from post-arc accretion mafic underplating (Eglington, 1987; Thomas et al., 1992; Eglington et al., 2010). It can now be postulated that the underplating was also responsible for lower crustal melting and formation of the Sezela syenitoids. In this model therefore, the Equeefa and Sezela Suites would represent the products of a phase of post-accretion extensional collapse of the orogen at this time. The depleted composition Hf and Nd isotopes of the Sezela and Equeefa Suites in comparison with the other units further imply the influx of depleted mantle derived material (Fig. 10).

Transcurrent deformation and Oribi magmatism: ca. 1050-1030 Ma

547 Following the accretion of the Margate Terrane with the Mzumbe/Kaapvaal margin and
548 the post-accretion alkaline/mafic magmatism, the accreted terranes were subjected to a
549 second low-pressure, (ultra)high-temperature metamorphic event associated with
550 emplacement of the voluminous A-Type charnockite plutons of the Oribi Gorge Suite.
551 This widespread low-pressure, (ultra)high-temperature granulite-facies magmatic-
552 metamorphic event had peak conditions between ~900 and ~1100 ºC at ~5 to 7 kbar
553 followed by an isobaric cooling path (Grantham, 1984; Evans et al., 1987; Thomas et al.,
554 1992; Grantham et al., 1993; van den Kerkhof and Grantham, 1999; Grantham et al.,
555 2001; Mendonidis and Grantham, 2003).
556 The age of this metamorphic event is constrained in this study by a number of
557 independent methods. Metamorphic zircons from the paragneissic two-pyroxene Leisure
558 Bay Formation granulites (see Grantham et al., 1991) yield a $^{207}Pb/^{206}Pb$ age of 1047 ± 17
559 Ma. Metamorphic ages from titanite in the Sezela Suite (1030 ± 9 Ma; Fig. 7) and
560 monazite from a mafic granulite sample from the Turtle Bay Formation (1042 ± 7 Ma)
561 also demonstrate a metamorphic event at this time (Fig. 9). The minimum age of this
562 event is constrained by the cross-cutting unmetamorphosed Mbizana microgranite dykes
563 in the Margate Terrane, which have an intrusive age of 1026 ± 3 Ma (Thomas et al.,
564 1993b).
565 This metamorphic event was also coeval with the intrusion of the Oribi Gorge Suite
566 (Thomas, 1988; Thomas et al., 1991) and the formation of charnockitic aureoles that
567 developed in the Margate Suite garnet leucogranites adjacent to large Oribi Gorge Suite
568 plutons (Thomas, 1988; see van den Kerkhof and Grantham, 1999; Grantham et al, 2012
569 and Mendonidis et al., 2014, this volume). As discussed above, we posit this magmatic

570 event took place over a narrow window of time at 1032 ± 5 Ma. Structural, petrologic,
571 geochemical, and isotopic evidence further imply the Oribi Suite granitoids represent a
572 series of intrusive events sourced from similar parent material (Thomas, 1988; Thomas et
573 al., 1991; Thomas et al., 1993; Thomas et al., 1996; Grantham et al., 2001; the
574 geochemistry from Eglington et al., 2003; Voordouw, 2010). Additionally, bulk-rock Nd,
575 and Hf analysis presented in this study (Fig. 10) give further support to the contention
576 that the Oribi Gorge Suite is dominantly composed of material reworked from the
577 Margate and Mzumbe terranes.
578 The high-temperature granulite-facies metamorphism and intrusion of the Oribi Gorge
579 Suite at ca. 1040 Ma were associated with synchronous transcurrent deformation in the
580 Natal Province (Thomas, 1988; Jacobs et al., 1993). This major (broadly D_2) deformation
581 event produced a series of wide, crustal-scale sinistral transcurrent faults (see Fig. 2).
582 These did not produce a totally pervasive penetrative fabric throughout the terranes
583 (Thomas, 1988; Voordouw, 2010), rather, the strain was partitioned into "steep belts"
584 (Thomas, 1989), up to several kilometres wide, of pervasive shear fabrics (S_2 in a broad
585 sense), separated by zones dominated by the older (S_1), collision-related ductile fabrics.
586 These steep shear zones are also manifest as major aeromagnetic anomalies known as the
587 Beattie set of anomalies (Du Plessis and Thomas, 1991; Scheiber-Enslin et al., 2014).
588 The clockwise P-T path followed by isobaric cooling which characterizes metamorphism
589 in the Mzumbe and Margate Terranes (Grantham et al., 1994; Mendonidis and Grantham,
590 2003) pose very interesting questions as to the tectonic mechanisms(s) responsible for
591 this polyphase metamorphic history. It has been suggested that the post-peak
592 metamorphism P-T path can be explained by the extensional collapse of the orogenic belt

(Thomas et al., 1992; Grantham et al., 1993; Grantham et al., 2012). We find this explanation untenable with an isobaric cooling path, as extensional collapse is associated in orogens worldwide with near isothermal decompression (Malavielle et al., 1990; Chauvet et al., 1992; Jacobs et al., 2003; Whitney et al., 2004). Rather, we propose that isobaric cooling could have been caused by advective cooling during transcurrent deformation, i.e. during convergence (orthogonal or oblique) the tectonic package is taken to peak pressure at which time the deformation vector shifts from convergence to transcurrent. The tectonic package remains at peak pressure during this transcurrent deformation while it cools advectively (Bohlen, 1987; Wakabayashi, 2004). Further work is need to constrain the timing of metamorphism in relation to sinistral deformation and intrusion of the Oribi Gorge plutons.

Conclusions

- New U-Pb zircon, monazite and titanite data provide important temporal constraints on the geological history of the NMP. These data provide some new controls, re-affirm many of the previous geochronological studies in the region and clarify the interpretation of previously conflicting data.
- A sample of the Mzumbe Granitoid Suite, dated in this study, is ca. 30 Ma younger than in a previous study, suggesting that this polyphase assemblage was emplaced over a protracted period of magmatism from 1207 ± 10 to 1175 ± 19 Ma and thus extending the duration of arc magmatism in the Mzumbe arc. Nd and Hf isotopes confirm that the Mzumbe Granitoid Suite formed in an island arc setting.

615 • Younger, but overlapping island arc magmatism in the Margate Granite ranged
616 between ~1181 Ma (Sikombe Granite) and ~1135 Ma (Margate Granite).
617 • Accretion of Tugela, Mzumbe, and Margate island arc complexes onto the
618 Kaapvaal Craton occurred in two stages at ~1150 Ma and ~1090 Ma. The former
619 involved the accretion of the Tugela and Mzumbe Terranes with the Kaapvaal
620 Craton, and the latter represents the accretion of the Margate Terrane. During the
621 Margate accretion, syn-tectonic intrusions such as the Margate Granite and
622 Glenmore Granite intruded the Margate Terrane, and juxtaposition of the Margate
623 and Mzumbe Terranes occurred along the Melville Thrust with the intrusion of
624 the associated Turtle Bay Suite.
625 • Arc accretion was followed by a phase of mafic and alkaline intermediate
626 magmatism represented by the Equeefa and Sezela Suites that are dated at ~1085
627 Ma. This magmatism possibly took place during a period of crustal thinning,
628 delamination and extensional collapse.
629 • Extensive transcurrent deformation took place at ca. 1050 to 1030 Ma, manifested
630 by low-pressure (~5-7 kbar), (ultra)high-temperature (~900-1100 ºC) granulite-
631 facies metamorphism, that was coeval with intrusion of the Oribi Gorge Suite.
632 The metamorphic event is constrained by titanite, monazite, and zircon ages at
633 1042 Ma, and the Oribi Gorge Suite intruded within uncertainty at 1032 ± 5 Ma.
634 Transcurrent deformation resulted in an isobaric cooling path interpreted to have
635 occurred during advective cooling.
636 • Nd and Hf isotopes show that the magmatic rocks produced in the NMP had a
637 single source extracted from the mantle during island arc magmatism associated

638 with the Mzumbe arc. Subsequent magmatic rocks simply reworked this island
639 arc material, with minimal contamination from significantly older crust and no
640 significant addition of mantle-derived material.

641 Acknowledgements

642 We would like to acknowledge Bruce Eglington for providing data from the DataView
643 Geochronology Database. Dan Condon, Carlyn Stewart, and Nicola Atkinson provided
644 analytical assistance at NIGL. Logistics in South Africa were facilitated with the help of
645 Greg Botha and Bevan Turner. Natural Environment Research Council (NERC grant
646 NE/J021822/1) provided financial support for this study. The NERC Isotope Geosciences
647 Facilities Steering Committee (IP-1366-0513) provided additional analytical support.
648 Helpful reviews from Bruce Eglington and Bernard Bingen resulted in considerable
649 improvements of the paper and are gratefully acknowledged.

650 Figure Captions

651 1: Simplified geological map of southern Africa outlining the regional extent to the
652 Namaqua-Natal belt, modified after Schlüter (2006).

653 2: a) Simplified geological map of the NMP showing the areal extent and relative
654 positions of the Margate, Mzumbe, and Tugela Terranes along with the Kaapvaal Craton
655 and the Oribi Gorge Suite; b) inset of the southern NMP with sample localities.
656 Geological maps fashioned after Thomas (1988).

657 3: CL images of representative zircons from samples analyzed in this study. Smaller
658 circles represent 25 μm U-Pb analytical locations and larger circles represent 36 μm Hf
659 analytical locations. $^{207}Pb/^{206}Pb$, $^{206}Pb/^{238}U$, and epsilon Hf uncertainties are 2 sigma
660 (analytical uncertainty and excess variance using a quadratic sum). On grains with

multiple U-Pb analytical spots, grouped analyses are either concordant (grains CS13-16.20, CS13-20.15, CS13-26.8) or have an upper concordia intercept age indicated.

4: Summary plot of U-Pb ages. Grey bars are $^{207}Pb/^{206}Pb$ ages of individual zircon grains (with exception of CS13-28 which are $^{206}Pb/^{238}U$). The colored bars across the zircon analyses in each sample are weighted averages of the analyses. Weighted 2 sigma uncertainties of colored bars include analytical uncertainties and excess variance only. Black outlined boxes are 2 sigma analytical uncertainties upon which systematic uncertainties of long-term variance (1.5%) and decay constant uncertainties (Schoene et al., 2006) are propogated. Intrusive relationships are based upon field observations described by Evans et al. (1991), Mendonidis et al. (1991), Thomas et al. (1991), and Thomas (1991a,b,c,d). Location of the Melville Thrust spanning the Turtle Bay Suite and boundaries of the Mzumbe and Margate Terranes is described by Thomas (1991d).

5: Summary plots of CA-ID-TIMS U-Pb zircon data. Figures and calculations were done using UPb_Redux (Bowring et al., 2011). Uncertainties are presented at the 2σ level in the form x/y/z, whereby: x=analytical uncertainty only; y=analytical and tracer calibration uncertainties (for comparison with LA-ICP-MS data); and z=total uncertainty.

6: Comparison between the least discordant (< 2%) subset of LA-ICP-MS analyses and the CA-ID-TIMS analyses.

7: Tera-Wasserburg inverse concordia plot of titanite analyses from the Sezela Syenite Suite (sample CS13-12).

8: Wetherill concordia plot of monazite analyses from the Turtle Bay Suite (sample CS13-28). $^{207}Pb/^{206}Pb$ ages of individual analyses are displayed in the inset. Backscatter,

683 Th and Y X-ray maps display minimal zonation. Spot analyses of monazite are 25 μm in
684 diameter.
685 9: $\varepsilon Hf_{(t)}$ analyses for each of the samples in this study. $\varepsilon Hf_{(t)}$ is calculated using the age
686 listed in Table 2. Weighted average uncertainties are 2 sigma.
687 10: $\varepsilon Hf_{(t)}$ (whole rock and zircon) and $\varepsilon Nd_{(t)}$ (whole rock) of samples in this study. Grey
688 field corresponds to Hf and Nd isotopic evolution trends with respective Lu/Hf and
689 Sm/Nd ratios of 0.012 and 0.14 (the average ratios of sample in this study). New crust in
690 εHf space from Dhuime et al. (2011).
691 11: Summary age plot of the Oribi Gorge Granitoid Suite including samples from
692 Eglington et al. (2003, in *italics*) and this study. The weighted average age of the Oribi
693 Gorge Granitoid Suite is calculated using samples CS13-10, -19, -27 (this study) and
694 UND199, UND215, and the rim ages from sample B1 (Eglington et al., 2003). This
695 results in a statically robust age of 1032 ± 5 Ma. The multi-grain zircon evaporation age
696 of the Mgeni pluton (Eglington et al., 1989) is not used in the average calculation but
697 supports the 1032 ± 5 Ma date. The other zircons from Oribi Gorge Suite plutons that are
698 not included in this calculation are assumed to be inherited from the basement rocks
699 within the Mzumbe and Margate Terrane respectively. Ages of the basement rocks are
700 shown in Fig. 12.
701 12: Compilation of magmatic, sedimentary, and metamorphic data associated with the
702 three terranes of the NMP. These data indicate that Tugela Ocean closure, ophiolite
703 obduction and arc accretion took place at ~1140 Ma. This was followed by continued arc
704 magmatism in the Margate Terrane until its accretion ~1090 Ma. This second accretion
705 event was also associated with the formation of the Melville Thrust, intrusion of the

706 Turtle Bay Suite and juxtaposition of the Mzumbe and Margate Terranes. It was
707 followed by ~1080 Ma alkaline and mafic magmatism potentially linked to mafic
708 underplating and/or extensional collapse. At ~1030 Ma, transcurrent deformation and
709 syntectonic magmatism is recorded by low-P, high-T granulite facies metamorphism and
710 the intrusion of the Oribi Gorge Suite.
711 S1 (online): Compiled U-Pb-Hf analyses of zircon (U-Pb-Hf), titanite (U-Pb), and
712 monazite (U-Pb) reference materials.
713 S2: Concordia Diagrams of the samples analyzed in this study. Analyses with resolvable
714 common lead are excluded. Least discordant (< 2%) data used in age calculation is shown
715 in blue. Excluded discordant data (< 2%) are shown in red. Analyses that are interpreted
716 to be inherited are shown in green.
717 Tables Captions
718 1: Table of sample name, locality, lithology, and dominant mineral assemblage for the
719 samples in discussed in this study.
720 2: Zircon U-Pb weighted average ages for samples within the Mzumbe and Margate
721 Teranes. Acceptable MSWD criteria adopted after Wendt and Carl (1999).
722 3: Whole rock Nd and Hf isotope data. Age of sample CS13-29 is approximate base upon
723 cross cutting relations.
724 S1: LA-ICP-MS U-Pb data of zircon
725 S2: LA-ICP-MS U-Pb data of titanite
726 S3: LA-ICP-MS U-Pb data of monazite
727 S4: LA-ICP-MS Hf data of zircon
728 S5: CA-ID-TIMS data of zircon

729 Other Supplementary Materials

730 KMZ of sample locations.

731 Supplementary text 1: Analytical methods

732 References

733 Arima, M., Johnston, S., 2001. Crustal evolution of the Tugela Terrane, Natal Belt, South Africa.
734 Gondwana Res. 563–564.
735 Barkhuizen, J.G., Matthews, P., 1990. Gravity modelling of the Natal Thrust Front: A Mid-Proterozoic
736 crustal suture in southeastern Africa. Geol. Soc. South Africa Geocongress'90 Johannesburg. Ext.
737 Abstr. Vol. 32.35.
738 Bickford, M., 2000. Geology and geochronology of Grenville-age rocks in the Van Horn and Franklin
739 Mountains area, west Texas: Implications for the tectonic evolution of Laurentia during the Grenville.
740 Geol. Soc. Am. Bull. 112, 1134–1148. doi:10.1130/0016-7606(2000)112<1134
741 Bisnath, A., McCourt, S., Frimmel, H., Buthelezi, S.B.N., 2009. The metamorphic evolution of mafic rocks
742 in the Tugela Terrane, Natal Belt, South Africa. South African J. Geol. 111, 369–386.
743 doi:10.2113/gssajg.111.4.369
744 Bohlen, S., 1987. Pressure-Temperature-Time Paths and a Tectonic Model for the Evolution of Granulites.
745 J. Geol. 95, 617–632.
746 Bowring, J.F., McLean, N.M., Bowring, S.A., 2011. Engineering cyber infrastructure for U-Pb
747 geochronology: Tripoli and U-Pb_Redux. Geochemistry, Geophys. Geosystems 12, n/a–n/a.
748 doi:10.1029/2010GC003479
749
750 Chauvet, A., Dallmeyer, R., 1992. 40Ar/39Ar mineral dates related to Devonian extension in the
751 southwestern Scandinavian Caledonides. Tectonophysics 210, 155–177. doi:10.1016/0040-
752 1951(92)90133-Q
753 Cornell, D.H., Thomas, R.J., 2006. Age and tectonic significance of the Banana Beach Gneiss , KwaZulu-
754 Natal South Coast , South Africa. South African J. Geol. 109, 335–340.
755 Dalziel, I., Mosher, S., Gahagan, L., 2000. Laurentia – Kalahari Collision and the Assembly of Rodinia. J.
756 Geol. 108, 499–513.
757 Dhuime, B., Hawkesworth, C., Cawood, P., 2011. When continents formed. Science 331, 154–5.
758 doi:10.1126/science.1201245
759 Eglington, B., Thomas, R., Armstrong, R., Walraven, F., 2003a. Zircon geochronology of the Oribi Gorge
760 Suite, KwaZulu-Natal, South Africa: constraints on the timing of trans-current shearing in the
761 Namaqua–Natal Belt. Precambrian Res. 123, 29–46. doi:10.1016/S0301-9268(03)00016-0
762 Eglington, B., Thomas, R., Armstrong, R., Walraven, F., 2003b. Zircon geochronology of the Oribi Gorge
763 Suite, KwaZulu-Natal, South Africa: constraints on the timing of trans-current shearing in the
764 Namaqua–Natal Belt. Precambrian Res. 123, 29–46. doi:10.1016/S0301-9268(03)00016-0
765 Eglington, B.M., 1987. Field, Geochemical and Isotope Studies of Selected Areas of Proterozoic Crust in
766 South-central Natal. University of Natal.
767 Eglington, B.M., 2006. Evolution of the Namaqua-Natal Belt, southern Africa – A geochronological and
768 isotope geochemical review. J. African Earth Sci. 46, 93–111. doi:10.1016/j.jafrearsci.2006.01.014
769 Eglington, B.M., Harmer, R.E., Kerr, A., 1986. Petrographic, Rb-Sr isotope and geochemical
770 characteristics of intrusive granitoids from the Port Edward-Port Shepstone area, Natal.
771 Eglington, B.M., Harmer, R.E., Kerr, A., 1989. Rb-Sr isotopic constraints on the ages of the Mgeni and
772 Nqwadolo Granites, Valley of a Thousand Hills, Natal.
773 Eglington, B.M., Kerr, A., 1989. Rb-Sr and Pb-Pb geochronology of Proterozoic intrusions from the
774 Scottburgh area of southern Natal.
775 Eglington, B.M., Thomas, R.J., Armstrong, R. a., 2010. U-Pb Shrimp Zircon Dating of Mesoproterozoic
776 Magmatic Rocks From the Scottburgh Area, Central Mzumbe Terrane, Kwazulu-Natal, South Africa.
777 South African J. Geol. 113, 229–235. doi:10.2113/gssajg.113.2.229
778 Evans, D. a. D., 2009. The palaeomagnetically viable, long-lived and all-inclusive Rodinia supercontinent
779 reconstruction. Geol. Soc. London, Spec. Publ. 327, 371–404. doi:10.1144/SP327.16

780 Evans, D. a. D., 2013. Reconstructing pre-Pangean supercontinents. Geol. Soc. Am. Bull. 125, 1735–1751.
781 doi:10.1130/B30950.1
782 Evans, M.J., Eglington, B.M., Kerr, A., Saggerson, E.P., 1987. The geology of the Proterozoic rocks
783 around Umzinto, southern Natal, South Africa. South African J. Geol. 90, 471–488.
784 Evans, M.J., Thomas, R.J., Eglington, B.M., 1991. Mzimlilo Granite, in: Johnson, M.R. (Ed.), Catalogue of
785 South African Lithostratigraphic Units 3. South African Committee for Stratigraphy, Council For
786 Geoscience, South Africa, pp. 29–30.
787 Gose, W. a., Johnston, S.T., Thomas, R.J., 2004. Age of magnetization of Mesoproterozoic rocks from the
788 Natal sector of the Namaqua-Natal belt, South Africa. J. African Earth Sci. 40, 137–145.
789 doi:10.1016/j.jafrearsci.2004.11.003
790 Grantham, G., Thomas, R., Mendonidis, P., 1994. Contrasting PTt loops from southern East Africa, Natal
791 and East Antarctica. J. African Earth … 19, 225–235.
792 Grantham, G.H., 1984. The tectonic, metamorphic and intrusive history of the Natal mobile belt between
793 Glenmore and Port Edward, Natal. University of Natal (Pietermaritzburg).
794 Grantham, G.H., Eglington, B.M., Thomas, R.J., Mendonidis, P., 2001. The nature of the Grenville-age
795 charnockitic A-type magmatism from the Natal, Namaqua and Maud Belts of southern Africa and
796 western Dronning Maud Land, Antarctica. Mem. Natl. Inst. Polar Res. Spec. issue 55, 59–86.
797 Grantham, G.H., Mendonidis, P., Thomas, R.J., Satish-Kumar, M., 2012. Multiple origins of charnockite in
798 the Mesoproterozoic Natal belt, Kwazulu-Natal, South Africa. Geosci. Front. 3, 755–771.
799 doi:10.1016/j.gsf.2012.05.006
800 Grantham, G.H., Storey, B.C., Thomas, R.J., Jacobs, J., n.d. The pre-break-up position of Haag Nunataks
801 within Gondwana: possible correlatives in Natal and Dronning Maud Land, in: Ricci, C.A. (Ed.), The
802 Antarctica Region, Geological Evolution and Processes. pp. 13–20.
803 Grantham, G.H., Thomas, R.J., Eglington, B.M., de Bruin, D., Atanasov, A., Evans, M.J., 1993. Corona
804 textures in Proterozoic olivine melanorites of the Equeefa Suite, Natal Metamorphic Province, South
805 Africa. Mineral. Petrol. 49, 91–102. doi:10.1007/BF01162928
806 Grantham, G.H., Thomas, R.J., Mendonidis, P., 1991. Leisure Bay Formation, in: Johnson, M.R. (Ed.),
807 Catalogue of South African Lithostratigraphic Units 3. South African Committee for Stratigraphy,
808 Council For Geoscience, South Africa, pp. 17–18.
809 Grimes, S.W., Copeland, P., 2004. Thermochronology of the Grenville Orogeny in west Texas,
810 Precambrian Research. doi:10.1016/j.precamres.2003.12.004
811 Hoffman, P.F., 1991. Did the breakout of laurentia turn gondwanaland inside-out? Science 252, 1409–12.
812 doi:10.1126/science.252.5011.1409
813 Huw Davies, J., von Blanckenburg, F., 1995. Slab breakoff: A model of lithosphere detachment and its test
814 in the magmatism and deformation of collisional orogens. Earth Planet. Sci. Lett. 129, 85–102.
815 doi:10.1016/0012-821X(94)00237-S
816 Jacobs, J., Bauer, W., Fanning, C.M., 2003. New age constraints for Grenville-age metamorphism in
817 western central Dronning Maud Land (East Antarctica), and implications for the palaeogeography of
818 Kalahari in Rodinia. Int. J. Earth Sci. 92, 301–315. doi:10.1007/s00531-003-0335-x
819 Jacobs, J., Pisarevsky, S., Thomas, R.J., Becker, T., 2008. The Kalahari Craton during the assembly and
820 dispersal of Rodinia. Precambrian Res. 160, 142–158. doi:10.1016/j.precamres.2007.04.022
821 Jacobs, J., Thomas, R., 1994. Oblique collision at about 1.1 Ga along the southern margin of the Kaapvaal
822 continent, south-east Africa. Geol. Rundschau 322–333.
823 Jacobs, J., Thomas, R.J., Armstrong, R.A., Henjes-Kunst, F., 1999. Age and thermal evolution of the
824 Mesoproterozoic Cape Meredith Complex, West Falkland. J. Geol. Soc. London. 156, 917–928.
825 doi:10.1144/gsjgs.156.5.0917
826 Jacobs, J., Thomas, R.J., Weber, K., 1993. Accretion and indentation tectonics at the southern edge of the
827 Kaapvaal craton during the Kibaran (Grenville) orogeny. Geology 21, 203. doi:10.1130/0091-
828 7613(1993)021<0203:AAITAT>2.3.CO;2
829 Jacobson, C.E., Grove, M., Pedrick, J.N., Barth, a. P., Marsaglia, K.M., Gehrels, G.E., Nourse, J. a., 2010.
830 Late Cretaceous-early Cenozoic tectonic evolution of the southern California margin inferred from
831 provenance of trench and forearc sediments. Geol. Soc. Am. Bull. 123, 485–506.
832 doi:10.1130/B30238.1
833 Johnston, S., Armstrong, R., Heaman, L., 2001. Preliminary U-Pb geochronology of the Tugela terrane,
834 Natal belt, eastern South Africa. Mem. Natl. ….

Kerkhof, A. van den, Grantham, G., 1999. Metamorphic charnockite in contact aureoles around intrusive enderbite from Natal, South Africa. Contrib. to Mineral. ….

Kerr, A., Finlay, C.A., 1981. A comparison between the Mvoti Granite and the Nqwadolo Granite. Petros 10, 71–83.

Kusiak, M.A., Whitehouse, M.J., Wilde, S.A., Nemchin, A. a., Clark, C., 2013. Mobilization of radiogenic Pb in zircon revealed by ion imaging: Implications for early Earth geochronology. Geology 41, 291–294. doi:10.1130/G33920.1

Lange, U., Brocker, M., Armstrong, R., Trapp, E., Mezger, K., 2005. Sm-Nd and U-Pb dating of high-pressure granulites from the Zlote and Rychleby Mts (Bohemian Massif, Poland and Czech Republic). J. Metamorph. Geol. 23, 133–145. doi:10.1111/j.1525-1314.2005.00566.x

Leloup, P.H., Boutonnet, E., Davis, W.J., Hattori, K., 2011. Long-lasting intracontinental strike-slip faulting: new evidence from the Karakorum shear zone in the Himalayas. Terra Nov. no–no. doi:10.1111/j.1365-3121.2011.00988.x

Li, Z.X., Bogdanova, S.V., Collins, A.S., Davidson, A., De Waele, B., Ernst, R.E., Fitzsimons, I.C.W., Fuck, R. a., Gladkochub, D.P., Jacobs, J., Karlstrom, K.E., Lu, S., Natapov, L.M., Pease, V., Pisarevsky, S. a., Thrane, K., Vernikovsky, V., 2008. Assembly, configuration, and break-up history of Rodinia: A synthesis. Precambrian Res. 160, 179–210. doi:10.1016/j.precamres.2007.04.021

Loewy, S.L., Dalziel, I.W.D., Pisarevsky, S., Connelly, J.N., Tait, J., Hanson, R.E., Bullen, D., 2011. Coats Land crustal block, East Antarctica: A tectonic tracer for Laurentia? Geology 39, 859–862. doi:10.1130/G32029.1

Malavieille, J., Guihot, P., Costa, S., Lardeaux, J.M., Gardien, V., 1990. Collapse of the thickened Variscan crust in the French Massif Central: Mont Pilat extensional shear zone and St. Etienne Late Carboniferous basin. Tectonophysics 177, 139–149. doi:10.1016/0040-1951(90)90278-G

Matthews, P.E., 1972. Possible Precambrian Obduction and Plate Tectonics in Southeastern Africa. Nature 240, 37–39. doi:10.1038/10.1038/physci240037a0

Mattinson, J.M., 2005. Zircon U–Pb chemical abrasion ("CA-TIMS") method: Combined annealing and multi-step partial dissolution analysis for improved precision and accuracy of zircon ages. Chem. Geol. 220, 47–66. doi:10.1016/j.chemgeo.2005.03.011

McCourt, S., Armstrong, R. a., Grantham, G.H., Thomas, R.J., 2006. Geology and evolution of the Natal belt, South Africa. J. African Earth Sci. 46, 71–92. doi:10.1016/j.jafrearsci.2006.01.013

Mendonidis, P., 1989. The Tectonic Evolution of a Portion of the Southern Granulite Zone of the Natal Mobile Belt, Between Southbroom and Glenmore, Natal. University of Natal, Pietermaritzburg.

Mendonidis, P., Armstrong, R., 2002. Metamorphic history and U-Pb Zircon (SHRIMP) geochronology of the Glenmore Granite: Implications for the tectonic evolution of the Natal Metamorphic Province. South African J. … 105, 325–336.

Mendonidis, P., Armstrong, R.A., 2009. A New U-Pb Zircon Age For The Portobello Granite From The Southern Part Of The Natal Metamorphic Belt. South African J. Geol. 112, 197–208. doi:10.2113/gssajg.112.2.197

Mendonidis, P., Grantham, G., 2003. Petrology, Origin, and Metamorphic History of Proterozoic-aged Granulites of the Natal Metamorphic Province, Southeastern Africa. Gondwana Res. 607–628.

Mendonidis, P., Grantham, G.H., Thomas, R.J., 1991. Glenmore Granite, in: Johnson, M.R. (Ed.), South African Catalogue of Lithostratigraphic Units 3. South African Committee for Stratigraphy, Council For Geoscience, South Africa, pp. 13–14.

Millar, I.L., Pankhurst, R.J., 1987. Gondwana Six: Structure, Tectonics, and Geophysics, Geophysical Monograph Series, Geophysical Monograph Series. American Geophysical Union, Washington, D. C. doi:10.1029/GM040

Mosher, S., Levine, J.S.F., Carlson, W.D., 2008. Mesoproterozoic plate tectonics: A collisional model for the Grenville-aged orogenic belt in the Llano uplift, central Texas. Geology 36, 55. doi:10.1130/G24049A.1

Pisarevsky, S. a., Wingate, M.T.D., Powell, C.M., Johnson, S., Evans, D. a. D., 2003. Models of Rodinia assembly and fragmentation. Geol. Soc. London, Spec. Publ. 206, 35–55. doi:10.1144/GSL.SP.2003.206.01.04

Scheiber-Enslin, S., Ebbing, J., Webb, S.J., 2014. An integrated geophysical study of the Beattie Magnetic Anomaly, South Africa. Tectonophysics. doi:10.1016/j.tecto.2014.08.021

890 Schlüter, T., 2006. Geological Atlas of Africa: With Notes on Stratigraphy, Tectonics, Economic Geology,
891 Geohazards and Geosites of Each Country. Springer.
892 Siebel, W., Shang, C.K., Thern, E., Danišík, M., Rohrmüller, J., 2012. Zircon response to high-grade
893 metamorphism as revealed by U–Pb and cathodoluminescence studies. Int. J. Earth Sci. 101, 2105–
894 2123. doi:10.1007/s00531-012-0772-5
895 Smith, D.R., Barnes, C., Shannon, W., Roback, R., James, E., 1997. Petrogenesis of Mid-Proterozoic
896 granitic magmas: examples from central and west Texas. Precambrian Res. 85, 53–79.
897 doi:10.1016/S0301-9268(97)00032-6
898 Spencer, C., Roberts, N., 2014. Intermontane basins and bimodal volcanism at the onset of the
899 Sveconorwegian Orogeny, southern Norway. Precambrian … 252, 107–118.
900 Talbot, C.J., Grantham, G.H., 1987. The Proterozoic intrusion and deformation of deep crustal "sills" along
901 the south coast of Natal. South African J. Geol. 90, 520–538.
902 Tapponnier, P., Molnar, P., 1976. Slip-line field theory and large-scale continental tectonics. Nature 264,
903 319–324. doi:10.1038/264319a0
904 Tapponnier, P., Peltzer, G., Le Dain, A.Y., Armijo, R., Cobbold, P., 1982. Propagating extrusion tectonics
905 in Asia: New insights from simple experiments with plasticine. Geology 10, 611–616.
906 doi:10.1130/0091-7613(1982)10
907 Thomas, R., Ashwal, L., Andreoli, M., 1992. The petrology of the Turtle Bay Suite: a mafic-felsic granulite
908 association from southern Natal, South Africa.,African Earth Sci. 15, 187–206.
909 Thomas, R.J., 1988. The geology of the Port Shepstone area. Explanation of sheet 3030 Port Shepstone.
910 Thomas, R.J., 1989. A tale of two tectonic terranes. South African J. Geol. 92, 306–321.
911 Thomas, R.J., 1989. The petrogenesis of the Mzumbe Gneiss Suite, a tonalite-trondhjemite orthogneiss
912 suite from the southern part of the Natal Structural and Metamorphic Province.
913 Thomas, R.J., 1990. Mzumbe Gneiss Suite, in: Johnson, M.R. (Ed.), Catalogue of South African
914 Lithostratigraphic Units 2. South African Committee for Stratigraphy, Council For Geoscience, South
915 Africa, pp. 35–36.
916 Thomas, R.J., 1991a. Mkomazi Gneiss, in: Johnson, M.R. (Ed.), Catalogue of South African
917 Lithostratigraphic Units 3. South African Committee for Stratigraphy, Council For Geoscience, South
918 Africa, pp. 27–28.
919 Thomas, R.J., 1991b. Oribi Gorge Granitoid Suite, in: Johnson, M.R. (Ed.), Catalogue of South African
920 Lithostratigraphic Units 3. South African Committee for Stratigraphy, Council For Geoscience, South
921 Africa, pp. 37–40.
922 Thomas, R.J., 1991c. Banana Beach Gneiss, in: Johnson, M.R. (Ed.), Catalogue of South African
923 Lithostratigraphic Units 3. South African Committee for Stratigraphy, Council For Geoscience, South
924 Africa, pp. 1–2.
925 Thomas, R.J., 1991d. Turtle Bay Suite, in: Johnson, M.R. (Ed.), Catalogue of South African
926 Lithostratigraphic Units 3. South African Committee for Stratigraphy, Council For Geoscience, South
927 Africa, pp. 47–48.
928 Thomas, R.J., 1992. Mbizana Microgranite, in: Johnson, M.R. (Ed.), South African Catalogue of
929 Lithostratigraphic Units 4. South African Committee for Stratigraphy, Council For Geoscience, South
930 Africa, pp. 15–16.
931 Thomas, R.J., 2003. Geochronology of the Sikombe Granite, Transkei, Natal Metamorphic Province, South
932 Africa. South African J. Geol. 106, 403–408. doi:10.2113/106.4.403
933 Thomas, R.J., Agenbacht, A.L.D., Cornell, D.H., Moore, J.M., 1994. The Kibaran of southern Africa:
934 Tectonic evolution and metallogeny. Ore Geol. Rev. 9, 131–160. doi:10.1016/0169-1368(94)90025-6
935 Thomas, R.J., Cornell, D.H., Armstrong, R.A., 1999. Provenance age and metamorphic history of the Quha
936 Formation, Natal metamorphic province; a U-Th-Pb zircon SHRIMP study. South African J. Geol.
937 102, 83–92.
938 Thomas, R.J., Eglington, B.M., 1990. A Rb-Sr, Sm-Nd and U-Pb zircon isotopic study of the Mzumbe
939 Suite, the oldest intrusive granitoid in southern Natal, South Africa. South African J. Geol. 93, 761–
940 765.
941 Thomas, R.J., Eglington, B.M., Bowring, S.A., 1993a. Dating the cessation of Kibaran magmatism in
942 Natal, South Africa. J. African Earth Sci. (and Middle East) 16, 247–252. doi:10.1016/0899-
943 5362(93)90046-S

944 Thomas, R.J., Eglington, B.M., Bowring, S.A., Retief, E.A., Walraven, F., 1993b. New isotope data from a
945 neoproterozoic porphyritic garnitoid-charnockite suite from Natal, South Africa. Precambrian Res.
946 62, 83–101. doi:10.1016/0301-9268(93)90095-J
947 Thomas, R.J., Eglington, B.M., Kerr, A., 1990. The geology and geochronology of the Belmont pluton and
948 microgranite dykes from the Margate area.
949 Thomas, R.J., Jacobs, J., Weber, K., 1997. Geology of the Mesoproterozoic Cape Meredith Complex, West
950 Falkland, in: Ricci, C.A. (Ed.), The Antarctica Region, Geological Evolution and Processes. Siena
951 Terra Antarctica Publications, pp. 21–30.
952 Thomas, R.J., Mendonidis, P., Grantham, G.H., 1991. Margate Granite Suite, in: Johnson, M.R. (Ed.),
953 Catalogue of South African Lithostratigraphic Units 3. South African Committee for Stratigraphy,
954 Council For Geoscience, South Africa, pp. 33–36.
955 Tohver, E., D'Agrella-Filho, M.S., Trindade, R.I.F., 2006a. Paleomagnetic record of Africa and South
956 America for the 1200–500Ma interval, and evaluation of Rodinia and Gondwana assemblies.
957 Precambrian Res. 147, 193–222. doi:10.1016/j.precamres.2006.01.015
958 Tohver, E., Pluijm, B.A. Van Der, Scandola, J.E., Essene, E.J., 2005. Late Mesoproterozoic Deformation of
959 SW Amazonia (Rondonia , Brazil): Geochronological and Structural Evidence for Collision with
960 Southern Laurentia. J. Geol. 113, 309–323.
961 Tohver, E., Teixeira, W., van der Pluijm, B., Geraldes, M.C., Bettencourt, J.S., Rizzotto, G., 2006b.
962 Restored transect across the exhumed Grenville orogen of Laurentia and Amazonia, with implications
963 for crustal architecture. Geology 34, 669. doi:10.1130/G22534.1
964 Valley, J.W., Cavosie, A.J., Ushikubo, T., Reinhard, D.A., Lawrence, D.F., Larson, D.J., Clifton, P.H.,
965 Kelly, T.F., Wilde, S.A., Moser, D.E., Spicuzza, M.J., 2014. Hadean age for a post-magma-ocean
966 zircon confirmed by atom-probe tomography. Nat. Geosci. 7, 219–223. doi:10.1038/ngeo2075
967 Valli, F., Arnaud, N., Leloup, P.H., Sobel, E.R., Mahéo, G., Lacassin, R., Guillot, S., Li, H., Tapponnier,
968 P., Xu, Z., 2007. Twenty million years of continuous deformation along the Karakorum fault, western
969 Tibet: A thermochronological analysis. Tectonics 26, n/a–n/a. doi:10.1029/2005TC001913
970 Vander Auwera, J., Bolle, O., Bingen, B., Liégeois, J.-P., Bogaerts, M., Duchesne, J.C., De Waele, B.,
971 Longhi, J., 2011. Sveconorwegian massif-type anorthosites and related granitoids result from post-
972 collisional melting of a continental arc root. Earth-Science Rev. 107, 375–397.
973 doi:10.1016/j.earscirev.2011.04.005
974 Voordouw, R.J., 2010. a D3 Shear Zone in the Margate Terrane and Its Implications for Regional
975 Deformation in the Natal Metamorphic Province (South Africa). South African J. Geol. 113, 183–
976 194. doi:10.2113/gssajg.113.2.183
977 Voordouw, R.J., Rajesh, H.M., 2012. Granitoids From the Margate Terrane and Their Implications for
978 Tectono-Magmatic Models of the Natal Metamorphic Province (South Africa). South African J.
979 Geol. 115, 47–64. doi:10.2113/gssajg.115.1.47
980 Wakabayashi, J., 2004. Tectonic mechanisms associated with P–T paths of regional metamorphism:
981 alternatives to single-cycle thrusting and heating. Tectonophysics 392, 193–218.
982 doi:10.1016/j.tecto.2004.04.012
983 Wendt, I., Carl, C., 1991. The statistical distribution of the mean squared weighted deviation. Chem. Geol.
984 Isot. Geosci. Sect. 86, 275–285. doi:10.1016/0168-9622(91)90010-T
985 Whitehouse, M.J., Ravindra Kumar, G.R., Rimša, A., 2014. Behaviour of radiogenic Pb in zircon during
986 ultrahigh-temperature metamorphism: an ion imaging and ion tomography case study from the Kerala
987 Khondalite Belt, southern India. Contrib. to Mineral. Petrol. 168, 1042. doi:10.1007/s00410-014-
988 1042-2
989 Whitney, D.L., Teyssier, C., Fayon, A.K., 2004. Isothermal decompression, partial melting and exhumation
990 of deep continental crust. Geol. Soc. London, Spec. Publ. 227, 313–326.
991 doi:10.1144/GSL.SP.2004.227.01.16

Captions

Click here to view linked References

Figure Captions

1: Simplified geological map of southern Africa outlining the regional extent to the Namaqua-Natal belt, modified after Schlüter (2006).

2: a) Simplified geological map of the NMP showing the areal extent and relative positions of the Margate, Mzumbe, and Tugela Terranes along with the Kaapvaal Craton and the Oribi Gorge Suite; b) inset of the southern NMP with sample localities. Geological maps fashioned after Thomas (1988).

3: CL images of representative zircons from samples analyzed in this study. Smaller circles represent 25 μm U-Pb analytical locations and larger circles represent 36 μm Hf analytical locations. $^{207}Pb/^{206}Pb$, $^{206}Pb/^{238}U$, and epsilon Hf uncertainties are 2 sigma (analytical uncertainty and excess variance using a quadratic sum). On grains with multiple U-Pb analytical spots, grouped analyses are either concordant (grains CS13-16.20, CS13-20.15, CS13-26.8) or have an upper concordia intercept age indicated.

4: Summary plot of U-Pb ages. Grey bars are $^{207}Pb/^{206}Pb$ ages of individual zircon grains (with exception of CS13-28 which are $^{206}Pb/^{238}U$). The colored bars across the zircon analyses in each sample are weighted averages of the analyses. Weighted 2 sigma uncertainties of colored bars include analytical uncertainties and excess variance only. Black outlined boxes are 2 sigma analytical uncertainties upon which systematic uncertainties of long-term variance (1.5%) and decay constant uncertainties (Schoene et al., 2006) are propogated. Intrusive relationships are based upon field observations described by Evans et al. (1991), Mendonidis et al. (1991), Thomas et al. (1991), and Thomas (1991a,b,c,d). Location of the Melville Thrust spanning the Turtle Bay Suite and boundaries of the Mzumbe and Margate Terranes is described by Thomas (1991d).

5: Summary plots of CA-ID-TIMS U-Pb zircon data. Figures and calculations were done using UPb_Redux (Bowring et al., 2011). Uncertainties are presented at the 2σ level in the form x/y/z, whereby: x=analytical uncertainty only; y=analytical and tracer calibration uncertainties (for comparison with LA-ICP-MS data); and z=total uncertainty.

6: Comparison between the least discordant (< 2%) subset of LA-ICP-MS analyses and the CA-ID-TIMS analyses.

7: Tera-Wasserburg inverse concordia plot of titanite analyses from the Sezela Syenite Suite (sample CS13-12).

8: Wetherill concordia plot of monazite analyses from the Turtle Bay Suite (sample CS13-28). $^{207}Pb/^{206}Pb$ ages of individual analyses are displayed in the inset. Backscatter, Th and Y X-ray maps display minimal zonation. Spot analyses of monazite are 25 μm in diameter.

9: $\varepsilon Hf_{(t)}$ analyses for each of the samples in this study. $\varepsilon Hf_{(t)}$ is calculated using the age listed in Table 2. Weighted average uncertainties are 2 sigma.

10: $\varepsilon Hf_{(t)}$ (whole rock and zircon) and $\varepsilon Nd_{(t)}$ (whole rock) of samples in this study. Grey field corresponds to Hf and Nd isotopic evolution trends with respective Lu/Hf and Sm/Nd ratios of 0.012 and 0.14 (the average ratios of sample in this study). New crust in εHf space from Dhuime et al. (2011).

11: Summary age plot of the Oribi Gorge Granitoid Suite including samples from Eglington et al. (2003, in *italics*) and this study. The weighted average age of the Oribi Gorge Granitoid Suite is calculated using samples CS13-10, -19, -27 (this study) and UND199, UND215, and the rim ages from sample B1 (Eglington et al., 2003). This results in a statically robust age of 1032 ± 5 Ma. The multi-grain zircon evaporation age

of the Mgeni pluton (Eglington et al., 1989) is not used in the average calculation but supports the 1032 ± 5 Ma date. The other zircons from Oribi Gorge Suite plutons that are not included in this calculation are assumed to be inherited from the basement rocks within the Mzumbe and Margate Terrane respectively. Ages of the basement rocks are shown in Fig. 12.

12: Compilation of magmatic, sedimentary, and metamorphic data associated with the three terranes of the NMP. These data indicate that Tugela Ocean closure, ophiolite obduction and arc accretion took place at ~1140 Ma. This was followed by continued arc magmatism in the Margate Terrane until its accretion ~1090 Ma. This second accretion event was also associated with the formation of the Melville Thrust, intrusion of the Turtle Bay Suite and juxtaposition of the Mzumbe and Margate Terranes. It was followed by ~1080 Ma alkaline and mafic magmatism potentially linked to mafic underplating and/or extensional collapse. At ~1030 Ma, transcurrent deformation and syntectonic magmatism is recorded by low-P, high-T granulite facies metamorphism and the intrusion of the Oribi Gorge Suite.

S1 (online): Compiled U-Pb-Hf analyses of zircon (U-Pb-Hf), titanite (U-Pb), and monazite (U-Pb) reference materials.

S2: Concordia Diagrams of the samples analyzed in this study. Analyses with resolvable common lead are excluded. Least discordant (< 2%) data used in age calculation is shown in blue. Excluded discordant data (< 2%) are shown in red. Analyses that are interpreted to be inherited are shown in green.

Tables Captions

1: Table of sample name, locality, lithology, and dominant mineral assemblage for the samples in discussed in this study.

2: Zircon U-Pb weighted average ages for samples within the Mzumbe and Margate Teranes. Acceptable MSWD criteria adopted after Wendt and Carl (1999).

3: Whole rock Nd and Hf isotope data. Age of sample CS13-29 is approximate base upon cross cutting relations.

S1: LA-ICP-MS U-Pb data of zircon

S2: LA-ICP-MS U-Pb data of titanite

S3: LA-ICP-MS U-Pb data of monazite

S4: LA-ICP-MS Hf data of zircon

S5: CA-ID-TIMS data of zircon

Other Supplementary Materials

KMZ of sample locations.

Supplementary text 1: Analytical methods

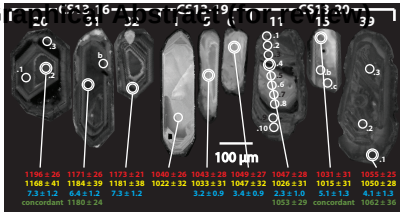

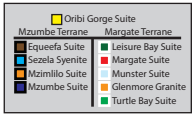

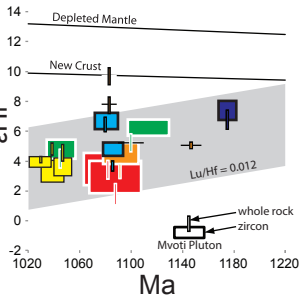

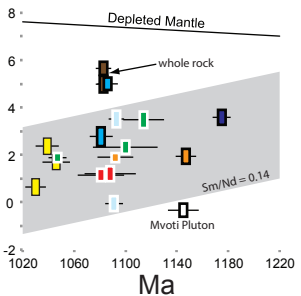

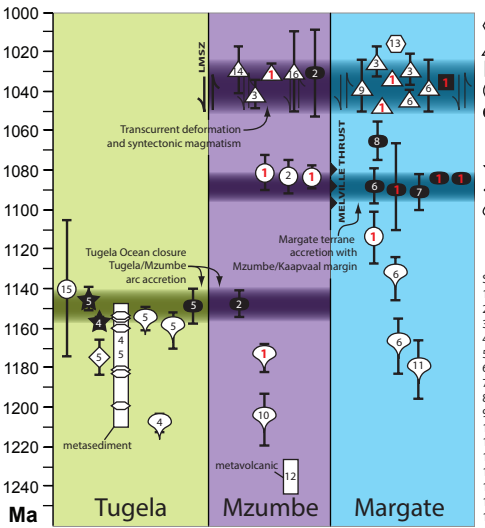

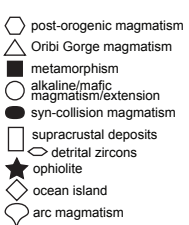

Sources for the data:
1: this study (in **red**)
2: Eglington et al. (2010)
3: Eglington et al. (2003)
4: McCourt (Geocongress 2000)
5: McCourt et al. (2010)
6: Mendonidis and Thomas (2014)
7: Mendonidis et al. (2002)
8: Cornell and Thomas (2006)
9: Thomas (1988)
10: Thomas and Eglington (1990)
11: Thomas et al. (2003)
12: Thomas et al. (1999)
13: Thomas et al. (1993a)
14: Thomas et al. (1993b)
15: Scogings (1991)
16: Eglington et al. (1989)

Crustal growth during islandIsland arc accretion and transcurrent deformationoblique continental collision, Natal Metamorphic Province, South Africa: new isotopic constraints

Christopher J Spencer[1,2*], Robert J Thomas[3], Nick M W Roberts[2], Peter A Cawood[1], Ian Millar[2], Simon Tapster[2]

[1]Department of Earth and Environmental Sciences, University of St Andrews, St Andrews, KY16 9AL, UK

[2]NERC Isotope Geosciences Facilities, British Geological Survey, Keyworth, Nottingham, NG12 5GG, UK

[3] Council for Geoscience, P.O. Box 572, Bellville, 7535, South Africa

*Corresponding author; current address: Department of Applied Geology, Curtin University, Perth WA 6845, Australia; cspencer@curtin.edu.au

*spenchristoph@gmail.com

Keywords: Natal orogeny; accretion; oblique collision, crustal growth; zircon U-Pb-Hf

Abstract

The Natal Metamorphic Province consists of, from north to south, the Tugela, Mzumbe, and Margate terranes. These were accreted to the southeastern margin of the Kaapvaal Craton in the late Mesoproterozoic, and followed by intrusion of a large suite of A-type granitoid bodies.collision of the craton with another continental block. New U-Pb data from zircon, titanite, and monazite further constrains the temporal framework ofwith these geological events.

Formatted: Space After: 0 pt

Formatted: Space After: 0 pt

Formatted: Space After: 0 pt

The Tugela and Mzumbe terranes record protracted magmatism in an island arc complex from ~1200 Ma to 1160 Ma, followed by the accretion of these terranes onto the southern margin of the Kaapvaal Craton at ~1150 Ma. Arc magmatism in the Margate Terrane continued until ~1120 Ma and was followed by extension and bimodal volcanism immediately prior to accretion to the Kaapvaal/Mzumbe continental margin at ~1090 Ma. This accretion was accompanied by high-pressure and high-temperature metamorphism, juxtaposition of the Mzumbe and Margate terranes along the Melville Thrust, and the formation of a number of syntectonic intrusive units derived from melting of the pre-existing arc crust. After accretion, extensional collapse is evidenced by the intrusion of mafic/ultramafic and alkaline intermediate magmatic suites at ~1085 Ma, resulting from mafic underplating and/or lower crustal delamination. Nd and Hf isotopic data imply the magmatic rocks of the Natal Metamorphic Province were derived from relatively juvenile continental crust, initially generated by island arc magmatism and subsequently reworked during the accretion event(s).~~and collision events.~~ The combined Kaapvaal-NMP region (the southern margin of the enlarged Kalahari Craton) then experienced extensive sinistral transcurrent deformation centered along a series of discrete steep shear zones that are found from the Kaapvaal cratonic margin to the southernmost portion of the Natal Metamorphic Province. This deformation~~collided with another continental fragment, which has been variously ascribed as Laurentia, or eastern Australia. The continental collision~~ is accompanied~~manifested~~ by low-pressure, (ultra)high-temperature metamorphism, isobaric cooling, and intrusion of the voluminous A-type Oribi Gorge Suite porphyritic granites and charnockites throughout the Mzumbe and Margate

Terranes. ~~This was contemporaneous with crustal scale sinistral shearing, and along with the recorded isobaric cooling path, is compatible with an escape tectonic setting.~~

1. Introduction

The Mesoproterozoic Natal Metamorphic Province (NMP) is comprised of ~1.3 to 1.0 Ga lithotectonic terranes which were accreted onto the SE margin of the Archaean Kaapvaal Craton (Figs. 1 and 2). From south to north these terranes are the Margate, Mzumbe, and Tugela terranes (Thomas, 1989a). The NMP, along with a similar age metamorphic province in the Northern Cape of South Africa and southern Namibia, form part of the Namaqua-Natal belt that is thought to be~~traditionally~~ associated with arc ~~and continental collision during the formation of the Rodinia supercontinent. Jacobs et al. (1993) showed that the Namaqua-Natal belt represents an example of arc~~ accretion and~~followed by~~ escape tectonics~~,~~ whereby late sinistral shearing in Natal is mirrored by conjugate dextral shears in Namaqualand (Jacobs et al., 1993) that formed immediately prior to the assembly of the Rodinia supercontinent.~~-~~ The timing of intrusion, deformation and metamorphism, and the geochemical/isotopic composition of the rocks within the NMP, has been the focus of many studies (see references and data compilations within Eglington, 2006 and McCourt et al., 2006). This study adds to the growing body of geochronological and isotopic data of the NMP, places further constraints on its orogenic evolution, and will address several outstanding questions concerning the temporal framework of the Natal Orogeny. Most of the previous studies have been conducted piecemeal over the last 25 years, and employed a variety of geochronological techniques by various laboratories. This approach has ensured that there still remain several ambiguities, unresolved questions and untested hypotheses. In order to provide a

Formatted: Indent: First line: 0 cm, Space After: 0 pt

Formatted: Space After: 0 pt

consistent U-Pb zircon geochronological data framework by ~~modern~~ laser ablation inductively coupled plasma-mass spectrometry (ICP-MS) and isotope-dilution thermal ionization mass spectrometry (ID-TIMS) techniques, we have re-sampled most of the main intrusive units from the Mzumbe and Margate Terranes ~~(Sezela Suite, Mzumbe Granitoid Suite, Glenmore Granite, Oribi Gorge Suite, Margate Granite Suite)~~ and dated some units for the first time. ~~(Mvoti pluton, Kwa-Lembe pluton, Leisure Bay Formation, Nicholson's Point Granite, Turtle Bay Suite).~~ This geochronological framework is augmented by the first whole-rock and zircon Hf isotope data from Natal, coupled with U-Pb zircon, titanite, and monazite age data recording metamorphism and whole-rock Nd isotopes of many of the intrusive units throughout the Mzumbe and Margate terranes. This ~~precise~~ dataset is used to provide an up-to-date -and comprehensive interpretation of the timing and nature of the tectono-magmatic events in the NMP.

2. Regional Setting

The Tugela Terrane comprises a series of NE directed, flat-lying thrust nappes, predominantly composed of supracrustal sequences; mainly layered amphibolites with subordinate quartzofeldspathic gneisses and ultramafic rocks with some intrusive tonalitic orthogneisses (Matthews, 1972; Thomas et al., 1994, Johnston et al., 2003). The terrane underwent upper-amphibolite to lower-granulite grade metamorphism, overprinted by greenschist facies assemblages (Bisnath et al., 2008). Matthews (1972) interpreted the terrane as an ophiolite complex, which was obducted over the rigid Kaapvaal cratonic margin at about 1135 Ma (Jacobs et al., 1997). The southern margin of the Tugela Terrane is defined by the major sub-vertical Lilani-Matigulu Shear Zone, which coincides with the southernmost geophysical boundary of the Kaapvaal Craton (de

Formatted: Indent: First line: 0 cm, Space After: 0 pt

Formatted: Space After: 0 pt

Beer and Meyer, 1984; Barkhiuzen and Matthews, 1990; Jacobs and Thomas 1994; de Wit and Tinker, 2004). South of the Lilani-Matigulu Shear Zone, the Mzumbe and Margate terranes are composed of arc-related, felsic to mafic metavolcanic and metasedimentary gneisses, the oldest of which (Quha gneiss) have been dated at ca. 1235 Ma (Thomas et al., 1999). The supracrustal gneisses were intruded at about ~1200 Ma by juvenile calc-alkaline I-type granitoids (e.g. the Mzumbe gneiss), likely in an island arc setting (Thomas and Eglington, 1990). The Mzumbe and Margate Terranes are separated by the Melville Thrust, a ~1 km wide, southerly dipping zone of high-strain (Thomas, 1989a). Apart from differing rock assemblages, the most apparent difference between the terranes is the metamorphic grade; the Margate Terrane displays (ultra)high-temperature granulite-facies metamorphism, whereas the Mzumbe Terrane is dominated by amphibolite-facies rocks (Thomas, 1989a; Thomas et al., 1992; Jacobs and Thomas, 1994). The three Natal terranes accreted northwards during the first phase of the Natal Orogeny during a tectonic phase generally termed D_1 (e.g. Jacobs and Thomas, 1994; Jacobs et al., 1997). The Mzumbe and Margate Terranes are intruded by several suites of granitic and subordinate mafic rocks. The most voluminous of these are the large metaluminous, A-type granite/charnockite plutons known as the Oribi Gorge Suite (Thomas, 1988, 1991b), which intrudes both the Mzumbe and Margate terranes after they were juxtaposed. These are interpreted to have been derived from the partial melting of lower crustal rocks (Thomas, 1988). The plutons exhibit ductile deformation especially near their contacts with the supracrustal gneisses, and were emplaced during a major phase of sinistral ductile transcurrent shearing, generally termed D_2 (Jacobs et al., 1993; Fig 12; Jacobs and Thomas, 1994). Published U-Pb zircon determinations point to a

protracted timescale for this tectono-magmatic event between ~1080 and 1030 Ma (see review in Eglington et al., 2003). Following transcurrent deformation, the latest stage of magmatism in the Natal Province is represented by a restricted number of undeformed granitic dykes in the Margate Terrane (Mbizana Microgranite) dated at 1026 ± 3 Ma (Thomas et al., 1993b). In the sections that follow, we provide a new set of isotopic data that cover a large portion of the Mzumbe and Margate Terrane, with which many of the models discussed are tested and modified.

3. Unit description, Petrography, and Zircon textures

Formatted: Indent: First line: 0 cm, Space After: 0 pt

Formatted: Space After: 0 pt

Sample lithologies and mineral assemblages are listed in Table 1.

3.1. Mzumbe Granitoid Suite

The Mzumbe Granitoid Suite forms the oldest pre-tectonic granitoid in the Mzumbe Terrane (Thomas, 1989a). It intrudes the supracrustal rocks of the Mapumulo Group. The age of the Mzumbe Granitoid Suite has been previously constrained by an 8-point Rb-Sr isochron age of 1212 ± 56 Ma and a TIMS U-Pb multigrain zircon age of 1207 +10/-11 Ma (Thomas and Eglington, 1990). This suite comprises a complex series of sheet-like granitoid bodies ranging from quartz diorite to leucogranodiorite which Thomas (1989b) interpreted as a comagmatic series of primitive, low-K, calc-alkaline granitoids formed from the partial melting of a descending slab of oceanic lithosphere adjacent to the Kaapvaal continental margin during the earliest phase of convergence in the NMP.

A sample of gneissic quartz-diorite from the Mzumbe Suite (CS13-16) was collected along the Fafa River near Ifafa. The sample is composed of quartz, plagioclase, poikiloblastic hornblende and altered biotite. Thomas (1989) reported colorless clinopyroxene replacing hornblende in some samples, which he interpreted as having

formed during prograde metamorphism. CL imaging of zircons in sample CS13-16 demonstrates oscillatory zonation, distinct core and rim growth phases and apatite and opaque mineral inclusions (Fig. 3).

3.2. Sezela Syenite Suite

This suite is composed of alkaline intrusive syenitic rocks which were sampled at the type localities in the Sezela pluton documented by Evans et al. (1991). The pluton comprises an inner relatively mafic grey quartz-monzonite and an outer envelope of pink quartz-monzonite and fluorite-bearing quartz-syenite (Thomas, 1988). The outer pink syenite displays a weak foliation with progressively decreasing amounts of strain in the interior of the pluton (Evans et al., 1987). The pink syenite sample exhibits patchy perthite mantling plagioclase, quartz, and biotite (see also Evans et al., 1991). Plagioclase is variably altered to sericite and biotite is found in greenish clots, altered to chlorite. The grey quartz monzonite sample exhibits perthitic feldspar, plagioclase, with altered biotite and hornblende. CL images of zircons in the two Sezela Suite samples (pink syenite: CS13-12, grey quartz monzonite: CS12-13) show a range of morphologies and textures. The majority of the zircons are complexly zoned and variably metamict (Fig. 3). Many zircons display distinct core and rim zircon growth phases. The Sezela Syenite Suite was originally defined as one of the youngest intrusive suites in the Mzumbe Terrane. It intrudes the supracrustal rocks of the Mapumulo Group, Humberdale Granite, and Equeefa Amphibolite Suite. Eglington and Kerr (1989) report a 9-point Rb-Sr whole-rock isochron age of 951 ± 16 Ma, which was interpreted as an intrusive age. This age and the presence of minimal deformation fabrics led this suite to be classified late to post-tectonic

(Evans et al., 1991), but data from this study discussed below calls this interpretation into question.

3.3. Leisure Bay Formation

The Leisure Bay Formation is part of the Mzimkulu Group, forming the oldest rocks of the Margate Terrane. The formation comprises a sequence of inter-layered pelite, psammite, and calcic granulite-facies migmatitic gneisses with chemical compositions akin to average shales, greywackes, and calcarenites respectively (Mendonidis, 1989). Three generations of folds with their associated axial planar foliations have been recognized (Grantham et al., 1991). The Leisure Bay Formation underwent (ultra)high-temperature, low-pressure (900-1100~~(> 850~~ ºC, ~5-74~~~ kbar) granulite-facies metamorphism and biotite/hornblende dehydration melting to produce garnet+orthopyroxene leucosomes and garnet+cordierite restites (Mendonidis and Grantham, 2003). Mendonidis and Grantham (2003) interpreted inclusions of hercynite in cordierite and garnet+quartz symplectites after orthopyroxene+plagioclase, as indicating isobaric cooling after the peak metamorphism. ~~(M_1), which they related to the intrusion of the Munster Metbasite Suite during the D_1 accretion event. Mendonidis and Grantham (2003) noted that M_1 was followed by a second metamorphism (M_2), which took place at lower temperatures (~ 800 ºC) and higher pressures (7.5–9 kbar) than M_1. M_2 was characterized by a clockwise pressure–temperature (P–T) loop, attributed to the intrusion of the Oribi Gorge Suite and subsequent isobaric cooling.~~ A sample of the Leisure Bay Formation (CS13-20) was collected from the type section as described by Grantham et al. (1991). CL imaging of zircons from this sample reveal oscillatory zonation, distinct core and rim growth phases, and minor opaque mineral inclusions. The zircons are subrounded,

and in some cases the zoning is truncated by abraded edges (Fig. 3); this is consistent with the metasedimentary interpretation of Mendonidis, (1989).

3.4. Margate Granite Suite

The most widespread and diverse intrusive unit in the Margate Terrane, covering about ~200 km^{2}, is known as the Margate Granite Suite (Thomas et al., 1991). It is made up of three variably foliated lithotypes: garnet-biotite augen gneiss, charnockite and more than one generation of leucogranite (± garnet). The intrusions range in form from thin boudinaged veins up to large sheet-like plutons (Thomas et al., 1991). Initially this suite was classified as being made up of peraluminous S-type granites, interpreted as syn-collisional melts generated during the accretion of the Margate Terrane ~~main regional tectonothermal event~~ (M_2; Thomas et al., 1991). Recently however, Voordouw and Rajesh (2012) reinvestigated the geochemistry of the rocks and found that ~75% of the Margate Suite granites are magnesian, calc-alkalic, and peraluminous, while the remaining 25% are ferroan, calc-alkalic, and metaluminous to peraluminous. They interpreted the suite to represent a large granitic batholith and the Margate Terrane as a continental magmatic arc. The polyphase Margate Suite is poorly dated, and the timing of intrusion has been constrained by a zircon SHRIMP U-Pb age of 1057 ± 27 Ma on one of the minor later phases of intrusion (Mendonidis and Armstrong, 2009). Two Rb-Sr whole-rock isochrons of 1011 ± 14 Ma (Nicholson's Point pluton; Eglington et al., 1986) and 1055 ± 60 Ma (Belmont pluton Thomas et al., 1990) have also been reported. The complexity of the Margate Suite is examined by Mendonidis et al. (this issue) who report U-Pb SHRIMP zircon dates from several phases of the suite, which reveal four distinct zircon-forming events: an earliest phase of magmatism (1169 ± 14 Ma), similar to that

reported for the Sikombe Granite (Thomas et al., 2003), three intrusive pulses of garnetiferous leucogranite (1135 ± 8, 1088 ± 9, and 1043 ± 4 Ma), and a phase of charnockitisation synchronous with the intrusion, and within the thermal aureole of the Oribi Gorge Granitoid suite (1037 ± 13 Ma). Two samples of the Margate Granite Suite were also taken as part of this study from the type locality (CS13-26) and from Nicholson's Point (CS13-21). They are composed of medium- to fine-grained garnet-bearing leucogranite with myrmekitic orthoclase and albite-rimmed plagioclase. Biotite is mostly chloritised, often associated with garnet, and is likely secondary. CL imaging of zircons in the samples show a low CL response and oscillatory zonation (Fig. 3).

3.5. Glenmore Granite

The Glenmore Granite is an irregular shaped body with an outcrop extent of ~28 km^2 that has been interpreted as a sheet, folded along east-west axes (Talbot and Grantham, 1987). The granite is strongly foliated, peraluminous, with biotite, garnet and occasional rapakivi feldspar textures (Grantham, 1983; Mendonidis, 1989; Mendonidis et al., 1991). It intrudes the Leisure Bay Formation to the south and Margate Granite Suite to the north, with contacts generally concordant to the regional foliation. The granite locally contains enclaves of Margate Granite, some phases of which, at least, must be older (Thomas, 1988). The Glenmore Granite has given a SHRIMP U-Pb zircon age of 1091 ± 9 Ma (Mendonidis et al., 2002). A sample of the granite was collected from the type locality described by Mendonidis et al. (1991). Poikilitic orthoclase is the dominant feldspar with inclusions of quartz and plagioclase, with abundant myrmekite. Grantham (1983) also reported biotite-quartz symplectites, typically in contact with garnet. CL images of

zircons in the granite (sample CS13-22) show oscillatory zonation, distinct core and rim growth phases with minor opaque mineral inclusions (Fig. 3).

3.6. Turtle Bay Suite

The Turtle Bay Suite comprises a bimodal association of two-pyroxene mafic granulites and felsic charnockites (orthopyroxene-bearing granites), spatially associated with the Melville Shear Zone, which constitutes the boundary between the Mzumbe and Margate terranes (Thomas et al., 1992). The two units are interlayered and are likely sheet intrusions. Strong compositional banding is observed in the mafic granulites comprising hydrous (hornblende and biotite-bearing) and anhydrous (pyroxene-rich) layers. The felsic charnockites contains large orthopyroxene poikiloblasts (< 10 mm) with biotite myrmekite. These rocks structurally overlie the Margate Granite Suite along the eastern coastal type section and are intruded by the Mvenyane pluton of the Oribi Gorge Suite in the western section (Thomas, 1988). Previous work has interpreted the two distinct rock types in this suite to genetically unrelated sources (Thomas, 1991d). These are represented by an earlier mafic plagioclase-rich cumulate and a later partial melt of this cumulate leading to highly fractionated pyroxene-bearing granites. A sample of both mafic granulite and felsic charnockite were collected from the coastal type section described by Thomas (1991d). CL images of zircons in the mafic granulite (CS13-28) reveal very complicated internal structures and show them to be metamict. Zircons from the felsic charnockite (CS13-29) have a low CL response and are metamict with oscillatory zonation (Fig. 3).

3.7. Oribi Granitoid Suite

The Oribi Granitoid Suite comprises ten plutons of very coarse-grained, megacrystic, and locally rapakivi granite/charnockite plutons, which intrude the supracrustal rocks and older granitoids of the Mzumbe and Margate terranes (Fig. 2). Some of the plutons are biotite/hornblende granite-dominated, with very little to no orthopyroxene (Mvenyane) whereas other are nearly exclusively charnockiticcharnockite (Port Edward, KwaLembe) (Thomas, 1988; Grantham et al., 2012). The plutons are predominately elliptical in map view and become progressively more elongate parallel to the regional foliation towards the northern part of the Mzumbe terrane (Thomas, 1988). Strong regional fabrics are seen along the plutonic margins forming distinct augen gneiss textures. In most plutons, strain partitioning during the D_2 deformation has left the plutonic core devoid of deformation, whereas the Glendale and Umgeni plutons exhibit discrete ductile shear zones that cut through the plutonic core (Fig. 2; Thomas, 1989a; Thomas et al., 1991). Samples were collected from two plutons in the Mzumbe Terrane (Mvoti and KwaLembeKwa Lembe) and two plutons in the Margate Terrane (Port Edward and Oribi Gorge).

3.7.1. Mvoti pluton

The Mvoti pluton occurs as an elongate granitoid/charnockite body (~240 km^2), and intrudes the Mapumulo Group and often hosts enclaves of the host rock (Thomas, 1992). The plutonic margins are generally sharp and occasionally mylonitic (Kerr and Finlay, 1981). Plagioclase in the Mvoti pluton is often replaced by sericite and antiperthite and biotite is partially chloritised. This pluton is previously undated, but displays the same intrusive relationships as the other units of the Oribi Gorge plutonic suite. A sample of the Mvoti pluton (CS13-4) was collected along the Mvoti River south of the Embezeni village near the inferred margin of the pluton. Cathodoluminescence (CL) imaging shows

the zircons in the Mvoti pluton are complexly zoned and often metamict; many have lozenge shaped apatite inclusions (Fig. 3).

3.7.2. KwaLembe~~Kwa-Lembe~~ pluton

The previously undated KwaLembe~~Kwa Lembe~~ pluton is an elliptical granitoid/charnockite (~420 km^2), which intrudes the undated Mkomazi granitic gneiss on its southern margin and is covered by the overlying Paleozoic Natal Group sedimentary rocks to the north (Evans et al., 1991). Contacts with the Mkomazi gneiss are sharp and concordant with the dominant steep foliation, which lies within the major D_2 Amanzimtoti Shear Zone. Plagioclase is the dominant feldspar with minor myrmekite when in contact with quartz. Secondary biotite is partially chloritised. A sample of the KwaLembe~~Kwa-Lembe~~ pluton was collected south of the Songeni village along the Mkomazi River. CL images of zircons in the KwaLembe~~Kwa-Lembe~~ pluton (sample CS13-10) exhibit complex zoning and intense metamictisation (Fig. 3).

3.7.3. Port Edward pluton

The Port Edward pluton is an irregularly shaped ~~charnockite to~~ enderbite bodypluton~~~~ (> 300 km^2) that intrudes the Munster Metabasite and the Margate Granite suites and often displays diffuse contacts (Grantham, 1983) interpreted to be caused by contact metamorphism (Eglington et al., 1986).~~)~~ Andesine and orthoclase are the dominant feldspars, which often have myrmekitic margins. Orthopyroxene is the main mafic mineral with minor amounts of secondary biotite. Previous studies have dated the Port Edward pluton at 1025 ± 8 Ma (SHRIMP zircon U-Pb) and 987 ± 19 Ma (whole-rock Rb-Sr), which have been interpreted to represent igneous emplacement and cooling respectively (Eglington et al., 2003). A sample of the Port Edward pluton was collected

along the coast of the Indian Ocean along the type section described by Thomas (1991c). Zircons in the Port Edward pluton (sample CS13-19) have sector and oscillatory zonation with minor opaque mineral inclusions as revealed by CL imaging (Fig. 3).

3.7.4. Oribi Gorge pluton

The Oribi Gorge pluton is a large elliptical granitoid/charnockite body (~880 km^2) that intrudes the granulite-facies Margate Granite Suite along its southern side. This pluton is predominately orthopyroxene-bearing ± fayalite and garnet and relatively minor volumes of porphyritic hornblende-biotite granite. The multi-facies relationship in the Oribi Gorge is similar to that of the Farsund charnockite of southern Norway, in which this variation is attributed to heterogeneous assimilation of varying lower crustal lithologies (Vander Auwera et al., 2014). Eglington et al. (2003) report a series of complex inheritance, emplacement, and overgrowth SHRIMP zircon U-Pb ages ranging from 1071 ± 12 Ma to 1029 ± 8 Ma. Thomas (1988) and Thomas et al. (1993) report a U-Pb zircon age for the pluton of 1037 ± 14 Ma and Rb-Sr ages of 1003 ± 29 Ma (whole-rock isochron), 924 ± 49 Ma (biotite), and 882 ± 18 Ma (biotite), probably reflecting emplacement and cooling. A sample (CS13-27) was collected from the type locality within the Oribi Gorge Nature Reserve along the Mzimkhulwana River as described by Thomas (1991c). CL images of zircons in the Oribi Gorge pluton (sample CS13-27) show sector and oscillatory zonation with minor opaque mineral inclusions (Fig. 3).

4. Methods

Full methods are explained in supplementary text 1.

4.1. Whole-rock Hf and Nd isotopes

Formatted: Indent: First line: 0 cm, Space After: 0 pt

Formatted: Space After: 0 pt

Whole-rock Hf isotopes were performed on a Thermo Scientific Neptune+ multi-collector inductively coupled plasma mass spectrometer system at the NERC Isotope Geoscience Laboratories (NIGL). Nd isotopes were collected using a Thermo Scientific Trition thermal ionization mass spectrometer also at NIGL.

4.2. Laser ablation U-Pb geochronology and Hf isotopes

U-Pb geochronology of zircon, titanite, and monazite were analyzed by single- and multi-collector sector-field inductively coupled plasma mass spectrometry (LA-SC/MC-SF-ICP-MS) coupled to a New Wave Research UP193UC ArF excimer laser ablation system at the NERC Isotope Geosciences Facilities following the methods described in Spencer et al. (2014). Near concordant (>95% concordance) U-Pb zircon ablation sites were then re-analyzed to measure their Lu-Hf isotopic compositions using a Thermo Scientific Neptune Plus MC-ICP-MS with a New Wave Research UP193UC ArF excimer laser ablation system at the NERC Isotope Geosciences Facilities.

4.3. CA-ID-TIMS U- Pb geochronology

A subset of the most concordant zircons was removed from epoxy mounts for chemical abrasion isotope dilution thermal ionization mass spectrometry (CA-ID-TIMS). Chemical abrasion following Mattinson (2005), ion exchange chemistry and isotopic analysis using a Thermo-Electron Triton were conducted at NIGL. See supplementary materials for complete methodology.

5. Results

5.1. U-Pb Geochronology

Results of U-Pb zircon, titanite, and monazite geochronology are presented in figures 4, 5, 6, 7, 8, S1, S2 and supplementary tables S1, S2, S3, and S4. Laser ablation analyses~~S3.~~

Formatted: Indent: First line: 0 cm, Space After: 0 pt

Formatted: Space After: 0 pt

~~Analyses~~ that display lead loss (> 2% discordance) or inheritance are filtered from the weighted average calculation. Weighted averages of $^{207}Pb/^{206}Pb$ or $^{206}Pb/^{238}U$ ages are reported based on the relative magnitude of 2 sigma uncertainties. For the ID-TIMS analyses, crystallization ages are determined using weighted averages of $^{207}Pb/^{206}Pb$ are used given the ~zero age lower intercepts of sample discordias.

5.2. Zircon Hf isotopes

Weighted averages of Hf isotopic analyses of zircon from each of the above samples are displayed in Fig. 10~~figure 7~~ and supplementary table S4 and have $\varepsilon Hf_{(t)}$ values between 7.4 and 2.9 with the exception of the Mvoti pluton which has an average of -0.8 ± 0.4. Reduced chi-squared tests reveal that Hf analyses for each sample represent single populations (see Wendt and Carl, 1999) and weighted average uncertainties vary between 0.4 and 1.4 epsilon units.

5.3. Whole-rock Nd, and Hf isotopes

Whole-rock isotope data are summarized in Table 3 and Fig. 10~~8~~. εNd ranges from -0.3 to 5.6, and εHf from -0.2 to 14.7. Sm/Nd ratios range from 0.21-0.10 and Lu/Hf ratios range from 0.057-0.002.

6. Discussion of the new U-Pb zircon ages and isotopic data

In detail, many of the dates determined in this study are in accordance with prior geochronological studies, although several do not agree with previous ages, requiring a re-evaluation of the timing of tectono-magmatic events. In the following section we review each new determination and compare it with previously published data.

6.1. Mzumbe Granitoid Suite (Mzumbe Terrane): sample CS13-16

Formatted: Indent: First line: 0 cm, Space After: 0 pt

Formatted: Space After: 0 pt

The sample of the gneissic quartz diorite of the Mzumbe Granitoid Suite analyzed in this study gave an age of 1175 ± 19 Ma. This is ~30 Ma younger than the previously reported multi-grain TIMS age of 1207 ± 10 Ma (Thomas and Eglington, 1990). Sample CS13-16 showed distinct core-rim relationships; however, each of the core/rim analyses yielded the same age within uncertainty. It is possible there is an older population or grains with older cores that were not captured by our analyses in this sample, which might explain why the age presented by Thomas and Eglington (1990) is older than the crystallization age determined in this study. An alternative is simply that the Mzumbe Granitoid Suite has a protracted magmatic history spanning from ~1175 to ~1207 Ma or includes two temporally discrete phases. Certainly, multiple intrusive phases are apparent in most outcrops.

Formatted: Space After: 0 pt

Whole-rock Nd, and Hf isotope data (Thomas and Eglington, 1990; this study) demonstrate that the Mzumbe Suite incorporated variable, but small, amounts of isotopically enriched material during petrogenesis (Fig. 108). Furthermore, the lack of reworking of significantly older crustal material, that might have been derived from the nearby Kaapvaal Craton for example, suggests the Mzumbe magmatic arc had a subduction polarity dipping away from the craton, as in the model of Jacobs and Thomas (1994). The incorporation of minor amounts of isotopically enriched crust in island arc settings is not unusual (e.g. see the Honshu, Luzon, and Lesser Antilles island arcs), as reviewed by Dhuime et al. (2011). The Hf and Nd isotope data from the younger sequences (with a few exceptions) fall within a narrow field between εHf of ~3-5 and

εNd of ~1-3, indicating the reworking of this arc material with minor incorporation of older material.

6.2. Sezela Syenite Suite (Mzumbe Terrane): samples CS13-12 and CS13-13

The Sezela pluton of the Sezela Syenite Suite, comprises two phases, an outer pink syenite and an inner grey quartz monzonite. Both phases were sampled in this study and gave statistically identical ages of 1081 ± 19 and 1085 ± 18 Ma, respectively. Both dates are considered to represent the age of crystallization/intrusion showing that the phases are coeval. The Sezela Suite has not previously been dated by zircon, except for an unpublished zircon evaporation Pb-Pb age of 1058 ± 6 Ma (B.M. Eglington, pers. comm., 2014). The suite has been defined as post-tectonic intrusive as it does not have clear cross cutting deformation fabrics (Evans et al., 1991). This interpretation was ~~apparently~~ supported by a Rb-Sr whole-rock isochron age of 951 ± 16 Ma, interpreted as an intrusive age by Eglington and Kerr (1989). Our new data shows that this young age and interpretation is no longer tenable. Furthermore, the grey quartz monzonite phase also yielded a titanite upper intercept U-Pb age of 1030 ± 9 Ma, interpreted as dating the metamorphic growth of titanite in the sample as it coincides with the emplacement ages of the Oribi Gorge Suite. This data clearly means a re-evaluation of the tectonic setting of the Sezela Suite is needed.

6.3. Leisure Bay Formation (Margate Terrane): sample CS13-20

A meta-psammitic sample from the Leisure Bay Formation yielded a $^{207}Pb/^{206}Pb$ laser ablation age of 1047 ± 17 (MSWD = 0.7) from a population of 15 analyses. Despite complex growth zoning revealed by CL imaging, multiple analyses of single grains either

yielded overlapping concordant analyses or discordant analyses with intercepts within uncertainty of the weighted average of the sample.

Given the metasedimentary nature of this sample, these ages either represent a single detrital population and thus the maximum depositional age, or a granulite-facies metamorphic event based upon the mineral assemblages. Based upon field relations and geochronology of the granites, which intrude the Leisure Bay Formation and overlap in uncertainty (ID-TIMS age of the Port Edward Pluton: 1034.5 ± 0.5~~1039 ± 9~~ Ma), such a young age cannot represent the maximum depositional age, so the grains are interpreted as being of metamorphic origin. It is curious that no other detrital component is apparent despite zircon zoning. This is possibly due to a complete resetting of the zircon age during granulite-facies metamorphism. Although these zircons do not have depleted Th/U ratios (0.7-4.4) they have very similar textures to those described from other high-temperature granulite terranes that are detrital in nature but completely reset in terms of U-Pb (Lange et al., 2005; Siebel et al., 2012). Further work is needed to more fully assess the distribution of U and Pb in the zircon lattice, as very high temperature systems have been shown to drastically alter their distribution (Kusiak et al., 2013; Valley et al., 2014; Whitehouse et al., 2014).

6.4. Turtle Bay Suite (Margate Terrane): CS13-28

A mafic granulite sample taken from the mafic phase of the Turtle Bay Suite, interpreted to be of metaigneous origin by Thomas et al. (1992) produced a $^{206}Pb/^{238}U$ age of 1114 ± 19 Ma. Selected analyses were between 4 and 7 % discordant. This date is interpreted to represent an estimate of the crystallization age of the metabasic rock. The same sample also yielded a U-Pb monazite age of 1042 ± 7 Ma (weighted average of 17 analyses from

Formatted: Space After: 0 pt

5 different grains; MSWD = 1.5), interpreted as dating a metamorphic event. Monazites from mineral separates were unzoned in Th and Y content (Fig. 8~~6~~).

6.5. Glenmore Granite (Margate Terrane): sample CS13-22

Magmatic zircons from the Glenmore Granite gave a laser ablation~~an~~ age of 1092 ± 20 Ma and an ID-TIMS age of 1084.5 ± 0.9 Ma (Figs. 5 and 6).~~.~~ This is identical to the SHRIMP U-Pb zircon age of 1091 ± 9 Ma reported in Mendonidis et al. (2002). CL imaging did reveal thin bright rims on the zircons from the Glenmore Granite, although these rims were too thin to analyze (see Fig. 3).

6.6. Margate Granite Suite (Margate Terrane): samples CS13-21 and CS13-26)

Two intrusions of the Margate Suite from Margate beach (CS13-26) and Nicholson Point (CS13-21) localities gave ages of 1088 ± 20 and 1099 ± 35 Ma, respectively. The Nicholson Point granite also yielded an ID-TIMS age of 1084.4 ± 1.7 Ma (Figs. 5 and 6). These ages, interpreted to represent the time of intrusion and crystallization of the granites, are statistically identical to that of the older garnet leucogranite phase of the Margate suite reported in Mendonidis et al. (2014; this volume). It is also coeval with the Glenmore Granite. For this reason, Mendonidis et al. (2014; this volume) consider the Glenmore Granite to be part of the Margate Suite.

6.7. Oribi Gorge Suite (both terranes): samples CS13-4, 10, 19, 27

The Oribi Gorge Suite comprises several highly distinctive plutons. The dating of the suite has, however, proved problematical. Four plutons have given simple, consistent dates (see Fig. 2): Mgeni (1030 ± 20 Ma; Eglington et al., 1989), KwaLembe (1030 ± 16 Ma; this study), Fafa (1037 ± 10; Eglington et al., 2003) and Port Edward (1025 ± 8 Ma; Eglington et al., 2003; 1039 ± 18 Ma; this study).

The dating of the Oribi Gorge pluton itself has been more complex. Thomas (1988) obtained a U-Pb zircon age of 1037 ± 14 Ma, within uncertainty to that we have obtained in this study (1046 ± 19 Ma), and the other four plutons. However, Thomas et al (1993a/b) and Eglington et al., (2003) obtained a range of dates, interpreted as intrusive, from 1082 to 1029 Ma. In these studies the zircons were often complex, core-rim relationships were common and an inherited component of many grains acknowledged. For example, the interpreted magmatic age (ca. 1080 Ma), attributed by Eglington et al., (2003) to a sample of the pluton from the Bomela locality was taken right at the contact with the Margate Granite. This age likely represents~~can probably represent~~ an inherited, Margate Granite, age (Mendonidis et al. 2014; this volume) rather than an emplacement age (Fig. ~~11).~~

To further assess the temporal constraints of the Oribi Gorge Suite, zircons from the Port Edward and Oribi Gorge plutons were also analyzed using ID-TIMS which yielded weighted average $^{207}Pb/^{206}Pb$ ages of 1034.4 ± 0.6 Ma (Port Edward pluton) and 1049.3 ± 0.8 Ma (Oribi Gorge pluton) (Figs. 5, 6, 9).

Although the *in situ* data from this study and those preceding it yielded a suite of imprecise data centered around ~1030 Ma with inheritance as old as ~1080 Ma, the ID-TIMS data presented here provides high-precision ages with at least 13.5 Ma separation between the crystallization of the zircons in the Port Edward and Oribi Gorge plutons (the difference between the minimum uncertainty of the Oribi Gorge pluton and maximum uncertainty of the Port Edward pluton). This separation implies the individual Oribi Gorge plutons were emplaced independently.~~The combined SHRIMP U-Pb zircon data of Eglington et al. (2003) and the LA-ICP-MS data from this study (Fig. 9) reveal a striking~~

Formatted: Space After: 0 pt

~~similarity of the youngest $^{207}Pb/^{206}Pb$ ages, centered at 1032 ± 5 Ma (MSWD = 1.03), including the zircon rims from sample B1. The older zircon populations reported in Eglington et al. (2003) cannot be separated from the youngest using geochemical differences, although the older ages lie conspicuously within the range of the basement rocks within the Mzumbe and Margate Terranes. Here, it is pertinent to point out that only in situ U-Pb zircon data was included in our study (see Eglington et al., 2003 for excluded data compilations).~~

The observed span of ages~~simplified age assignment~~ of the Oribi Gorge Suite (along with the assumption this applies to the other plutons in the suite) has considerable implications for the timing and duration of tectonic events. This~~For example, to account for the spread of ages of the Oribi Gorge pluton, Eglington et al. (2003)~~ suggests that the sinistral transcurrent deformation, with which the suite is intimately associated, continued for at least 13.5~~50~~ Ma and possibly longer.~~ Such a long duration of movement along discrete shear zones has not been documented in modern tectonic settings. Even in the largest of the modern orogenic systems such as the Himalaya, intracontinental transcurrent shear zones show deformation for ~ 20 million years which is considered extraordinary (Valli et al., 2007; Leloup et al., 2011).~~

~~The new, very restricted, age of the Oribi Gorge Suite solves several outstanding issues with the temporal framework in the Natal Province. For example, McCourt et al. (2006) argue that the ~ 1070 Ma age for the Oribi Gorge pluton of the Margate Terrane and the 1065 ± 15 inferred age of the Ntimbankulu pluton of the Mzumbe terrane (based on 1065 ± 15 Ma zircon rims in the Quha Formation which it intrudes) require the Margate and Mzumbe Terranes to have been juxtaposed by ~ 1070 Ma. They further use the 1082 ± 2~~

~~Ma age of the Equeefa Suite of the Mzumbe Terrane (age unpublished in McCourt et al., 2006 and later published in Eglington et al., 2010) and the near equivalent age of Bomela locality of the Oribi Gorge pluton of the Margate Terrane to support a ~1070 Ma juxtaposition. However, our interpretation that the Oribi Gorge plutons were all emplaced at ~1030 Ma age invalidates this supposition and can only put a minimum age on the terrane juxtaposition event.~~

The new dataset has, however, introduced a new complexity with regard to the age of the Oribi Gorge Suite. One of the northern intrusions, the Mvoti pluton, situated over 100 km north of the KwaLembe intrusion, yielded a $^{207}Pb/^{206}Pb$ age of 1145 ± 18 Ma, some 115 Ma older than the southern plutons (Fig. 4). It also exhibits much lower whole rock and zircon εHf and whole rock εNd values. This age and isotopic signature is strikingly similar to the adjacent Mzumbe Terrane basement, and the sample, like the one from the Bomela locality of the Oribi Gorge pluton, was collected from the contact area. It is thus suggested that the Mvoti age in this study represents inheritance and significant assimilation of the adjacent basement rocks and is not an intrusive age.

7. Tectonic Model

The data presented allow for a reassessment of the tectonic and temporal framework of the NMP, as summarised in Fig. 12~~10~~.

Arc magmatism: ca. 1250 to 1150 Ma

The earliest event recorded in the Mzumbe and Margate terranes is the formation of the volcanic arc phase of the Quha Formation, dated at 1235 ± 9 Ma (Thomas et al., 1999). The Quha Formation was subsequently intruded by the Mzumbe Granitoid Suite, which is dated at 1207 ± 10 Ma (Thomas and Eglington, 1990) and 1175 ± 19 Ma (this study).

Formatted: Space After: 0 pt

Formatted: Indent: First line: 0 cm, Space After: 0 pt

Formatted: Space After: 0 pt

This implies either protracted arc magmatism with synchronous volcano-sedimentary deposition, or two discrete pulses of arc magmatism.

The Mzumbe Suite is characterized by I-type granitoids interpreted, together with the Quha Formation, to have formed in an essentially juvenile island arc setting above a south-dipping subduction zone (see also Thomas, 1989b; Jacobs and Thomas, 1994). εHf and εNd display varied isotopic compositions all of which are within uncertainty of, and greater than, the chondritic uniform reservoir, implying limited reworking of significantly older crust (Figs. 10, 11~~Fig. 8~~).

Evidence of an early stage of arc magmatism is also present in the Tugela Terrane, within the northernmost Tugela and Madidima thrust sheets (Arima and Johnson, 2001). The timing of this arc magmatism is imprecisely constrained between ~1200 and ~1150 Ma, within uncertainty of the Mzumbe arc magmatism, although McCourt et al. (2006) posit the Tugela and Mzumbe arc magmatism formed in two separate island arc systems.

Terrane accretion and first regional metamorphism: 1150 to 1100 Ma

The Tugela and Mzumbe terranes were accreted to the Kaapvaal Craton by ~1140 Ma (Fig. 10~~8~~; Jacobs et al., 1997; McCourt et al., 2006). This is evidenced by the emplacement of the syntectonic granite sheets of the Mzimlilo Suite of the Mzumbe Terrane (1147 ± 17 Ma; Eglington, et al. 2010) and the aplitic dykes cross-cutting the Mkondeni arc rocks (McCourt et al., 2010).

During this time, arc magmatism continued until ~1135 Ma (Margate Granite; Mendonidis et al., 2014, this volume) in the outboard Margate Terrane along with the likely equivalent Sikombe Granite (Thomas, 1990; Thomas et al., 2003). The latest stages of Margate arc magmatism was accompanied by the intrusion of the bimodal Turtle Bay

Suite comprising two-pyroxene mafic units (now granulites) and felsic pyroxene granitoids. This magmatism is interpreted to represent a phase of extensional activity during the latest stages of arc magmatism (Thomas et al., 1992). The Turtle Bay Suite is spatially closely related with, and deformed by, the Melville thrust, which juxtaposes the granulite-facies rocks of the Margate Terrane northwards over the amphibolite grade rocks of the Mzumbe Terrane (Thomas, 1989; 1991d; Thomas et al., 1992).

The accretion of the Margate Terrane with the Mzumbe/Kaapvaal margin is constrained by the emplacement and deformation of several syn-collision intrusions and zircon overgrowths from ~1100 Ma to ~1090 Ma (e.g. Banana Beach Gneiss, Margate Granite, Glenmore Granite; see Fig. 12~~9~~ caption for references). Each of these syn-collision igneous bodies, along with older, pre-collision intrusions has a strong penetrative ductile fabric (broadly S_1) associated with crustal thickening and regional low-pressure granulite-facies metamorphism in the Margate Terrane (~4 kbar and >850º) (Evans et al., 1987; Mendonidis and Grantham, 2003), and upper amphibolite facies metamorphism in the Mzumbe Terrane.

The assigned age (~1090 Ma) of this metamorphism roughly coincides with the intrusion of the syn-tectonic granitoids found throughout the Margate Terrane followed by the extensional collapse and alkaline/mafic magmatism of the Sezela and Equeefa Suites in the Mzumbe Terrane (see Fig. 11~~9~~ and references therein). It also explains the presence of Margate Suite type garnet leucogranite plutons, such as the Belmont and Stiebel Rocks plutons north of the Mellville Shear Zone, in the southern Mzumbe Terrane. Although undated by U-Pb zircon the Belmont pluton gave a Rb-Sr isochron dates od ca. 1055 Ma

(Thomas et al., 1993), suggesting that it belongs to the latest, post-accretion phase of the Margate Suite, dated at ca. 1040 Ma (Mendonidis et al., 2014; this volume).

Post-accretion extension: ca. 1080 Ma

The cessation of this tectonomagmatic event can be constrained by the ages of the relatively undeformed Equeefa and Sezela suites. The age of the Equeefa Suite was determined by Eglington et al. (2010) at 1083 ± 6 Ma (SHRIMP zircon U-Pb). Our data shows that, for the first time, that the mafic/ultramafic Equeefa and the intermediate alkaline Sezela suites are coeval with both phases of the latter yielding U-Pb zircon ages of 1081 ± 9 and 1085 ± 8 Ma. Consequently, we interpret the Rb-Sr whole-rock isochron date of 951 ± 16 Ma of the Sezela Suite in Eglington and Kerr (1989) to represent a later cooling or alteration event as it is even younger than the U-Pb titanite age of 1030 ± 9 that we have obtained for the quartz monzonite phase.

Since it is now known that the Equeefa and Sezela suite are coeval, their tectonic significance can be better understood. The dated gabbro-norite body of Equeefa Suite probably resulted from post-arc accretion mafic underplating (Eglington, 1987; Thomas et al., 1992; Eglington et al., 2010). It can now be postulated that the underplating was also responsible for lower crustal melting and formation of the Sezela syenitoids. In this model therefore, the Equeefa and Sezela Suites would represent the products of a phase of post-accretion extensional collapse of the orogen at this time. The depleted composition Hf and Nd isotopes of the Sezela and Equeefa Suites in comparison with the other units further imply the influx of depleted mantle derived material (Fig. 10~~8~~).

Transcurrent deformation and Oribi magmatism~~Continental collision~~: ca. 1050-1030 Ma

Following the accretion of the Margate Terrane with the Mzumbe/Kaapvaal margin and the post-accretion alkaline/mafic magmatism, the accreted terranes were subjected to a second low-pressure, (ultra)high-temperature~~grade~~ metamorphic event associated with emplacement of the voluminous A-Type charnockite plutons of the Oribi Gorge Suite. This widespread low-pressure, (ultra)high-temperature granulite-facies magmatic-metamorphic event had peak conditions between ~900 and ~1100 ºC at ~5 to 7 kbar followed by an isobaric cooling path (Grantham, 1984; Evans et al., 1987; Thomas et al., 1992; Grantham et al., 1993; van den Kerkhof and Grantham, 1999; Grantham et al., 2001; Mendonidis and Grantham, 2003).

The age of this metamorphic event is ~~tightly~~ constrained in this study by a number of independent methods. Metamorphic zircons from the paragneissic two-pyroxene Leisure Bay Formation granulites (see Grantham et al., 1991) yield a $^{207}Pb/^{206}Pb$ age of 1047 ± 17 Ma. Metamorphic ages from titanite in the Sezela Suite (1030 ± 9 Ma; Fig. 7) and monazite from a mafic granulite sample from the Turtle Bay Formation (1042 ± 7 Ma) also demonstrate a metamorphic event at this time (Fig.~~Figure~~ 9). The minimum age of this event is constrained by the cross-cutting unmetamorphosed Mbizana microgranite dykes in the Margate Terrane, which have an intrusive age of 1026 ± 3 Ma (Thomas et al., 1993b).

This metamorphic event~~The second metamorphism~~ was also coeval with the intrusion of the Oribi Gorge Suite (Thomas, 1988; Thomas et al., 1991) and the formation of charnockitic aureoles that developed in the Margate Suite garnet leucogranites adjacent to large Oribi Gorge Suite plutons (Thomas, 1988; see van den Kerkhof and Grantham, 1999; Grantham et al, 2012 and Mendonidis et al., 2014, this volume). As discussed

above, we posit this magmatic event took place over a narrow window of time at 1032 ± 5 Ma. Structural, petrologic, geochemical, and isotopic evidence further imply the Oribi Suite granitoids represent a series of~~single~~ intrusive events~~event~~ sourced from similar parent material (Thomas, 1988; Thomas et al., 1991; Thomas et al., 1993; Thomas et al., 1996; Grantham et al., 2001; the geochemistry from Eglington et al., 2003; Voordouw, 2010). Additionally, bulk-rock Nd, and Hf analysis presented in this study (Fig. 10~~8~~) give further support to the contention that the Oribi Gorge Suite is dominantly composed of material reworked from the Margate and Mzumbe terranes~~represents a single comagmatic intrusive event~~.

The high-temperature granulite-facies metamorphism and intrusion of the Oribi Gorge Suite at ca. 1040 Ma were associated with synchronous transcurrent deformation in the Natal Province (Thomas, 1988; Jacobs et al., 1993). This major (broadly D_2) deformation event produced a series of wide, crustal-scale sinistral transcurrent faults (see Fig. 2). These did not produce a totally pervasive penetrative fabric throughout the terranes (Thomas, 1988; Voordouw, 2010), rather, the strain was partitioned into "steep belts" (Thomas, 1989), up to several kilometres wide, of pervasive shear fabrics (S_2 in a broad sense), separated by zones dominated by the older (S_1), collision-related ductile fabrics. These steep shear zones are also manifest as major aeromagnetic anomalies known as the Beattie set of anomalies (Du Plessis and Thomas, 1991; Scheiber-Enslin et al., 2014).

The clockwise P-T path followed by isobaric cooling which characterizes metamorphism~~characterises both metamorphic events (M_1 and M_2)~~ in the Mzumbe and Margate Terranes (Grantham et al., 1994; Mendonidis and Grantham, 2003) pose very interesting questions as to the tectonic mechanisms(s) responsible for this polyphase

metamorphic history. It has been suggested that the post-peak metamorphism P-T path can be explained by the extensional collapse of the orogenic belt (Thomas et al., 1992; Grantham et al., 1993; Grantham et al., 2012). We find this explanation untenable with an isobaric cooling path, as extensional collapse is associated in orogens worldwide with near isothermal decompression (Malavielle et al., 1990; Chauvet et al., 1992; Jacobs et al., 2003; Whitney et al., 2004). Rather, we propose that isobaric cooling could have been caused by advective cooling during transcurrent deformation, i.e. during convergence (orthogonal or oblique) the tectonic package is taken to peak pressure at which time the deformation vector shifts from convergence to transcurrent. The tectonic package remains at peak pressure during this transcurrent deformation while it cools advectively (Bohlen, 1987; Wakabayashi, 2004). Further work is need to constrain the timing of metamorphism in relation to sinistral deformation and intrusion of the Oribi Gorge plutons.

~~This type of tectono-thermal and magmatic regime is best explained by a continental collision at around 1040 Ma (Fig. 11). The question must be asked; collision with what?~~

~~*Paleogeography of the continental collision*~~

~~The nature of the major tectono-magmatic event at ca. 1030 to 1040 Ma, seen throughout the Mzumbe and Margate terranes (but not the Tugela Terrane with its thick, rigid, cold cratonic substrate) is typical of a continental collision zone such as the Himalayas (Tapponnier and Molnar, 1976; Tapponnier et al., 1982) as suggested by several previous studies (Jacobs et al., 1993; Jacobs and Thomas, 1994; Jacobs et al. 2003; McCourt et al., 2006). The putative collision would have represented one of the major late~~

~~Mesoproterozoic orogens associated with the assembly of the supercontinent of Rodinia (Hoffman, 1991; Li et al, 2008).~~

~~The identity of the "southern continental block" with respect to the Namaqua-Natal orogen remains an unanswered question (Fig. 11). Certainly, the missing continent is not apparent solely by matching conjugate orogens of similar geology in other continents. From the evidence in Natal, we can say with some assurance, that at ~ 1.2 Ga the southern margin of the composite Kalahari Craton (comprised of the Zimbabwe, Kaapvaal, and Grunehogna cratons) was characterized by ocean-ward subduction in the NMP and formation of the juvenile Tugela/Mzumbe/Margate island arcs, while the Namaqua Province to the west comprised a complex series of Mesoproterozoic volcanic arcs and Palaeoproterozoic continental fragments to the east (see Eglington, 2006 and Jacobs et al., 2008 for a review; Fig. 11).~~

~~Palaeomagnetic data suggest a plausible connection between the Kalahari Craton and southern Laurentia (Dalziel et al., 2000; Gose et al., 2004; Li et al., 2008; Evans, 2013), whereas other reconstructions have also been proposed linking the Kalahari with eastern Australia (Pisarevsky et al., 2003; Evans, 2009). From the literature, the following crustal blocks are possible candidates for the colliding fragment (see Fig. 12).~~

~~Laurentia~~

~~During the late Mesoproterozoic, Laurentia had a passive margin on its southern side (present coordinates, northern margin in this discussion) wherein craton-derived sediment was accumulating, currently represented by the Packsaddle domain of the Llano Uplift (Mosher et al., 2008). Dalziel et al. (2000) and Mosher et al. (2008) have suggested that~~

~~the subduction that led up to the ~1150-1120 Ma continental collisional orogenesis seen in the Llano Uplift was directed away from the Laurentian craton as no evidence for subduction magmatism is present in the Llano Uplift; an analogous situation to that proposed in Natal. Therefore, this would have resulted in the collision of two subduction zones facing away from the cratons, similar to the modern analogue of the Philippines (Yumul et al., 2003). The continental collision was followed by abundant juvenile granite intrusions similar in composition to the Oribi Gorge Suite that intruded the Llano Uplift, but significantly earlier, from 1120 to 1070 Ma (Smith et al., 1997) and possibly related to slab break-off and asthenospheric upwelling (Davies and von Blanckenbrug, 1995). West of the Llano Uplift, metamorphism in the Van Horn region of Texas took place between ~1060 and ~1020 Ma with continued contractional deformation from ~1030 to ~1000 Ma (Grimes and Copeland, 2004), so in this part of the Laurentian margin, the collision timing was comparable to that of the NMP. In view of this apparent diachronism of orogenic events along the Laurentian margin, the case for Laurentia to be the colliding continent with Natal cannot be unequivocally resolved.~~

~~Amazonia has also been proposed as the continent that collided with southern Laurentia (Tohver et al., 2005, 2006), in which case Kalahari would necessarily be excluded. However, Evans (2013) pointed out that this model requires a dynamically improbable rotation of Amazonia by nearly 180º as it translated along the Laurentian margin.~~

~~Australia~~

~~The eastern side of continental Australia is a palaeomagnetically permissible candidate as the colliding continent (Pisarevsky et al., 2003; Evans, 2009), but these reconstructions~~

~~place the NMP facing an ocean basin (passive margin/fringing arc system), which does not fit our interpretation of the geology.~~

~~Another crustal block~~

~~Multiple lines of evidence point towards a collisional/accretion event following the accretion of the Mzumbe and Margate terranes. These include granulite facies metamorphism ca. 1040 Ma, Oribi Gorge Suite plutonism ca. 1030 Ma and synchronous antithetic transcurrent shearing (escape tectonics) in the Namaqua Metamorphic Province; see Fig. 11. At the moment however, the palaeomagnetic constraints on the the precise configuration of this part of Rodinia are so imprecise that it is wholly plausible that there are other, as yet unidentified candidate fragments to have collided with southern Kalahari. This question will probably remain unresolved until such data become available.~~

Conclusions

- New U-Pb zircon, monazite and titanite data provide important temporal constraints on the geological history of the NMP. These data provide some new controls, re-affirm many of the previous geochronological studies in the region and clarify the interpretation of previously conflicting data.
- A sample of the Mzumbe Granitoid Suite, dated in this study, is ca. 30 Ma younger than in a previous study, suggesting that this polyphase assemblage~~the suite~~ was emplaced over a protracted period of magmatism from 1207 ± 10 to 1175 ± 19 Ma and thus extending the duration of arc magmatism in the Mzumbe arc. Nd and Hf isotopes confirm that the Mzumbe Granitoid Suite formed in an island arc setting.

Formatted: Space After: 0 pt

- Younger, but overlapping island arc magmatism in the Margate Granite ranged between ~1181 Ma (Sikombe Granite) and ~1135 Ma (Margate Granite).
- Accretion of Tugela, Mzumbe, and Margate island arc complexes onto the Kaapvaal Craton occurred in two stages at ~1150 Ma and ~1090 Ma. The former involved the accretion of the Tugela and Mzumbe Terranes with the Kaapvaal Craton, and the latter represents the accretion of the Margate Terrane. During the Margate accretion, syn-tectonic intrusions such as the Margate Granite and Glenmore Granite intruded the Margate Terrane, and juxtaposition of the Margate and Mzumbe Terranes occurred along the Melville Thrust with the intrusion of the associated Turtle Bay Suite.
- Arc accretion was followed by a phase of mafic and alkaline intermediate magmatism represented by the Equeefa and Sezela Suites that are dated at ~1085 Ma. This magmatism possibly took place during a period of crustal thinning, delamination and extensional collapse.
- Extensive transcurrent deformation~~Collision, with another, yet to be identified continental block~~ took place at ca. 1050~~1040~~ to 1030 Ma, manifested by low-pressure (~5-7 kbar), (ultra)high-temperature (~900-1100 ºC) granulite-facies metamorphism, that was coeval with intrusion of the Oribi Gorge Suite~~, and regional scale transcurrent deformation.~~ The metamorphic event is constrained by titanite, monazite, and zircon ages at 1042 Ma, and the Oribi Gorge Suite intruded within uncertainty at 1032 ± 5 Ma. Transcurrent deformation resulted in an isobaric cooling path interpreted to have occurred during advective cooling.

- Nd and Hf isotopes show that the magmatic rocks produced in the NMP had a single source extracted from the mantle during island arc magmatism associated with the Mzumbe arc. Subsequent magmatic rocks simply reworked this island arc material, with minimal contamination from significantly older crust and no significant addition of mantle-derived material.

Acknowledgements

We would like to acknowledge Bruce Eglington for providing data from the DataView Geochronology Database. Dan Condon, Carlyn Stewart, and Nicola Atkinson provided analytical assistance at NIGL. Logistics in South Africa were facilitated with the help of Greg Botha and Bevan Turner. Natural Environment Research Council (NERC grant NE/J021822/1) provided financial support for this study. The NERC Isotope Geosciences Facilities Steering Committee (IP-1366-0513) provided additional analytical support. Helpful reviews from Bruce Eglington and Bernard Bingen resulted in considerable improvements of the paper and are gratefully acknowledged.

Figure Captions

1: Simplified geological map of southern Africa outlining the regional extent to the Namaqua-Natal belt, modified after Schlüter (2006).

2: a) Simplified geological map of the NMP showing the areal extent and relative positions of the Margate, Mzumbe, and Tugela Terranes along with the Kaapvaal Craton and the Oribi Gorge Suite; b) inset of the southern NMP with sample localities. Geological maps fashioned after Thomas (1988).

3: CL images of representative zircons from samples analyzed in this study. Smaller circles represent 25 µm U-Pb analytical locations and larger circles represent 36 µm Hf

analytical locations. $^{207}Pb/^{206}Pb$, $^{206}Pb/^{238}U$, and epsilon Hf uncertainties are 2 sigma (analytical uncertainty and excess variance using a quadratic sum). On grains with multiple U-Pb analytical spots, grouped analyses are either concordant (grains CS13-16.20, CS13-20.15, CS13-26.8) or have an upper concordia intercept age indicated.

4: Summary plot of U-Pb ages. Grey bars are $^{207}Pb/^{206}Pb$ ages of individual zircon grains (with exception of CS13-28 which are $^{206}Pb/^{238}U$). The colored bars across the zircon analyses in each sample are weighted averages of the analyses. Weighted 2 sigma uncertainties of colored bars include analytical uncertainties and excess variance only. Black outlined boxes are 2 sigma analytical uncertainties upon which systematic uncertainties of long-term variance (1.5%) and decay constant uncertainties (Schoene et al., 2006) are propogated. Intrusive relationships are based upon field observations described by Evans et al. (1991), Mendonidis et al. (1991), Thomas et al. (1991), and Thomas (1991a,b,c,d). Location of the Melville Thrust spanning the Turtle Bay Suite and boundaries of the Mzumbe and Margate Terranes is described by Thomas (1991d).

5: Summary plots of CA-ID-TIMS U-Pb zircon data. Figures and calculations were done using UPb_Redux (Bowring et al., 2011). Uncertainties are presented at the 2σ level in the form x/y/z, whereby: x=analytical uncertainty only; y=analytical and tracer calibration uncertainties (for comparison with LA-ICP-MS data); and z=total uncertainty.

6: Comparison between the least discordant (< 2%) subset of LA-ICP-MS analyses and the CA-ID-TIMS analyses.

7~~5~~: Tera-Wasserburg inverse concordia plot of titanite analyses from the Sezela Syenite Suite (sample CS13-12).

Formatted: Space After: 0 pt

8~~6~~: Wetherill concordia plot of monazite analyses from the Turtle Bay Suite (sample CS13-28). $^{207}Pb/^{206}Pb$ ages of individual analyses are displayed in the inset. Backscatter, Th and Y X-ray maps display minimal zonation. Spot analyses of monazite are 25 µm in diameter.

9~~7~~: $\varepsilon Hf_{(t)}$ analyses for each of the samples in this study. $\varepsilon Hf_{(t)}$ is calculated using the age listed in Table 2. Weighted average uncertainties are 2 sigma.

10~~8~~: $\varepsilon Hf_{(t)}$ (whole rock and zircon) and $\varepsilon Nd_{(t)}$ (whole rock) of samples in this study. Grey field corresponds to Hf and Nd isotopic evolution trends with respective Lu/Hf and Sm/Nd ratios of 0.012 and 0.14 (the average ratios of sample in this study). New crust in εHf space from Dhuime et al. (2011).

11~~9~~: Summary age plot of the Oribi Gorge Granitoid Suite including samples from Eglington et al. (2003, in *italics*) and this study. The weighted average age of the Oribi Gorge Granitoid Suite is calculated using samples CS13-10, -19, -27 (this study) and UND199, UND215, and the rim ages from sample B1 (Eglington et al., 2003). This results in a statically robust age of 1032 ± 5 Ma. The multi-grain zircon evaporation age of the Mgeni pluton (Eglington et al., 1989) is not used in the average calculation but supports the 1032 ± 5 Ma date. The other zircons from Oribi Gorge Suite plutons that are not included in this calculation are assumed to be inherited from the basement rocks within the Mzumbe and Margate Terrane respectively. Ages of the basement rocks are shown in Fig. 12~~10~~.

12~~10~~: Compilation of magmatic, sedimentary, and metamorphic data associated with the three terranes of the NMP. These data indicate that Tugela Ocean closure, ophiolite obduction and arc accretion took place at ~1140 Ma. This was followed by continued arc

magmatism in the Margate Terrane until its accretion ~1090 Ma. This second accretion event was also associated with the formation of the Melville Thrust, intrusion of the Turtle Bay Suite and juxtaposition of the Mzumbe and Margate Terranes. It was followed by ~1080 Ma alkaline and mafic magmatism potentially linked to mafic underplating and/or extensional collapse. At ~1030 Ma, transcurrent deformation and syntectonic magmatism~~continental collision~~ is recorded by low-P, high-T granulite facies metamorphism and the intrusion of the Oribi Gorge Suite.

~~11: Schematic paleogeographic reconstruction of the Kalahari Craton and an unknown collider at ca. 1000 Ma. Kalahari Craton after Jacobs et al. (2008). Position of Coats Land (CL) after Loewy et al. (2011). A: Areachap Terrane; CKB: Choma-Kaloma Block; DML: Dronning Maud Land; FI: Falkland Islands; G: Grunehogna Craton; H: Haag Nunataks; K: Kaapvaal Craton; MMU: Marrupa-Malawi-Unango terrane; NAM: Nampula Province; Ri: Richtersveld Terrane; S: Sinclair Terrane; SR: Sør Rondane; Z: Zimbabwe Craton.~~

~~12: Schematic palaeogeographic reconstructions of Rodinia after a) Pisarevsky et al. (2003) which places the NMP adjacent to eastern Australia; b) Li et al. (2008) which shows the NMP next to Laurentia and c) Evans (2009) which shows the NMP in an outboard position with no nearby continental masses. Figure modified from Evans, 2013. Continents not discussed are shown in gray.~~

S1 (online~~inline~~): Compiled U-Pb-Hf analyses of zircon (U-Pb-Hf), titanite (U-Pb), and monazite (U-Pb) reference materials.

S2: Concordia Diagrams of the samples analyzed in this study. Analyses with resolvable common lead are excluded. Least discordant (< 2%) data used in age calculation is shown

Formatted: Space After: 0 pt

in blue. Excluded discordant data (< 2%) are shown in red. Analyses that are interpreted to be inherited are shown in green.

Tables Captions

1: Table of sample name, locality, lithology, and dominant mineral assemblage for the samples in discussed in this study.

2: Zircon U-Pb weighted average ages for samples within the Mzumbe and Margate Teranes. Acceptable MSWD criteria adopted after Wendt and Carl (1999).

3: Whole rock Nd and Hf isotope data. Age of sample CS13-29 is approximate base upon cross cutting relations.

S1: LA-ICP-MS U-Pb data of zircon~~zircons~~

S2: LA-ICP-MS U-Pb data of titanite

S3: LA-ICP-MS U-Pb data of monazite

S4: LA-ICP-MS Hf data of zircon

S5: CA-ID-TIMS data of zircon

Other Supplementary Materials

KMZ of sample locations.

Supplementary text 1: Analytical methods

References

Arima, M., Johnston, S., 2001. Crustal evolution of the Tugela Terrane, Natal Belt, South Africa. Gondwana Res. 563–564.

Barkhuizen, J.G., Matthews, P., 1990. Gravity modelling of the Natal Thrust Front: A Mid-Proterozoic crustal suture in southeastern Africa. Geol. Soc. South Africa Geocongress'90 Johannesburg. Ext. Abstr. Vol. 32.35.

Bickford, M., 2000. Geology and geochronology of Grenville-age rocks in the Van Horn and Franklin Mountains area, west Texas: Implications for the tectonic evolution of Laurentia during the Grenville. Geol. Soc. Am. Bull. 112, 1134–1148. doi:10.1130/0016-7606(2000)112<1134

Bisnath, A., McCourt, S., Frimmel, H., Buthelezi, S.B.N., 2009. The metamorphic evolution of mafic rocks in the Tugela Terrane, Natal Belt, South Africa. South African J. Geol. 111, 369–386. doi:10.2113/gssajg.111.4.369

Bohlen, S., 1987. Pressure-Temperature-Time Paths and a Tectonic Model for the Evolution of Granulites. J. Geol. 95, 617–632.

Formatted: Space After: 0 pt

Formatted: Space Before: 0 pt, After: 0 pt

Bowring, J.F., McLean, N.M., Bowring, S.A., 2011. Engineering cyber infrastructure for U-Pb geochronology: Tripoli and U-Pb_Redux. Geochemistry, Geophys. Geosystems 12, n/a–n/a. doi:10.1029/2010GC003479

Chauvet, A., Dallmeyer, R., 1992. 40Ar/39Ar mineral dates related to Devonian extension in the southwestern Scandinavian Caledonides. Tectonophysics 210, 155–177. doi:10.1016/0040-1951(92)90133-Q

Cornell, D.H., Thomas, R.J., 2006. Age and tectonic significance of the Banana Beach Gneiss , KwaZulu-Natal South Coast , South Africa. South African J. Geol. 109, 335–340.

Dalziel, I., Mosher, S., Gahagan, L., 2000. Laurentia - Kalahari Collision and the Assembly of Rodinia. J. Geol. 108, 499–513.

Dhuime, B., Hawkesworth, C., Cawood, P., 2011. When continents formed. Science 331, 154–5. doi:10.1126/science.1201245

Eglington, B., Thomas, R., Armstrong, R., Walraven, F., 2003a. Zircon geochronology of the Oribi Gorge Suite, KwaZulu-Natal, South Africa: constraints on the timing of trans-current shearing in the Namaqua–Natal Belt. Precambrian Res. 123, 29–46. doi:10.1016/S0301-9268(03)00016-0

Eglington, B., Thomas, R., Armstrong, R., Walraven, F., 2003b. Zircon geochronology of the Oribi Gorge Suite, KwaZulu-Natal, South Africa: constraints on the timing of trans-current shearing in the Namaqua–Natal Belt. Precambrian Res. 123, 29–46. doi:10.1016/S0301-9268(03)00016-0

Eglington, B.M., 1987. Field, Geochemical and Isotope Studies of Selected Areas of Proterozoic Crust in South-central Natal. University of Natal.

Eglington, B.M., 2006. Evolution of the Namaqua-Natal Belt, southern Africa – A geochronological and isotope geochemical review. J. African Earth Sci. 46, 93–111. doi:10.1016/j.jafrearsci.2006.01.014

Eglington, B.M., Harmer, R.E., Kerr, A., 1986. Petrographic, Rb-Sr isotope and geochemical characteristics of intrusive granitoids from the Port Edward-Port Shepstone area, Natal.

Eglington, B.M., Harmer, R.E., Kerr, A., 1989. Rb-Sr isotopic constraints on the ages of the Mgeni and Nqwadolo Granites, Valley of a Thousand Hills, Natal.

Eglington, B.M., Kerr, A., 1989. Rb-Sr and Pb-Pb geochronology of Proterozoic intrusions from the Scottburgh area of southern Natal.

Eglington, B.M., Thomas, R.J., Armstrong, R. a., 2010. U-Pb Shrimp Zircon Dating of Mesoproterozoic Magmatic Rocks From the Scottburgh Area, Central Mzumbe Terrane, Kwazulu-Natal, South Africa. South African J. Geol. 113, 229–235. doi:10.2113/gssajg.113.2.229

Evans, D. a. D., 2009. The palaeomagnetically viable, long-lived and all-inclusive Rodinia supercontinent reconstruction. Geol. Soc. London, Spec. Publ. 327, 371–404. doi:10.1144/SP327.16

Evans, D. a. D., 2013. Reconstructing pre-Pangean supercontinents. Geol. Soc. Am. Bull. 125, 1735–1751. doi:10.1130/B30950.1

Evans, M.J., Eglington, B.M., Kerr, A., Saggerson, E.P., 1987. The geology of the Proterozoic rocks around Umzinto, southern Natal, South Africa. South African J. Geol. 90, 471–488.

Evans, M.J., Thomas, R.J., Eglington, B.M., 1991. Mzimlilo Granite, in: Johnson, M.R. (Ed.), Catalogue of South African Lithostratigraphic Units 3. South African Committee for Stratigraphy, Council For Geoscience, South Africa, pp. 29–30.

Gose, W. a., Johnston, S.T., Thomas, R.J., 2004. Age of magnetization of Mesoproterozoic rocks from the Natal sector of the Namaqua-Natal belt, South Africa. J. African Earth Sci. 40, 137–145. doi:10.1016/j.jafrearsci.2004.11.003

Grantham, G., Thomas, R., Mendonidis, P., 1994. Contrasting PTt loops from southern East Africa, Natal and East Antarctica. J. African Earth … 19, 225–235.

Grantham, G.H., 1984. The tectonic, metamorphic and intrusive history of the Natal mobile belt between Glenmore and Port Edward, Natal. University of Natal (Pietermaritzburg).

Grantham, G.H., Eglington, B.M., Thomas, R.J., Mendonidis, P., 2001. The nature of the Grenville-age charnockitic A-type magmatism from the Natal, Namaqua and Maud Belts of southern Africa and western Dronning Maud Land, Antarctica. Mem. Natl. Inst. Polar Res. Spec. issue 55, 59–86.

Grantham, G.H., Mendonidis, P., Thomas, R.J., Satish-Kumar, M., 2012. Multiple origins of charnockite in the Mesoproterozoic Natal belt, Kwazulu-Natal, South Africa. Geosci. Front. 3, 755–771. doi:10.1016/j.gsf.2012.05.006

Formatted: Font: (Default) Academy Engraved LET

Grantham, G.H., Storey, B.C., Thomas, R.J., Jacobs, J., n.d. The pre-break-up position of Haag Nunataks within Gondwana: possible correlatives in Natal and Dronning Maud Land, in: Ricci, C.A. (Ed.), The Antarctica Region, Geological Evolution and Processes. pp. 13–20.

Grantham, G.H., Thomas, R.J., Eglington, B.M., de Bruin, D., Atanasov, A., Evans, M.J., 1993. Corona textures in Proterozoic olivine melanorites of the Equeefa Suite, Natal Metamorphic Province, South Africa. Mineral. Petrol. 49, 91–102. doi:10.1007/BF01162928

Grantham, G.H., Thomas, R.J., Mendonidis, P., 1991. Leisure Bay Formation, in: Johnson, M.R. (Ed.), Catalogue of South African Lithostratigraphic Units 3. South African Committee for Stratigraphy, Council For Geoscience, South Africa, pp. 17–18.

Grimes, S.W., Copeland, P., 2004. Thermochronology of the Grenville Orogeny in west Texas, Precambrian Research. doi:10.1016/j.precamres.2003.12.004

Hoffman, P.F., 1991. Did the breakout of laurentia turn gondwanaland inside-out? Science 252, 1409–12. doi:10.1126/science.252.5011.1409

Huw Davies, J., von Blanckenburg, F., 1995. Slab breakoff: A model of lithosphere detachment and its test in the magmatism and deformation of collisional orogens. Earth Planet. Sci. Lett. 129, 85–102. doi:10.1016/0012-821X(94)00237-S

Jacobs, J., Bauer, W., Fanning, C.M., 2003. New age constraints for Grenville-age metamorphism in western central Dronning Maud Land (East Antarctica), and implications for the palaeogeography of Kalahari in Rodinia. Int. J. Earth Sci. 92, 301–315. doi:10.1007/s00531-003-0335-x

Jacobs, J., Pisarevsky, S., Thomas, R.J., Becker, T., 2008. The Kalahari Craton during the assembly and dispersal of Rodinia. Precambrian Res. 160, 142–158. doi:10.1016/j.precamres.2007.04.022

Jacobs, J., Thomas, R., 1994. Oblique collision at about 1.1 Ga along the southern margin of the Kaapvaal continent, south-east Africa. Geol. Rundschau 322–333.

Jacobs, J., Thomas, R.J., Armstrong, R.A., Henjes-Kunst, F., 1999. Age and thermal evolution of the Mesoproterozoic Cape Meredith Complex, West Falkland. J. Geol. Soc. London. 156, 917–928. doi:10.1144/gsjgs.156.5.0917

Jacobs, J., Thomas, R.J., Weber, K., 1993. Accretion and indentation tectonics at the southern edge of the Kaapvaal craton during the Kibaran (Grenville) orogeny. Geology 21, 203. doi:10.1130/0091-7613(1993)021<0203:AAITAT>2.3.CO;2

Jacobson, C.E., Grove, M., Pedrick, J.N., Barth, a. P., Marsaglia, K.M., Gehrels, G.E., Nourse, J. a., 2010. Late Cretaceous-early Cenozoic tectonic evolution of the southern California margin inferred from provenance of trench and forearc sediments. Geol. Soc. Am. Bull. 123, 485–506. doi:10.1130/B30238.1

Johnston, S., Armstrong, R., Heaman, L., 2001. Preliminary U-Pb geochronology of the Tugela terrane, Natal belt, eastern South Africa. Mem. Natl. ….

Kerkhof, A. van den, Grantham, G., 1999. Metamorphic charnockite in contact aureoles around intrusive enderbite from Natal, South Africa. Contrib. to Mineral. ….

Kerr, A., Finlay, C.A., 1981. A comparison between the Mvoti Granite and the Nqwadolo Granite. Petros 10, 71–83.

Kusiak, M.A., Whitehouse, M.J., Wilde, S.A., Nemchin, A. a., Clark, C., 2013. Mobilization of radiogenic Pb in zircon revealed by ion imaging: Implications for early Earth geochronology. Geology 41, 291–294. doi:10.1130/G33920.1

Lange, U., Brocker, M., Armstrong, R., Trapp, E., Mezger, K., 2005. Sm-Nd and U-Pb dating of high-pressure granulites from the Zlote and Rychleby Mts (Bohemian Massif, Poland and Czech Republic). J. Metamorph. Geol. 23, 133–145. doi:10.1111/j.1525-1314.2005.00566.x

Leloup, P.H., Boutonnet, E., Davis, W.J., Hattori, K., 2011. Long-lasting intracontinental strike-slip faulting: new evidence from the Karakorum shear zone in the Himalayas. Terra Nov. no–no. doi:10.1111/j.1365-3121.2011.00988.x

Li, Z.X., Bogdanova, S.V., Collins, A.S., Davidson, A., De Waele, B., Ernst, R.E., Fitzsimons, I.C.W., Fuck, R. a., Gladkochub, D.P., Jacobs, J., Karlstrom, K.E., Lu, S., Natapov, L.M., Pease, V., Pisarevsky, S. a., Thrane, K., Vernikovsky, V., 2008. Assembly, configuration, and break-up history of Rodinia: A synthesis. Precambrian Res. 160, 179–210. doi:10.1016/j.precamres.2007.04.021

Loewy, S.L., Dalziel, I.W.D., Pisarevsky, S., Connelly, J.N., Tait, J., Hanson, R.E., Bullen, D., 2011. Coats Land crustal block, East Antarctica: A tectonic tracer for Laurentia? Geology 39, 859–862. doi:10.1130/G32029.1

Malavieille, J., Guihot, P., Costa, S., Lardeaux, J.M., Gardien, V., 1990. Collapse of the thickened Variscan crust in the French Massif Central: Mont Pilat extensional shear zone and St. Etienne Late Carboniferous basin. Tectonophysics 177, 139–149. doi:10.1016/0040-1951(90)90278-G

Matthews, P.E., 1972. Possible Precambrian Obduction and Plate Tectonics in Southeastern Africa. Nature 240, 37–39. doi:10.1038/10.1038/physci240037a0

Mattinson, J.M., 2005. Zircon U–Pb chemical abrasion ("CA-TIMS") method: Combined annealing and multi-step partial dissolution analysis for improved precision and accuracy of zircon ages. Chem. Geol. 220, 47–66. doi:10.1016/j.chemgeo.2005.03.011

McCourt, S., Armstrong, R. a., Grantham, G.H., Thomas, R.J., 2006. Geology and evolution of the Natal belt, South Africa. J. African Earth Sci. 46, 71–92. doi:10.1016/j.jafrearsci.2006.01.013

Mendonidis, P., 1989. The Tectonic Evolution of a Portion of the Southern Granulite Zone of the Natal Mobile Belt, Between Southbroom and Glenmore, Natal. University of Natal, Pietermaritzburg.

Mendonidis, P., Armstrong, R., 2002. Metamorphic history and U-Pb Zircon (SHRIMP) geochronology of the Glenmore Granite: Implications for the tectonic evolution of the Natal Metamorphic Province. South African J. … 105, 325–336.

Mendonidis, P., Armstrong, R.A., 2009. A New U-Pb Zircon Age For The Portobello Granite From The Southern Part Of The Natal Metamorphic Belt. South African J. Geol. 112, 197–208. doi:10.2113/gssajg.112.2.197

Mendonidis, P., Grantham, G., 2003. Petrology, Origin, and Metamorphic History of Proterozoic-aged Granulites of the Natal Metamorphic Province, Southeastern Africa. Gondwana Res. 607–628.

Mendonidis, P., Grantham, G.H., Thomas, R.J., 1991. Glenmore Granite, in: Johnson, M.R. (Ed.), South African Catalogue of Lithostratigraphic Units 3. South African Committee for Stratigraphy, Council For Geoscience, South Africa, pp. 13–14.

Millar, I.L., Pankhurst, R.J., 1987. Gondwana Six: Structure, Tectonics, and Geophysics, Geophysical Monograph Series, Geophysical Monograph Series. American Geophysical Union, Washington, D. C. doi:10.1029/GM040

Mosher, S., Levine, J.S.F., Carlson, W.D., 2008. Mesoproterozoic plate tectonics: A collisional model for the Grenville-aged orogenic belt in the Llano uplift, central Texas. Geology 36, 55. doi:10.1130/G24049A.1

Pisarevsky, S. a., Wingate, M.T.D., Powell, C.M., Johnson, S., Evans, D. a. D., 2003. Models of Rodinia assembly and fragmentation. Geol. Soc. London, Spec. Publ. 206, 35–55. doi:10.1144/GSL.SP.2003.206.01.04

Scheiber-Enslin, S., Ebbing, J., Webb, S.J., 2014. An integrated geophysical study of the Beattie Magnetic Anomaly, South Africa. Tectonophysics. doi:10.1016/j.tecto.2014.08.021

Schlüter, T., 2006. Geological Atlas of Africa: With Notes on Stratigraphy, Tectonics, Economic Geology, Geohazards and Geosites of Each Country. Springer.

Siebel, W., Shang, C.K., Thern, E., Danišík, M., Rohrmüller, J., 2012. Zircon response to high-grade metamorphism as revealed by U–Pb and cathodoluminescence studies. Int. J. Earth Sci. 101, 2105–2123. doi:10.1007/s00531-012-0772-5

Smith, D.R., Barnes, C., Shannon, W., Roback, R., James, E., 1997. Petrogenesis of Mid-Proterozoic granitic magmas: examples from central and west Texas. Precambrian Res. 85, 53–79. doi:10.1016/S0301-9268(97)00032-6

Spencer, C., Roberts, N., 2014. Intermontane basins and bimodal volcanism at the onset of the Sveconorwegian Orogeny, southern Norway. Precambrian … 252, 107–118.

Talbot, C.J., Grantham, G.H., 1987. The Proterozoic intrusion and deformation of deep crustal "sills" along the south coast of Natal. South African J. Geol. 90, 520–538.

Tapponnier, P., Molnar, P., 1976. Slip-line field theory and large-scale continental tectonics. Nature 264, 319–324. doi:10.1038/264319a0

Tapponnier, P., Peltzer, G., Le Dain, A.Y., Armijo, R., Cobbold, P., 1982. Propagating extrusion tectonics in Asia: New insights from simple experiments with plasticine. Geology 10, 611–616. doi:10.1130/0091-7613(1982)10

Thomas, R., Ashwal, L., Andreoli, M., 1992. The petrology of the Turtle Bay Suite: a mafic-felsic granulite association from southern Natal, South Africa.,African Earth Sci. 15, 187–206.

Thomas, R.J., 1988. The geology of the Port Shepstone area. Explanation of sheet 3030 Port Shepstone.

Thomas, R.J., 1989. A tale of two tectonic terranes. South African J. Geol. 92, 306–321.

Thomas, R.J., 1989. The petrogenesis of the Mzumbe Gneiss Suite, a tonalite-trondhjemite orthogneiss suite from the southern part of the Natal Structural and Metamorphic Province.

Thomas, R.J., 1990. Mzumbe Gneiss Suite, in: Johnson, M.R. (Ed.), Catalogue of South African Lithostratigraphic Units 2. South African Committee for Stratigraphy, Council For Geoscience, South Africa, pp. 35–36.

Thomas, R.J., 1991a. Mkomazi Gneiss, in: Johnson, M.R. (Ed.), Catalogue of South African Lithostratigraphic Units 3. South African Committee for Stratigraphy, Council For Geoscience, South Africa, pp. 27–28.

Thomas, R.J., 1991b. Oribi Gorge Granitoid Suite, in: Johnson, M.R. (Ed.), Catalogue of South African Lithostratigraphic Units 3. South African Committee for Stratigraphy, Council For Geoscience, South Africa, pp. 37–40.

Thomas, R.J., 1991c. Banana Beach Gneiss, in: Johnson, M.R. (Ed.), Catalogue of South African Lithostratigraphic Units 3. South African Committee for Stratigraphy, Council For Geoscience, South Africa, pp. 1–2.

Thomas, R.J., 1991d. Turtle Bay Suite, in: Johnson, M.R. (Ed.), Catalogue of South African Lithostratigraphic Units 3. South African Committee for Stratigraphy, Council For Geoscience, South Africa, pp. 47–48.

Thomas, R.J., 1992. Mbizana Microgranite, in: Johnson, M.R. (Ed.), South African Catalogue of Lithostratigraphic Units 4. South African Committee for Stratigraphy, Council For Geoscience, South Africa, pp. 15–16.

Thomas, R.J., 2003. Geochronology of the Sikombe Granite, Transkei, Natal Metamorphic Province, South Africa. South African J. Geol. 106, 403–408. doi:10.2113/106.4.403

Thomas, R.J., Agenbacht, A.L.D., Cornell, D.H., Moore, J.M., 1994. The Kibaran of southern Africa: Tectonic evolution and metallogeny. Ore Geol. Rev. 9, 131–160. doi:10.1016/0169-1368(94)90025-6

Thomas, R.J., Cornell, D.H., Armstrong, R.A., 1999. Provenance age and metamorphic history of the Quha Formation, Natal metamorphic province; a U-Th-Pb zircon SHRIMP study. South African J. Geol. 102, 83–92.

Thomas, R.J., Eglington, B.M., 1990. A Rb-Sr, Sm-Nd and U-Pb zircon isotopic study of the Mzumbe Suite, the oldest intrusive granitoid in southern Natal, South Africa. South African J. Geol. 93, 761–765.

Thomas, R.J., Eglington, B.M., Bowring, S.A., 1993a. Dating the cessation of Kibaran magmatism in Natal, South Africa. J. African Earth Sci. (and Middle East) 16, 247–252. doi:10.1016/0899-5362(93)90046-S

Thomas, R.J., Eglington, B.M., Bowring, S.A., Retief, E.A., Walraven, F., 1993b. New isotope data from a neoproterozoic porphyritic garnitoid-charnockite suite from Natal, South Africa. Precambrian Res. 62, 83–101. doi:10.1016/0301-9268(93)90095-J

Thomas, R.J., Eglington, B.M., Kerr, A., 1990. The geology and geochronology of the Belmont pluton and microgranite dykes from the Margate area.

Thomas, R.J., Jacobs, J., Weber, K., 1997. Geology of the Mesoproterozoic Cape Meredith Complex, West Falkland, in: Ricci, C.A. (Ed.), The Antarctica Region, Geological Evolution and Processes. Siena Terra Antarctica Publications, pp. 21–30.

Thomas, R.J., Mendonidis, P., Grantham, G.H., 1991. Margate Granite Suite, in: Johnson, M.R. (Ed.), Catalogue of South African Lithostratigraphic Units 3. South African Committee for Stratigraphy, Council For Geoscience, South Africa, pp. 33–36.

Tohver, E., D'Agrella-Filho, M.S., Trindade, R.I.F., 2006a. Paleomagnetic record of Africa and South America for the 1200–500Ma interval, and evaluation of Rodinia and Gondwana assemblies. Precambrian Res. 147, 193–222. doi:10.1016/j.precamres.2006.01.015

Tohver, E., Pluijm, B.A. Van Der, Scandola, J.E., Essene, E.J., 2005. Late Mesoproterozoic Deformation of SW Amazonia (Rondonia , Brazil): Geochronological and Structural Evidence for Collision with Southern Laurentia. J. Geol. 113, 309–323.

Tohver, E., Teixeira, W., van der Pluijm, B., Geraldes, M.C., Bettencourt, J.S., Rizzotto, G., 2006b. Restored transect across the exhumed Grenville orogen of Laurentia and Amazonia, with implications for crustal architecture. Geology 34, 669. doi:10.1130/G22534.1

Valley, J.W., Cavosie, A.J., Ushikubo, T., Reinhard, D.A., Lawrence, D.F., Larson, D.J., Clifton, P.H., Kelly, T.F., Wilde, S.A., Moser, D.E., Spicuzza, M.J., 2014. Hadean age for a post-magma-ocean zircon confirmed by atom-probe tomography. Nat. Geosci. 7, 219–223. doi:10.1038/ngeo2075

Valli, F., Arnaud, N., Leloup, P.H., Sobel, E.R., Mahéo, G., Lacassin, R., Guillot, S., Li, H., Tapponnier, P., Xu, Z., 2007. Twenty million years of continuous deformation along the Karakorum fault, western Tibet: A thermochronological analysis. Tectonics 26, n/a–n/a. doi:10.1029/2005TC001913

Vander Auwera, J., Bolle, O., Bingen, B., Liégeois, J.-P., Bogaerts, M., Duchesne, J.C., De Waele, B., Longhi, J., 2011. Sveconorwegian massif-type anorthosites and related granitoids result from post-collisional melting of a continental arc root. Earth-Science Rev. 107, 375–397. doi:10.1016/j.earscirev.2011.04.005

Voordouw, R.J., 2010. a D3 Shear Zone in the Margate Terrane and Its Implications for Regional Deformation in the Natal Metamorphic Province (South Africa). South African J. Geol. 113, 183–194. doi:10.2113/gssajg.113.2.183

Voordouw, R.J., Rajesh, H.M., 2012. Granitoids From the Margate Terrane and Their Implications for Tectono-Magmatic Models of the Natal Metamorphic Province (South Africa). South African J. Geol. 115, 47–64. doi:10.2113/gssajg.115.1.47

Wakabayashi, J., 2004. Tectonic mechanisms associated with P–T paths of regional metamorphism: alternatives to single-cycle thrusting and heating. Tectonophysics 392, 193–218. doi:10.1016/j.tecto.2004.04.012

Wendt, I., Carl, C., 1991. The statistical distribution of the mean squared weighted deviation. Chem. Geol. Isot. Geosci. Sect. 86, 275–285. doi:10.1016/0168-9622(91)90010-T

Whitehouse, M.J., Ravindra Kumar, G.R., Rimša, A., 2014. Behaviour of radiogenic Pb in zircon during ultrahigh-temperature metamorphism: an ion imaging and ion tomography case study from the Kerala Khondalite Belt, southern India. Contrib. to Mineral. Petrol. 168, 1042. doi:10.1007/s00410-014-1042-2

Whitney, D.L., Teyssier, C., Fayon, A.K., 2004. Isothermal decompression, partial melting and exhumation of deep continental crust. Geol. Soc. London, Spec. Publ. 227, 313–326. doi:10.1144/GSL.SP.2004.227.01.16

Formatted: Indent: Left: 0 cm, Hanging: 0.84 cm

Formatted: Indent: Left: 0 cm, Hanging: 0.84 cm

Table 1

Sample	Locality	Lithology	Mineral Assembalge
CS13-4	Mvoti	Charnockite	ksp+pl+qtz+opx+bt+tit+zr+ap
CS13-10	Kwa-Lembe	Charnockite	pl+ksp+qtz+opx+gt+bt+zr+ap
CS13-12	Sezela	Syenite	ksp+pl+qtz+bt+hbl+tit+zr+ap
CS13-13	Sezela	Quartz-monzonite	ksp+pl+qtz+bt+hbl+tit+zr+ap
CS13-16	Mzumbe	Quartz-diorite	ksp+pl+qtz+hbl+bt+gt+zr+ap
CS13-19	Port Edward	Charnockite	pl+ksp+qtz+opx+bt+zr+ap
CS13-20	Leisure Bay	Psammitic Granulite	qtz+pl+ksp+bt+opx+g+hbl+zr+ap
CS13-21	Nicholson Point	Granite	qtz+pl+ksp+bt+gt+zr+ap+tit+rt
CS13-22	Glenmore	Granite	ksp+qtz+pl+gt+bt+zr+ap
CS13-26	Margate	Granite	qtz+pl+ksp+bt+gt+zr+ap+tit+rt
CS13-27	Oribi Gorge	Charnockite	ksp+pl+qtz+opx+bt+zr+ap
CS13-28	Turtle Bay	Mafic Granulite	pl+hbl+opx+cpx+bt+ol+ap+zr
CS13-29	Turtle Bay	Charnockite	qtz+pl+ksp+opx+bt+hbl+cpx+zr+ap

mineral	abbrev.
K-feldspar	ksp
plagioclase	pl
quartz	qtz
biotite	bt
hornblende	hbl
titanite	tit
zircon	zr
apatite	ap
orthopyroxene	opx
clinopyroxene	cpx
garnet	gt
rutile	rt
olivine	ol

Table 2

Mzumbe Terrane

Locality	Sample	n	Age (Ma)	±2s	MSWD
Mzumbe	CS13-16	12	1175	8/19	1.1
Mvoti	CS13-4	15	1145	6/18	2.9
Sezela	CS13-12	9	1081	9/19	0.81
	titanite	7	1030	11	6.0
Sezela	CS13-13	13	1085	9/18	0.8
Kwa-Lembe	CS13-10	19	1030	4/16	1.5

Margate Terrane

Locality	Sample	n	Age (Ma)	±2s	MSWD
Turtle Bay	CS13-28	7	1114	13/19	0.7
	monazite	17	1042	7	1.5
Glenmore	CS13-22	5	1092	11/22	0.4
		3	**1084.5**	**0.9**	**3.8**
Margate	CS13-26	2	1088	20/26	1
Nicholson Point	CS13-21	6	1099	31/35	6.3
		3	**1084.4**	**1.7**	**2.9**
Leisure Bay	CS13-20	15	1047	8/17	0.7
Oribi Gorge	CS13-27	6	1046	11/19	0.7
		4	**1049.3**	**0.8**	**5.5**
Port Edward	CS13-19	9	1039	9/18	0.5
		4	**1034.4**	**0.6**	**2.3**

bold MSWD values are CA-ID-TIMS analyses

Table 3

Locality	Sample	Age	± 2s	Sm ppm	± 2SE	Nd ppm	± 2SE	$^{147}Sm/^{144}Nd$	$^{143}Nd/^{144}Nd$	± 2SE	eNd	± 2SE
Mvoti	CS13-04	1145	12	8.068	0.002	39.988	0.003	0.122	0.512059	0.000007	-0.3	0.3
Mzimlilo	CS13-09	1147	8	11.717	0.005	51.230	0.007	0.138	0.512297	0.000008	1.9	0.3
Kwa-Lembe	CS13-10	1030	8	20.031	0.521	75.414	0.011	0.161	0.512426	0.000009	0.6	0.4
Sezela	CS13-12	1081	9	22.442	0.625	134.559	0.033	0.101	0.512099	0.000010	2.8	0.4
Sezela	CS13-13	1086	8	5.167	0.004	17.583	0.001	0.178	0.512758	0.000007	5.0	0.3
Equeefa	CS13-14	1083	6	2.755	0.000	8.288	0.000	0.201	0.512957	0.000007	5.6	0.3
Equeefa	CS13-15	1083	6	3.151	0.002	9.805	0.001	0.194	0.512875	0.000009	5.0	0.4
Mzumbe	CS13-16	1175	7	4.180	0.004	18.711	0.001	0.135	0.512345	0.000008	3.6	0.3
Port Edward	CS13-19	1039	9	14.357	0.007	71.402	0.010	0.122	0.512247	0.000009	2.4	0.4
Leisure Bay	CS13-20	1047	7	6.414	0.007	35.555	0.002	0.109	0.512132	0.000005	1.9	0.2
Nicholson Point	CS13-21	1081	18	2.529	0.000	7.204	0.000	0.212	0.512807	0.000007	1.1	0.3
Glenmore	CS13-22	1092	14	9.458	0.056	54.982	0.004	0.104	0.512070	0.000005	1.9	0.2
Munster	CS13-23	1093	6	12.475	0.052	77.960	0.010	0.097	0.512100	0.000009	3.5	0.4
Munster	CS13-24	1091	7	20.690	0.694	88.972	0.014	0.141	0.512233	0.000008	-0.1	0.3
Margate	CS13-26	1088	20	6.936	0.001	31.013	0.002	0.135	0.512260	0.000008	1.2	0.3
Oribi Gorge	CS13-27	1046	11	19.820	0.237	94.021	0.017	0.127	0.512249	0.000008	1.7	0.3
Turtle Bay	CS13-28	1114	16	1.373	0.001	7.391	0.000	0.112	0.512199	0.000009	3.5	0.4
Turtle Bay	CS13-29	1100		3.329	0.001	14.553	0.001	0.138	0.512335	0.000007	2.3	0.3

Locality	Sample	Age	± 2s	Lu_ppm	± 2SE	Hf ppm	± 2SE	$^{176}Lu/^{177}Hf$	$^{176}Hf/^{177}Hf$	± 2SE	eHf	± 2SE
Mvoti	CS13-04	1145	12	0.4594	0.0004	7.658	0.001	0.009	0.282232	0.000007	-0.2	0.5
Mzimlilo	CS13-09	1147	8	0.6036	0.0003	12.558	0.002	0.007	0.282343	0.000003	5.0	0.2
Kwa-Lembe	CS13-10	1030	8	1.9705	0.0038	14.023	0.002	0.020	0.282629	0.000003	4.1	0.2
Sezela	CS13-12	1081	9	0.6926	0.0003	1.830	0.000	0.054	0.283284	0.000009	3.4	0.6
Sezela	CS13-13	1086	8	0.6103	0.0008	2.104	0.000	0.041	0.283115	0.000005	6.4	0.4
Equeefa	CS13-14	1083	6	0.3429	0.0000	0.857	0.000	0.057	0.283524	0.000008	9.7	0.6
Equeefa	CS13-15	1083	6	0.3955	0.0001	1.928	0.000	0.029	0.282905	0.000008	7.7	0.6
Mzumbe	CS13-16	1175	7	0.0950	0.0000	2.230	0.000	0.006	0.282360	0.000009	6.7	0.6
Port Edward	CS13-19	1039	9	0.6939	0.0005	15.332	0.004	0.006	0.282383	0.000006	4.8	0.4
Leisure Bay	CS13-20	1047	7	0.3851	0.0001	2.265	0.000	0.024	0.282720	0.000008	4.5	0.6
Nicholson Point	CS13-21	1081	18	0.9777	0.0039	5.851	0.001	0.024	0.282681	0.000007	3.6	0.5
Glenmore	CS13-22	1092	14	0.3147	0.0005	2.913	0.000	0.015	0.282497	0.000007	3.3	0.5
Munster	CS13-23	1093	6	0.4355	0.0004	11.587	0.001	0.005	0.282326	0.000005	4.5	0.4
Munster	CS13-24	1091	7	0.7689	0.0002	7.398	0.001	0.015	0.282524	0.000005	4.7	0.4
Margate	CS13-26	1088	20	0.1859	0.0001	2.303	0.000	0.011	0.282375	0.000010	1.7	0.7
Oribi Gorge	CS13-27	1046	11	0.8377	0.0029	5.715	0.001	0.021	0.282644	0.000009	4.1	0.6
Turtle Bay	CS13-28	1114	16	0.0575	0.0000	3.950	0.014	0.002	0.282534	0.000008	14.7	0.6
Turtle Bay	CS13-29	1100		0.1344	0.0000	1.736	0.000	0.011	0.282458	0.000009	5.2	0.6

Figure 1

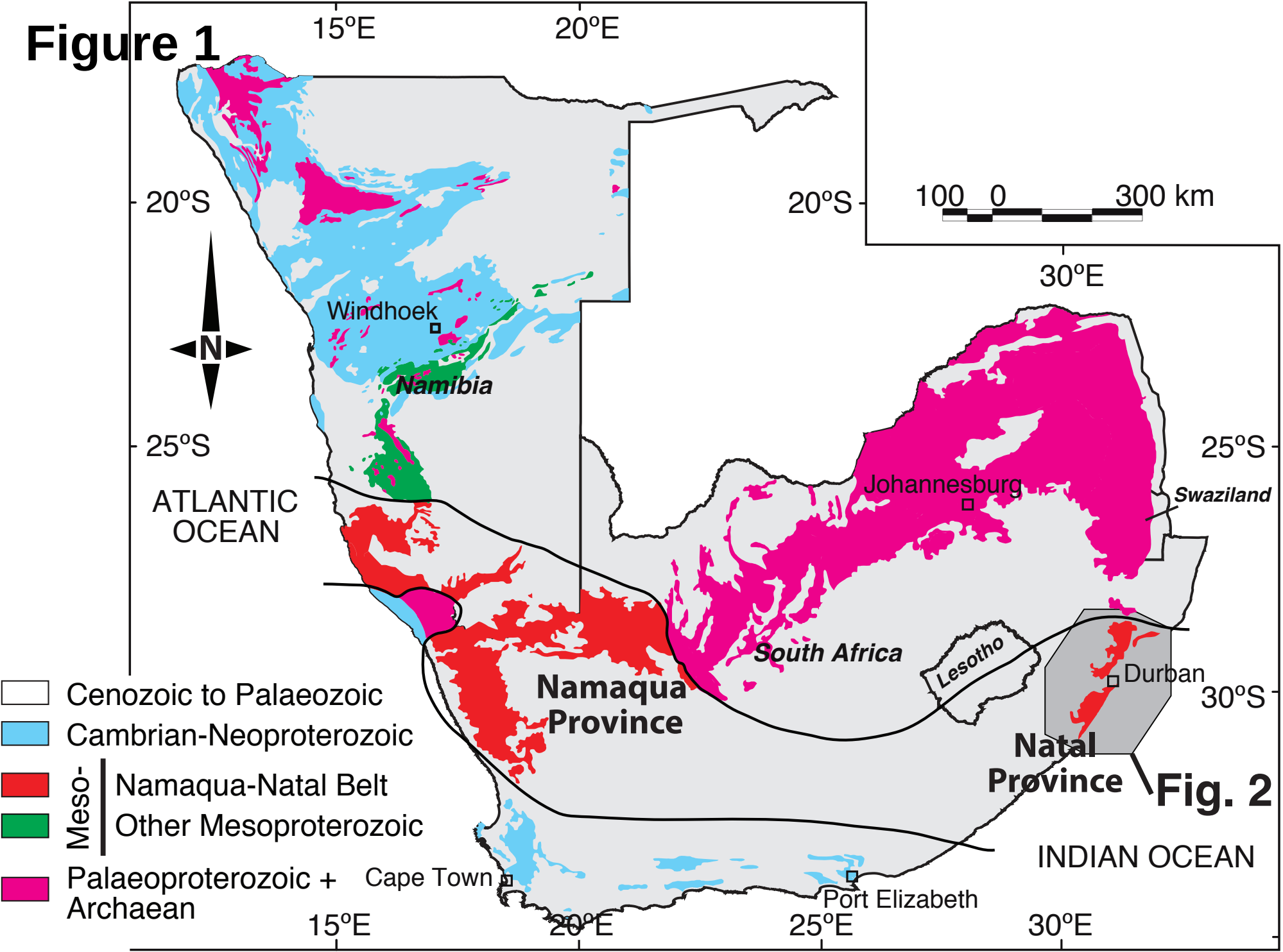
15ºE
20ºE
20ºS
25ºS
30ºE
100 0 300 km
N
Windhoek
Namibia
ATLANTIC OCEAN
Johannesburg
Swaziland
South Africa
Lesotho
Durban
Namaqua Province
Natal Province
Fig. 2
INDIAN OCEAN
Cape Town
Port Elizabeth
Cenozoic to Palaeozoic
Cambrian-Neoproterozoic
Meso-
Namaqua-Natal Belt
Other Mesoproterozoic
Palaeoproterozoic + Archaean

Figure 2

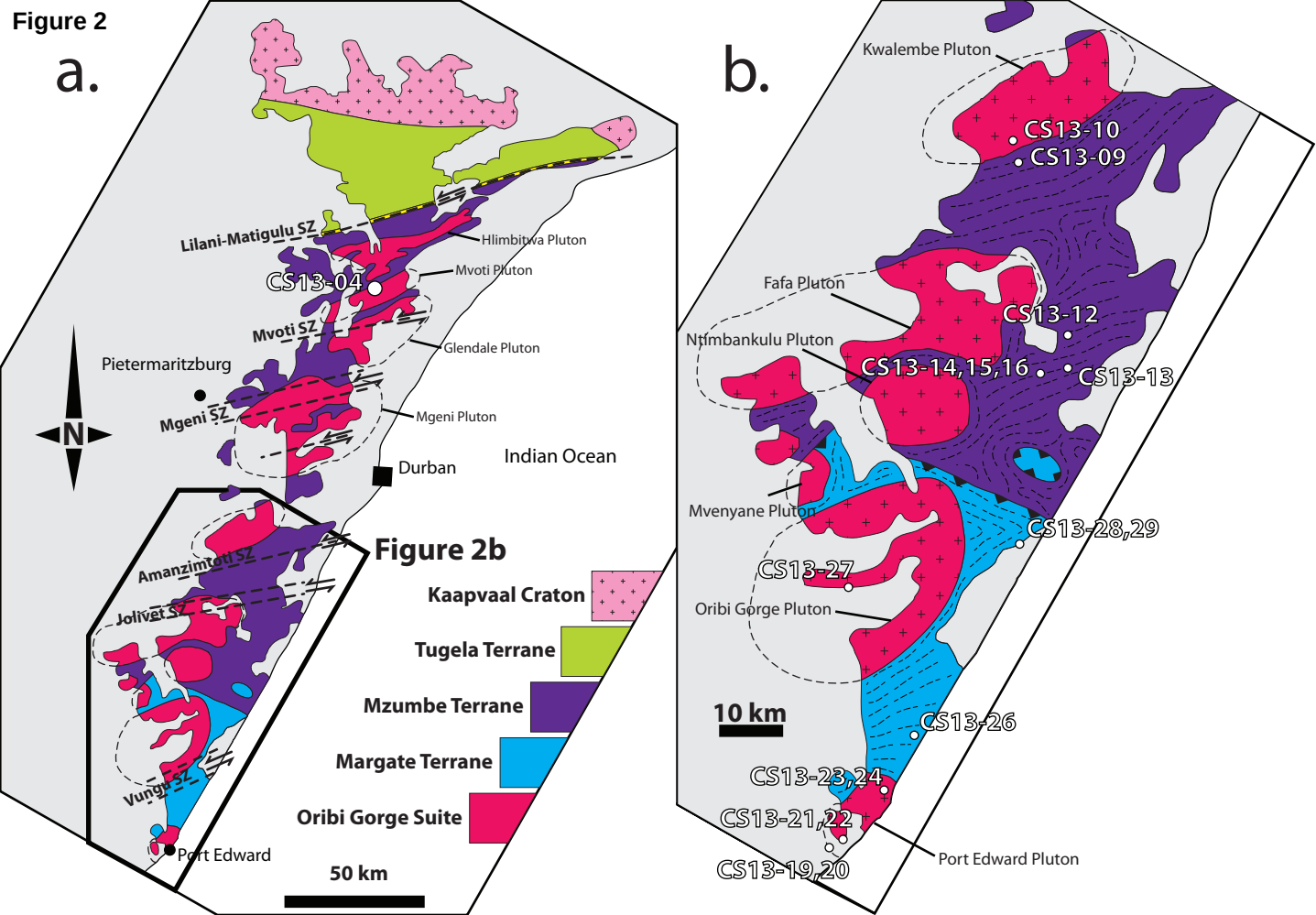
a.
Lilani-Matigulu SZ
Hlimbitwa Pluton
CS13-04
Mvoti Pluton
Mvoti SZ
Glendale Pluton
Pietermaritzburg
Mgeni SZ
Mgeni Pluton
N
Durban
Indian Ocean
Figure 2b
Amanzimtoti SZ
Jolivet SZ
Kaapvaal Craton
Tugela Terrane
Mzumbe Terrane
Margate Terrane
Oribi Gorge Suite
Vungu SZ
Port Edward
50 km
b.
Kwalembe Pluton
CS13-10
CS13-09
Fafa Pluton
CS13-12
Ntimbankulu Pluton
CS13-14,15,16
CS13-13
Mvenyane Pluton
CS13-28,29
CS13-27
Oribi Gorge Pluton
10 km
CS13-26
CS13-23,24
CS13-21,22
Port Edward Pluton
CS13-19,20

Figure 3

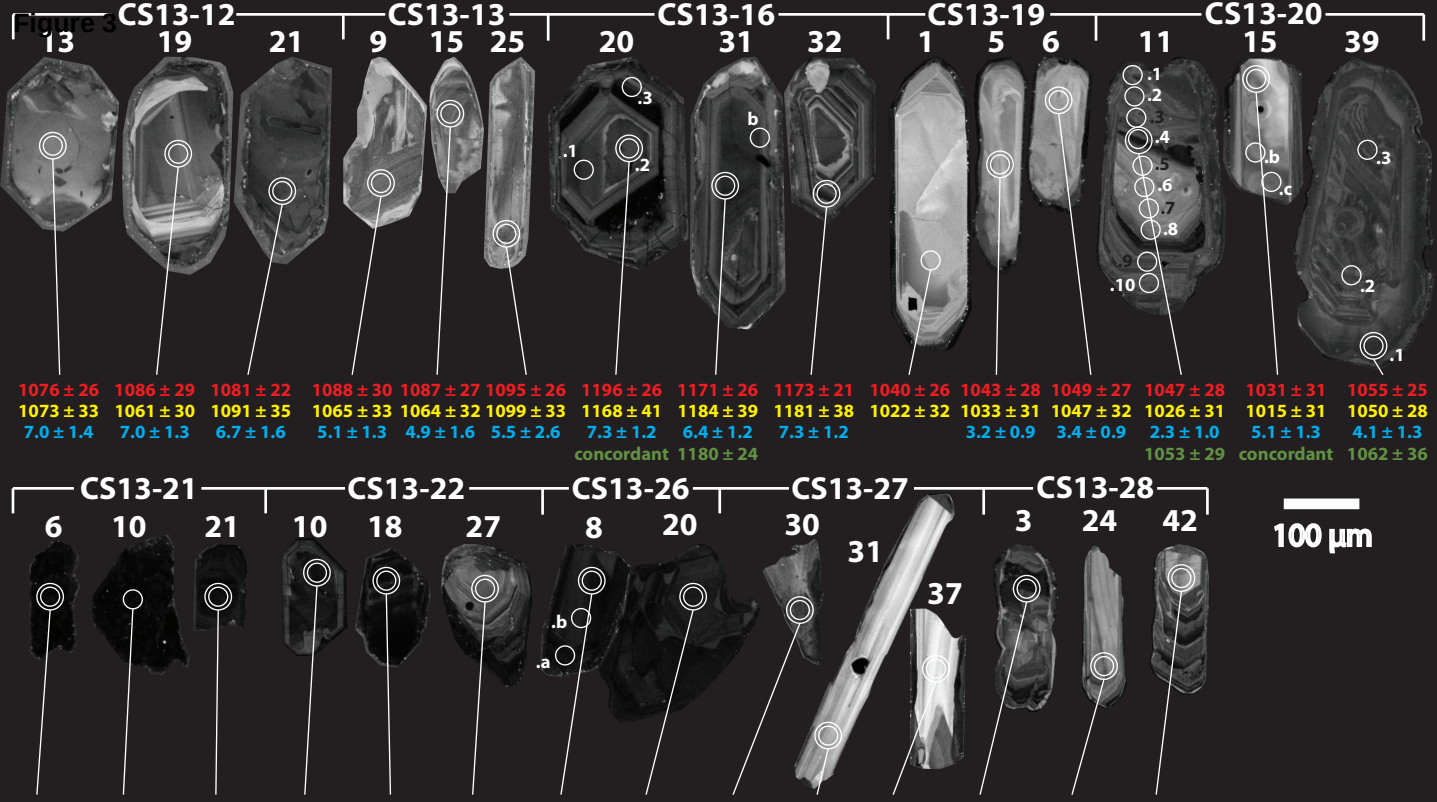
CS13-12
13
19
21
CS13-13
9
15
25
CS13-16
20
31
32
CS13-19
1
5
6
CS13-20
11
15
39
.1
.2
.3
.4
.5
.6
.7
.8
.9
.10
.a
.b
.c
1076 ± 26
1073 ± 33
7.0 ± 1.4
1086 ± 29
1061 ± 30
7.0 ± 1.3
1081 ± 22
1091 ± 35
6.7 ± 1.6
1088 ± 30
1065 ± 33
5.1 ± 1.3
1087 ± 27
1064 ± 32
4.9 ± 1.6
1095 ± 26
1099 ± 33
5.5 ± 2.6
1196 ± 26
1168 ± 41
7.3 ± 1.2
concordant
1171 ± 26
1184 ± 39
6.4 ± 1.2
1180 ± 24
1173 ± 21
1181 ± 38
7.3 ± 1.2
1040 ± 26
1022 ± 32
1043 ± 28
1033 ± 31
3.2 ± 0.9
1049 ± 27
1047 ± 32
3.4 ± 0.9
1047 ± 28
1026 ± 31
2.3 ± 1.0
1053 ± 29
1031 ± 31
1015 ± 31
5.1 ± 1.3
concordant
1055 ± 25
1050 ± 28
4.1 ± 1.3
1062 ± 36
CS13-21
6
10
21
CS13-22
10
18
27
CS13-26
8
20
CS13-27
30
31
37
CS13-28
3
24
42
100 µm
1062 ± 21
1060 ± 36
3.4 ± 1.8
1096 ± 22
1052 ± 33
1106 ± 25
1098 ± 37
3.6 ± 1.8
1091 ± 23
1087 ± 36
4.3 ± 1.4
1093 ± 22
1105 ± 36
5.1 ± 1.7
1104 ± 31
1089 ± 43
4.1 ± 1.7
1079 ± 27
1056 ± 32
3.0 ± 1.6
concordant
1099 ± 30
1075 ± 33
2.9 ± 1.8
1039 ± 26
1028 ± 35
4.8 ± 1.2
1043 ± 26
1032 ± 35
6.2 ± 1.4
1033 ± 28
1033 ± 39
4.7 ± 1.7
1176 ± 28
1125 ± 34
5.2 ± 1.4
1174 ± 25
1123 ± 33
5.9 ± 1.8
1140 ± 29
1111 ± 34
6.8 ± 1.8
207Pb/206Pb age (Ma)
206Pb/238U age (Ma)
epsilon Hf
Concordia intercept of multiple analyses of single grains (Ma)

Figure 4

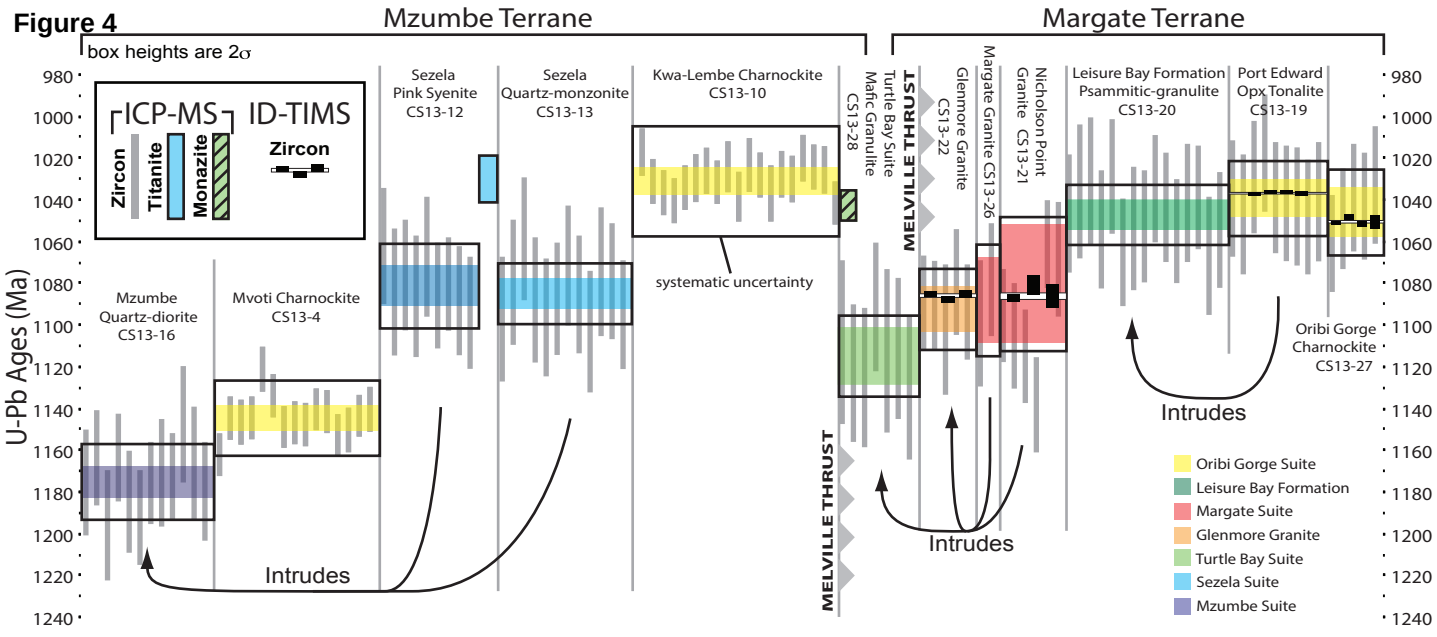
Mzumbe Terrane
Margate Terrane
box heights are 2σ
ICP-MS
ID-TIMS
Zircon
Titanite
Monazite
Zircon
U-Pb Ages (Ma)
980
1000
1020
1040
1060
1080
1100
1120
1140
1160
1180
1200
1220
1240
Mzumbe Quartz-diorite CS13-16
Mvoti Charnockite CS13-4
Sezela Pink Syenite CS13-12
Sezela Quartz-monzonite CS13-13
Kwa-Lembe Charnockite CS13-10
systematic uncertainty
Intrudes
Mafic Granulite CS13-28
Turtle Bay Suite
MELVILLE THRUST
Glenmore Granite CS13-22
Margate Granite CS13-26
Nicholson Point Granite CS13-21
Leisure Bay Formation Psammitic-granulite CS13-20
Port Edward Opx Tonalite CS13-19
Oribi Gorge Charnockite CS13-27
Intrudes
Intrudes
MELVILLE THRUST
Oribi Gorge Suite
Leisure Bay Formation
Margate Suite
Glenmore Granite
Turtle Bay Suite
Sezela Suite
Mzumbe Suite

Figure 5

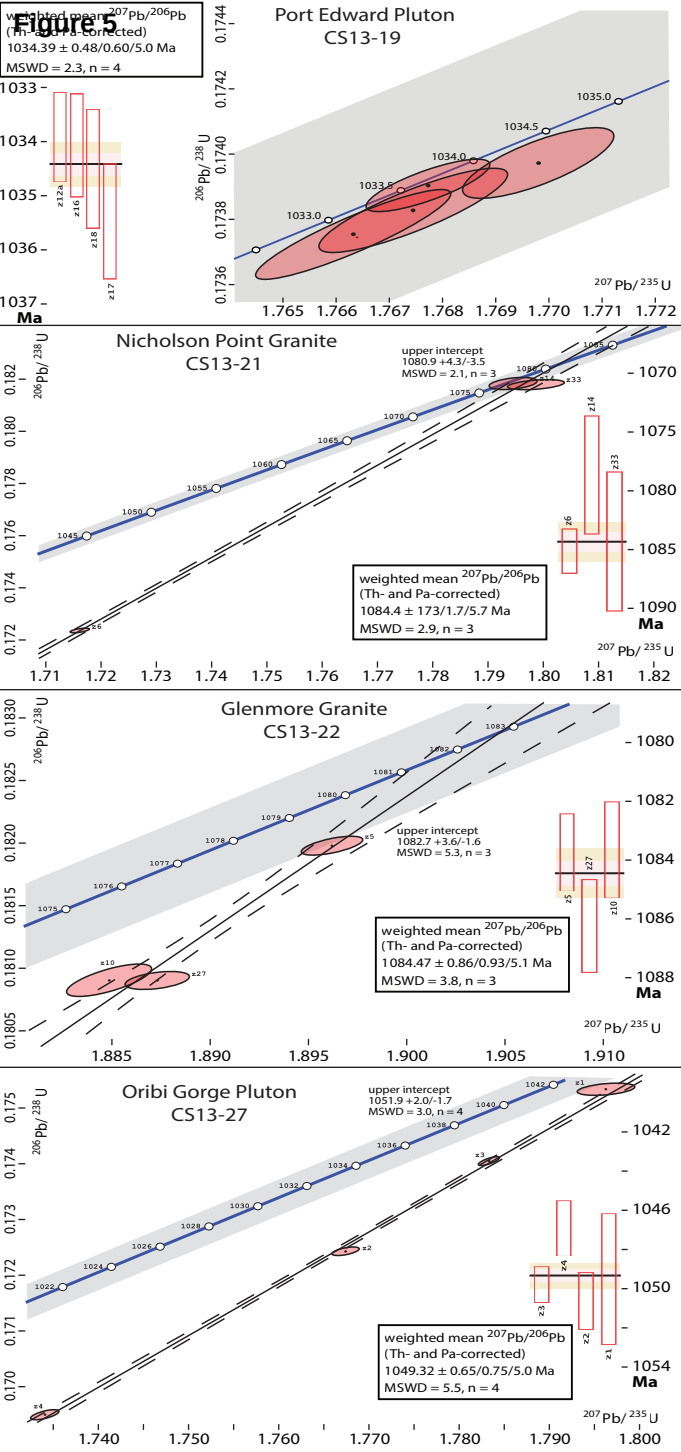
weighted mean 207Pb/206Pb
(Th- and Pa-corrected)
1034.39 ± 0.48/0.60/5.0 Ma
MSWD = 2.3, n = 4
Ma
z12a
z16
z18
z17
Port Edward Pluton
CS13-19
206Pb/238U
207Pb/235U
Nicholson Point Granite
CS13-21
upper intercept
1080.9 +4.3/-3.5
MSWD = 2.1, n = 3
weighted mean 207Pb/206Pb
(Th- and Pa-corrected)
1084.4 ± 173/1.7/5.7 Ma
MSWD = 2.9, n = 3
z33
z14
z6
z8
Glenmore Granite
CS13-22
upper intercept
1082.7 +3.6/-1.6
MSWD = 5.3, n = 3
weighted mean 207Pb/206Pb
(Th- and Pa-corrected)
1084.47 ± 0.86/0.93/5.1 Ma
MSWD = 3.8, n = 3
z5
z27
z10
z4
Oribi Gorge Pluton
CS13-27
upper intercept
1051.9 +2.0/-1.7
MSWD = 3.0, n = 4
weighted mean 207Pb/206Pb
(Th- and Pa-corrected)
1049.32 ± 0.65/0.75/5.0 Ma
MSWD = 5.5, n = 4
z1
z2
z3
z4

Figure 6

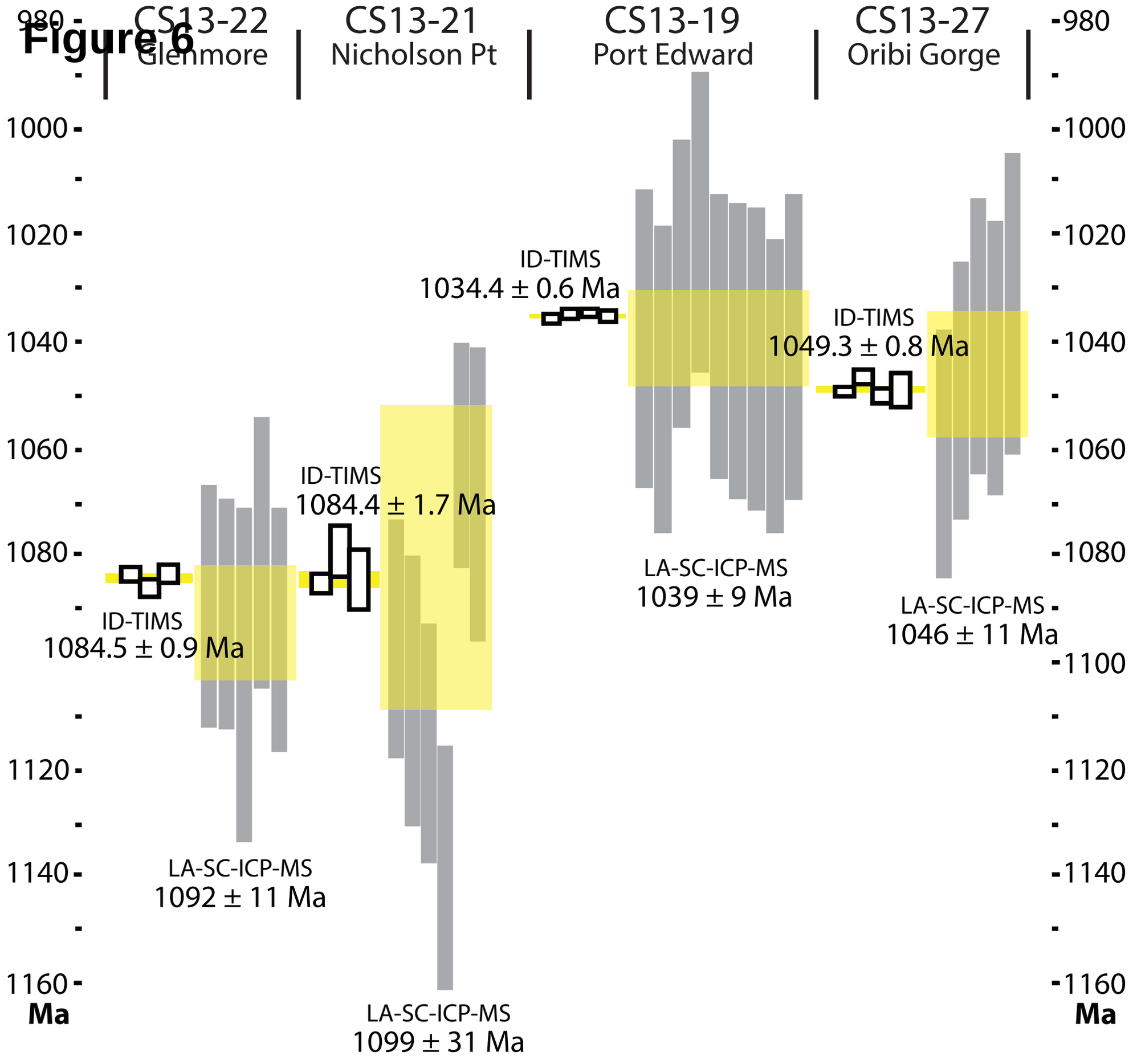
CS13-22
Glenmore
CS13-21
Nicholson Pt
CS13-19
Port Edward
CS13-27
Oribi Gorge
980
1000
1020
1040
1060
1080
1100
1120
1140
1160
Ma
ID-TIMS
1084.5 ± 0.9 Ma
LA-SC-ICP-MS
1092 ± 11 Ma
ID-TIMS
1084.4 ± 1.7 Ma
LA-SC-ICP-MS
1099 ± 31 Ma
ID-TIMS
1034.4 ± 0.6 Ma
LA-SC-ICP-MS
1039 ± 9 Ma
ID-TIMS
1049.3 ± 0.8 Ma
LA-SC-ICP-MS
1046 ± 11 Ma

Figure 7

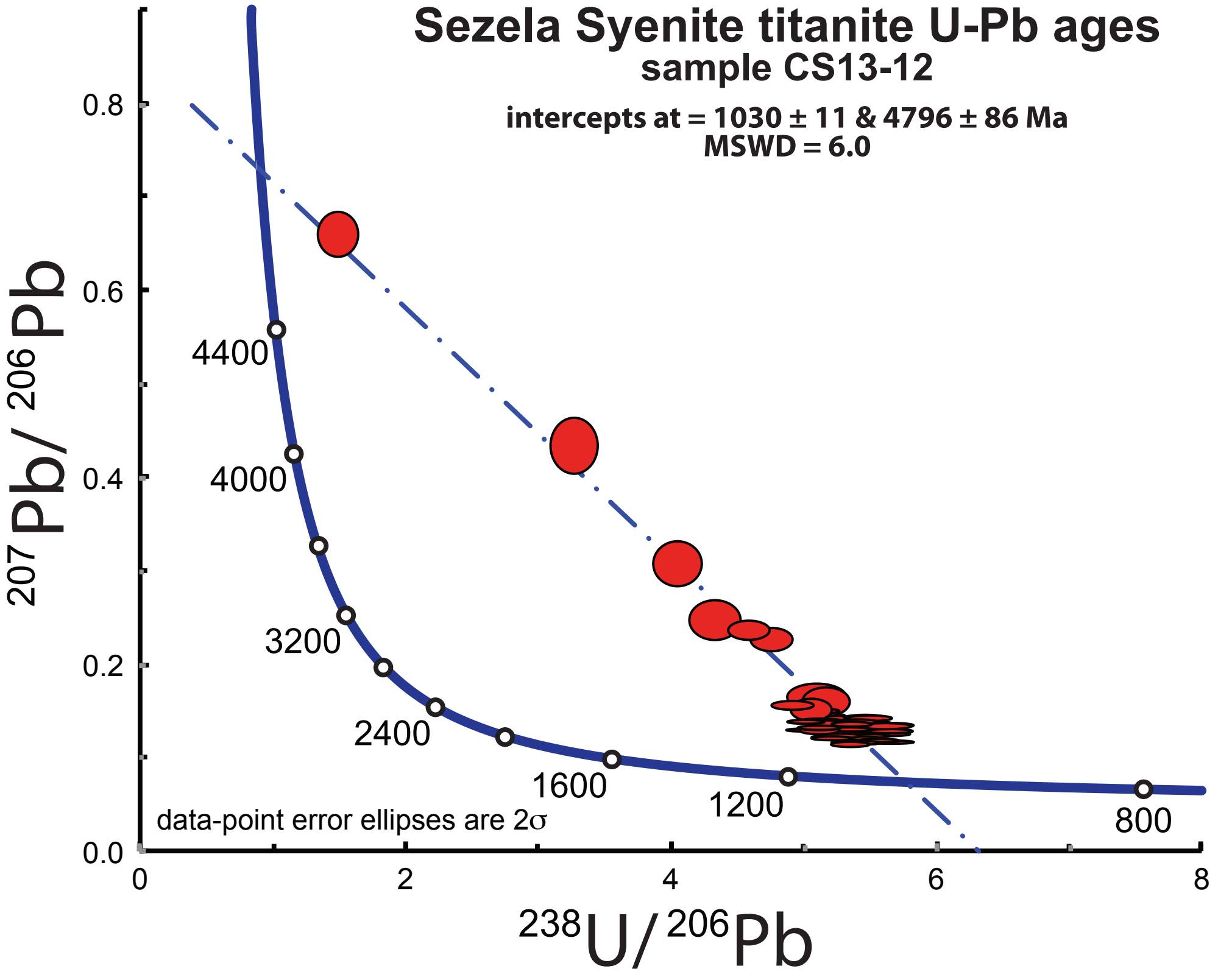
Sezela Syenite titanite U-Pb ages
sample CS13-12
intercepts at = 1030 ± 11 & 4796 ± 86 Ma
MSWD = 6.0
0.8
0.6
0.4
0.2
0.0
0
2
4
6
8
4400
4000
3200
2400
1600
1200
800
data-point error ellipses are 2σ
207Pb/206Pb
238U/206Pb

Figure 8 **Turtle Bay Suite monazite U-Pb ages**
sample CS13-28

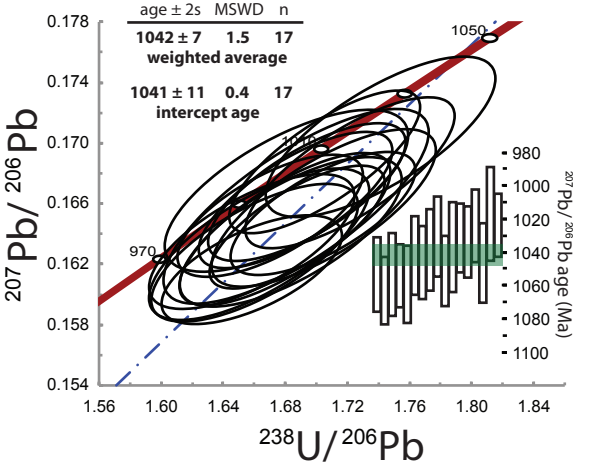

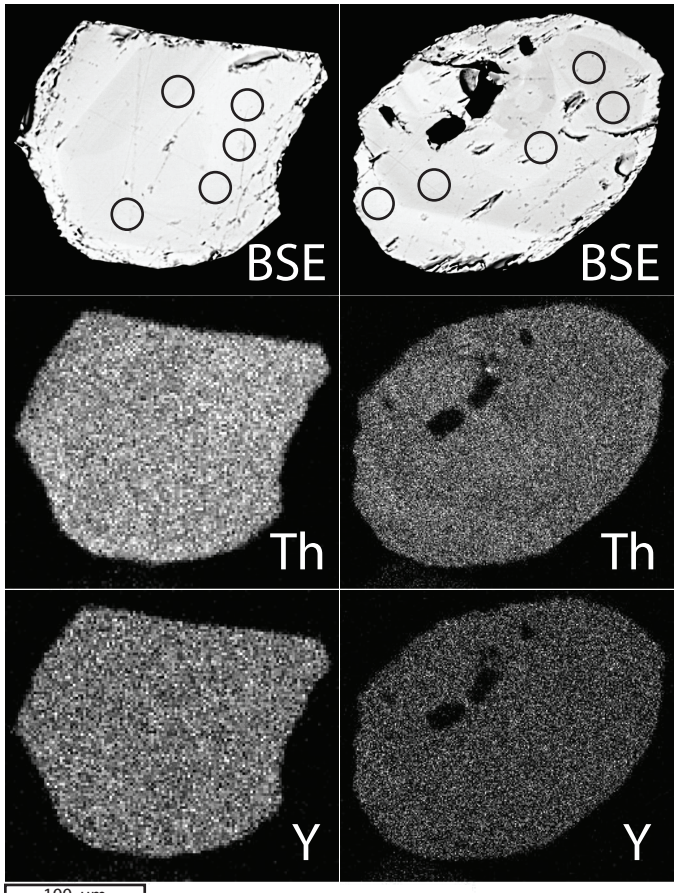

Figure 9

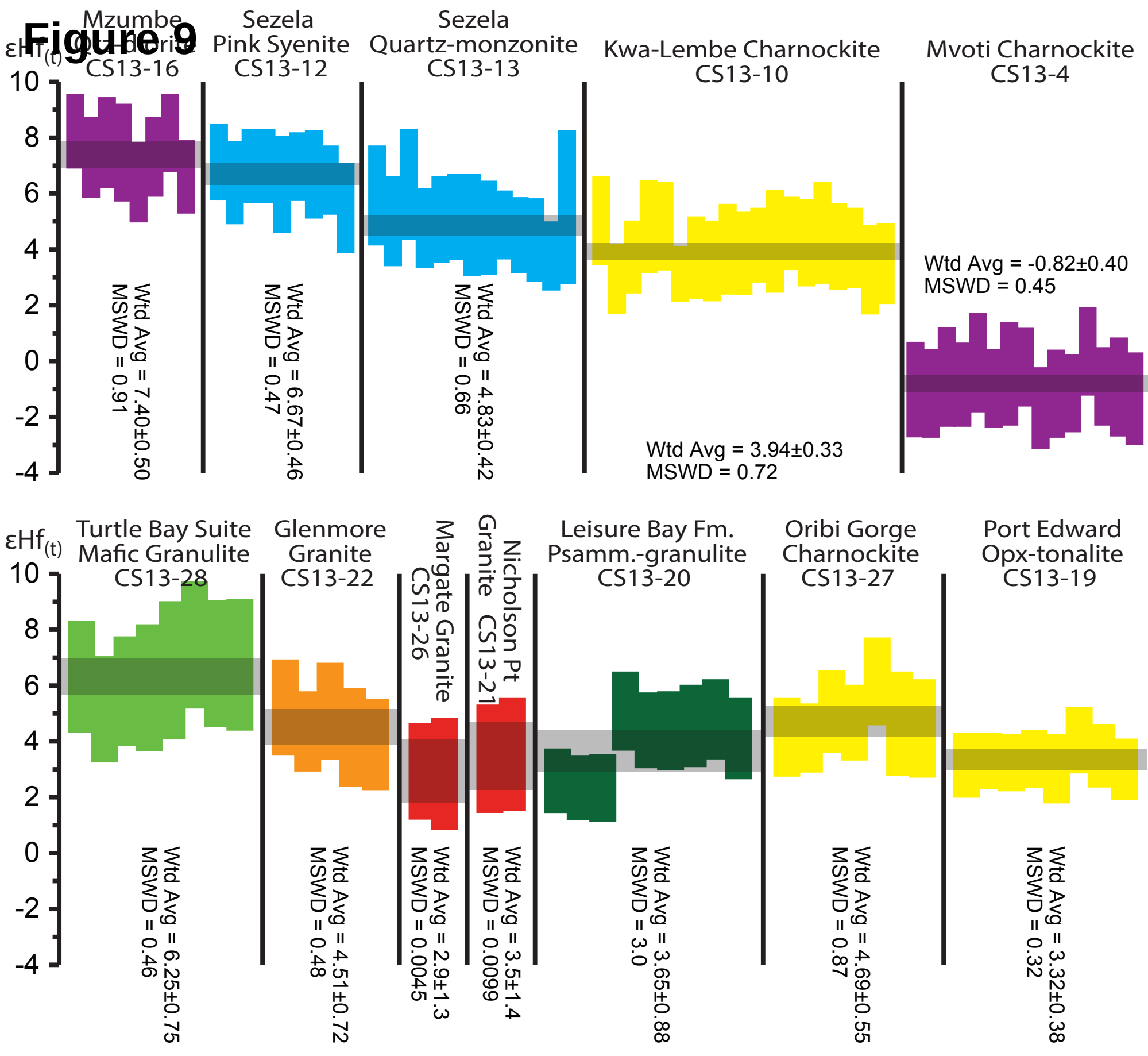
εHf(t)
10
8
6
4
2
0
-2
-4
Mzumbe Gabbronorite CS13-16
Wtd Avg = 7.40±0.50
MSWD = 0.91
Sezela Pink Syenite CS13-12
Wtd Avg = 6.67±0.46
MSWD = 0.47
Sezela Quartz-monzonite CS13-13
Wtd Avg = 4.83±0.42
MSWD = 0.66
Kwa-Lembe Charnockite CS13-10
Wtd Avg = 3.94±0.33
MSWD = 0.72
Mvoti Charnockite CS13-4
Wtd Avg = -0.82±0.40
MSWD = 0.45
Turtle Bay Suite Mafic Granulite CS13-28
Wtd Avg = 6.25±0.75
MSWD = 0.46
Glenmore Granite CS13-22
Wtd Avg = 4.51±0.72
MSWD = 0.48
Margate Granite CS13-26
Wtd Avg = 2.9±1.3
MSWD = 0.0045
Nicholson Pt Granite CS13-21
Wtd Avg = 3.5±1.4
MSWD = 0.0099
Leisure Bay Fm. Psamm.-granulite CS13-20
Wtd Avg = 3.65±0.88
MSWD = 3.0
Oribi Gorge Charnockite CS13-27
Wtd Avg = 4.69±0.55
MSWD = 0.87
Port Edward Opx-tonalite CS13-19
Wtd Avg = 3.32±0.38
MSWD = 0.32

Figure 10

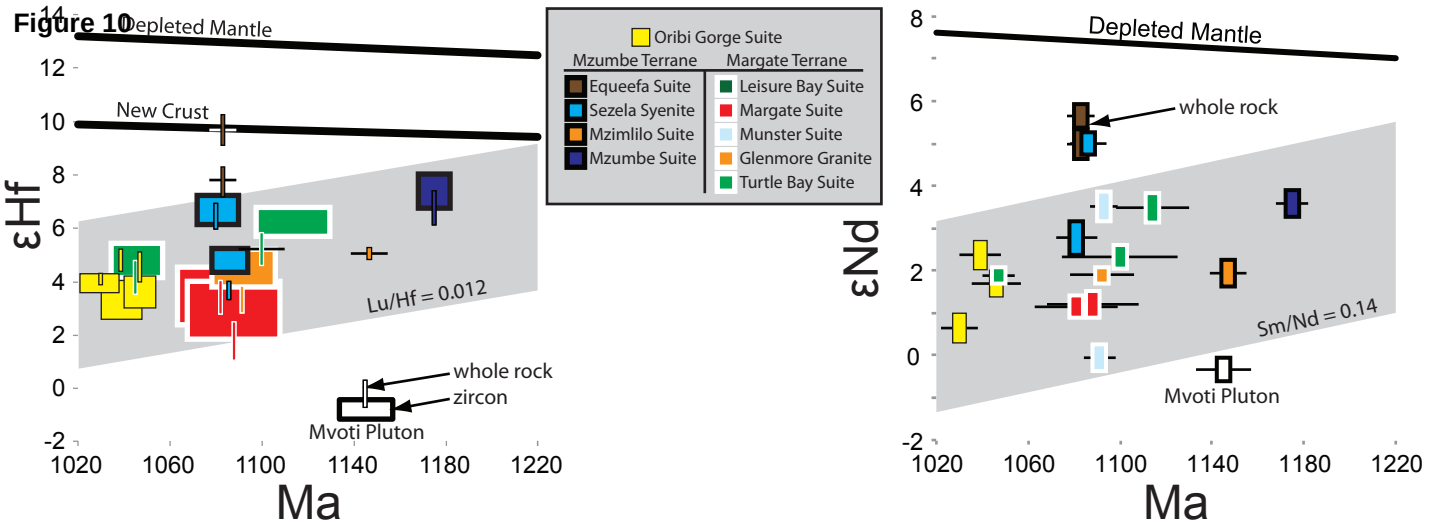
Depleted Mantle
New Crust
εHf
Lu/Hf = 0.012
whole rock
zircon
Mvoti Pluton
Ma
Oribi Gorge Suite
Mzumbe Terrane
Margate Terrane
Equeefa Suite
Sezela Syenite
Mzimlilo Suite
Mzumbe Suite
Leisure Bay Suite
Margate Suite
Munster Suite
Glenmore Granite
Turtle Bay Suite
Depleted Mantle
whole rock
εNd
Sm/Nd = 0.14
Mvoti Pluton
Ma

Figure 11

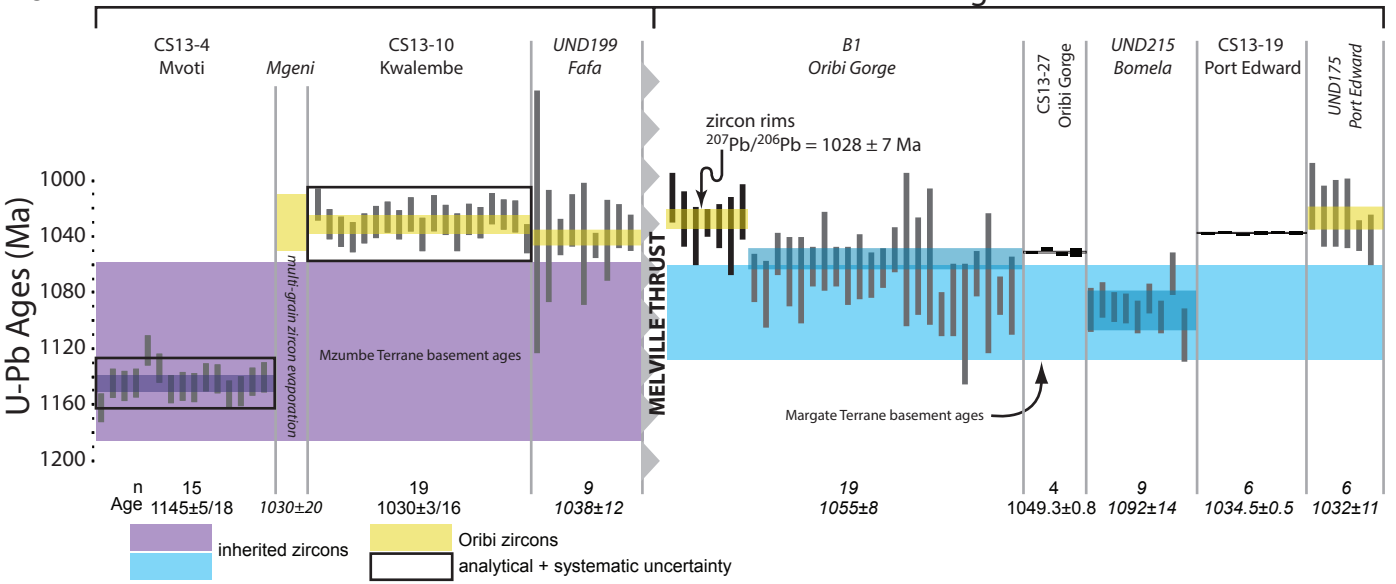
N
Mzumbe Terrane
Margate Terrane
S
CS13-4
Mvoti
Mgeni
CS13-10
Kwalembe
UND199
Fafa
B1
Oribi Gorge
zircon rims
207Pb/206Pb = 1028 ± 7 Ma
CS13-27
Oribi Gorge
UND215
Bomela
CS13-19
Port Edward
UND175
Port Edward
U-Pb Ages (Ma)
1000
1040
1080
1120
1160
1200
multi-grain zircon evaporation
Mzumbe Terrane basement ages
MELVILLE THRUST
Margate Terrane basement ages
n
Age
15
1145±5/18
1030±20
19
1030±3/16
9
1038±12
19
1055±8
4
1049.3±0.8
9
1092±14
6
1034.5±0.5
6
1032±11
inherited zircons
Oribi zircons
analytical + systematic uncertainty

Figure 12

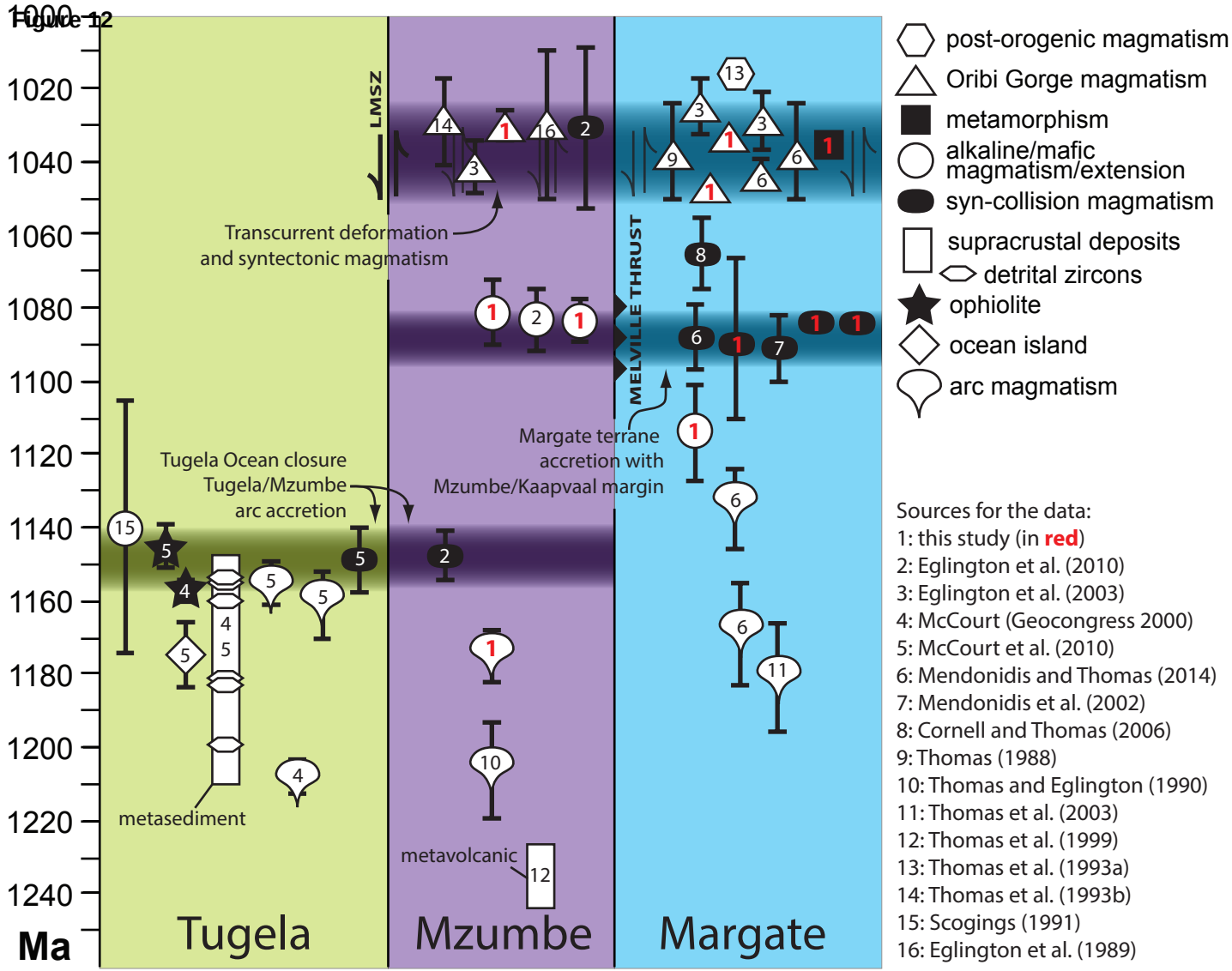

Sources for the data:
1: this study (in **red**)
2: Eglington et al. (2010)
3: Eglington et al. (2003)
4: McCourt (Geocongress 2000)
5: McCourt et al. (2010)
6: Mendonidis and Thomas (2014)
7: Mendonidis et al. (2002)
8: Cornell and Thomas (2006)
9: Thomas (1988)
10: Thomas and Eglington (1990)
11: Thomas et al. (2003)
12: Thomas et al. (1999)
13: Thomas et al. (1993a)
14: Thomas et al. (1993b)
15: Scogings (1991)
16: Eglington et al. (1989)

KML File (for GoogleMaps)

Click here to download KML File (for GoogleMaps): NNO Samples.kmz

Supplementary figure 2

Click here to download Supplementary material for on-line publication: S2 - Natal Concordias.pdf

Supplementary table 1

Click here to download Supplementary material for on-line publication: S1 - Natal Zircon.xls

Supplementary table 2

Click here to download Supplementary material for on-line publication: S2 - Natal Titanite.xls

Supplementary table 3

Click here to download Supplementary material for on-line publication: S3 - Natal Monazite.xls

Supplementary table 4

Click here to download Supplementary material for on-line publication: S4 - Natal Zircon Hf.xls

Supplementary text 1

Click here to download Supplementary material for on-line publication: Natal Methods.docx

Supplementary figure 1

Click here to download Inline Supplementary Figure: S1 - Natal STDs.pdf